Aus der Neurologischen Universitätsklinik Tübingen

Abteilung Neurologie mit Schwerpunkt neurovaskuläre Erkrankungen

Influence of sensorimotor μ rhythm phase and power on motor cortex excitability and plasticity induction, assessed with EEG-triggered TMS

Inaugural-Dissertation
zur Erlangung des Doktorgrades
der Medizin

der Medizinischen Fakultät
der Eberhard Karls Universität
zu Tübingen

vorgelegt von

El Hilany-Thies, Miriam Alison, geb. Thies

2022

Dekan:	Professor Dr. B. Pichler
1. Berichterstatter:	Professor Dr. U. Ziemann
2. Berichterstatter:	Professor Dr. C. Schwarz
Tag der Disputation:	10.02.2022

Contents

Page

1 Introduction **1**

1.1 Preface . . . 1

1.2 Statement of significance . . . 1

1.3 History of brain stimulation . . . 3

1.4 Foundations of TMS: Physicist's perspective . . . 4

1.5 Foundations of TMS: Neuroscientist's perspective . . . 5

1.5.1 From pulse to twitch . . . 6

1.5.2 Factors influencing current propagation . . . 7

1.6 Foundations of TMS: Neurologist's perspective . . . 10

1.6.1 Conceptual schema of TMS protocols . . . 10

1.6.2 Adverse Effects . . . 11

1.6.3 EEG-triggered TMS and EEG . . . 12

1.6.4 Alpha as Pulsed Inhibition . . . 14

1.6.5 Alpha in the visual cortex . . . 16

1.6.6 Alpha in the sensory cortex . . . 17

1.6.7 Alpha in the motor cortex: . . . 18

1.6.8 Objectives of the experiments: . . . 19

2 Methods **20**

2.1 Participants . . . 20

2.2 Recording and Stimulation . . . 21

2.3 Real-time EEG-triggered TMS . . . 21

2.4 Neuronavigation . . . 22

2.5 Statistical methods . . . 23

3 Experiment: MUPEX **24**

3.1 MUPEX. Introduction . . . 24

3.2 MUPEX. Session Design . . . 24

3.3 MUPEX. Data analysis . . . 25

3.4 MUPEX. Results . . . 26

3.5 MUPEX. Discussion . . . 29

3.5.1 Reported adverse effects . . . 29

3.5.2 Interpretation of MUPEX results . . . 31

3.6 MUPEX. Conclusion 39

4 Experiment: MUPAS **40**

4.1 MUPAS. Introduction 40

4.2 MUPAS. Methods 46

4.3 MUPAS. Session Design 47

4.4 MUPAS. Screening 50

4.5 MUPAS. Consistency Strategy 53

4.6 MUPAS. Results 53

4.6.1 Screening results 53

4.6.2 Main Sessions 54

4.7 MUPAS. Discussion 63

4.7.1 Limitation: Influences on plasticity induction not accounted for 63

4.7.2 Interpretation of MUPAS results 65

4.7.3 Applicability 72

4.8 MUPAS. Conclusion 76

5 Conclusion **77**

6 Summary **79**

7 Deutsche Zusammenfassung **81**

8 Bibliography **83**

9 Erklärung zum Eigenanteil **94**

10 Acknowledgments **95**

11 Attachments **96**

11.1 Detailed description of an exemplary measuring session 96

11.2 MUPAS single subject plots 97

List of Figures

1 TMS coil on motor hotspot 7
2 Sensory and motor homunculus 7
3 Monophasic TMS pulse 8
4 Schematic of TMS protocols 11
5 Relationship between µ power and excitability 18
6 C3 Hjorth montage 22
7 MUPEX: session design 24
8 Input-output curve 25
9 MUPEX: power-MEP slope 28
10 MUPEX: absolute power per bin 29
11 MUPEX: power spectra across bins 29
12 MUPEX: timing and topography of targeted power fluctuations . . . 30
13 Topography of μ-$alpha$ versus μ-$beta$ 33
14 PAS pathway 44
15 Median nerve stimulation 47
16 MUPAS: session design 48
17 MUPAS: hypotheses 50
18 MUPAS: screening session and exit points 52
19 MUPAS: group average changes from baseline 57
20 MUPAS: group average absolute MEP amplitudes 57
21 MUPAS: phase targeting analysis 58
22 MUPAS: power spectra across conditions 58
23 MUPAS: scatterplot of baseline amplitudes 60
24 MUPAS: scatterplot of μ power during PAS per condition 61
25 MUPAS: scatterplot of μ power during PAS per subject 61
26 MUPAS: scatterplot of PAS durations 62
27 MUPAS: single subject phase targeting 98
28 MUPAS: single subject power spectra 99
29 MUPAS: single subject changes from baseline 100
30 MUPAS: single subject absolute MEPs 101

List of Tables

1 EEG rhythms 14
2 MUPEX: results 30
3 Comparison of μ power-excitability studies 37
4 Schematic of TMS plasticity protocols 42
5 MUPAS: absolute MEP amplitudes 64
6 MUPAS: change from baseline 64
7 MUPAS: consistency across conditions 64
8 MUPAS: consistency across sessions 64

List of Abbreviations

Abbreviation or Acronym: **Meaning:**

ADL ..... activities of daily living
AEP ..... auditory evoked potential
AP ..... action potential
APB ..... abductor pollicis brevis muscle
AU ..... arbitrary units
avg ..... average
BCI ..... brain-computer interface
BOLD signal ..... blood oxygen level-dependent signal
CMAP ..... compound muscle action potential
CSE ..... corticospinal excitability
DBS ..... deep brain stimulation
dp-rtMS ..... double-pulse repetitive transcranial magnetic stimulation
ECoG ..... electrocorticography
EEG ..... electroencephalography
EMG ..... electromyography / electromyogram
EP ..... evoked potential
EPSP ..... excitatory post synaptic potential
FDI ..... first dorsal interosseus muscle
FFT ..... fast Fourier transformation
IA ..... interaction analysis
IOC ..... input-output curve
IPSP ..... inhibitory post synaptic potential
ISI ..... inter-stimulus interval: delay between stimuli within one trial
ITI ..... inter-trial interval: delay between two trials
LAI ..... long-latency afferent inhibition
M1 ..... primary motor cortex
MEP ..... motor-evoked potential
MEP1mV ..... 1-mV-MEP threshold
MNI ..... Montréal Neurological Institute (brain template)
MNS ..... median-nerve stimulation
MRI ..... Magnetic Resonance Imaging
MSO ..... maximum stimulator output
MUPAS ..... MU-rhythm and Paired Associative Stimulation (Experiment 2)
MUPEX ..... MU-rhythm Power and Motor EXcitability (Experiment 1)

N1 ..... latency of the peak at 140 ms latency (here in a MNS-evoked SSEP)
N20 ..... individual latency of the SSEP peak at about 20ms after stimulus
NIBS ..... non-invasive brain stimulation
NIRS ..... near-infrared spectroscopy
NMDA ..... N-methyl-D-aspartate receptor (ionotropic glutamate receptor)
rENS ..... repetitive electrical nerve stimulation
RMT ..... resting motor threshold
rTMS ..... repetitive transcranial magnetic stimulation
S1 ..... primary sensory cortex
SAI ..... short-latency afferent inhibition
SA-PEST ..... Simple Adaptive Parameter Estimation by Sequential Testing
SD ..... standard deviation
SI ..... stimulation intensity
SNR ..... signal to noise ratio
SSEP ..... somatosensory evoked potential
tACS ..... transcranial alternating current stimulation (form of TES)
TBS ..... theta-burst stimulation
tDCS ..... transcranial direct current stimulation (form of TES)
TEP ..... TMS-evoked EEG potential
tES ..... transcranial electrical stimulation (form of NIBS)
TMS ..... transcranial magnetic stimulation (form of NIBS)
tRNS ..... transcranial random noise stimulation

1 Introduction

1.1 Preface

The human brain largely acts in hidden ways, letting us observe only its 'output', i.e., in what manner the human body attached to this brain conducts itself. How the brain arrives at this output, what kind of processes lead to a certain behavior – all of this remains in the dark, sheltered within a secretive skull and coded in ways still not fully understood today.

Observations of patients with localized brain lesions were one of the first approaches to understanding how the brain works and led to the insight that different parts of this organ have distinct functions: By comparing the behavior of patients with that of individuals without brain damage, scientists could conclude upon a certain area's purpose. The most famous example is the oft-told tale of railroad construction worker Phineas Gage. In 1848, he survived an explosion which drove a tapered iron bar through his head, severely damaging one of his frontal lobes. His motor, sensory and memory functions as well as his general intelligence were unimpaired, but he displayed changes in personality and heightened impulsivity [O'Driscoll and Leach, 1998]. His symptoms serve to illustrate the role of the frontal cortex in social behavior and emotions to medical students even today.
In times of functional imaging methods such as fMRI and white matter tractography, questions about the location of brain areas involved during certain tasks and pathways connecting them are readily answerable. However, in order to advance understanding of a system, pure observation is eventually surpassed by purposeful manipulation, i.e., an experiment in the proper sense – or as Wagner et al. put it, brain stimulation can *"add causal information to the otherwise purely correlational insights of functional brain imaging"* [Wagner et al., 2007].

1.2 Statement of significance

Going one step further towards practical clinical application in curative neurology and psychiatry, harnessing and enhancing the brain's natural powers of adaptive change, i.e., plasticity, can perhaps be viewed as the 'crown jewel' of neurostimulation. Neuroplasticity is a decisive factor in rehabilitation processes, which in turn play a big role in neurology compared to other medical specialities. The possibility of translating neuroscience to clinical application explains a particular motivation exceeding scientific curiosity that draws clinical neurologists such as the author of this thesis towards this particular brand of neuroscience.

Despite the sometimes astonishing lengths to which 'naturally occurring' neuroplasticity can restore function after injury such as a stroke, and the vast expansion upon these improvements through targeted physio-, ergo- and logotherapy as employed in neurorehabilitation centers today, there are still too many patients with lasting deficits impacting their daily lives: According to the German Stroke Registry, about a third of stroke survivors need help with their daily activities at 3 months follow-up [Grau et al., 2001]. If neurostimulation protocols can support and intensify the benefits that are already today reaped from traditional methods of rehabilitation, this would constitute a practical use of the insights into the inner workings of the human brain which neuroscience has gained over the past centuries – a 'bench to bedside'-phenomenon arriving at the stage of rehabilitation where many are already in use in prevention, diagnosis and acute treatment.
Methods of non-invasive brain stimulation afford us a direct access to and impact on many cortical regions and hence the power to suppress or enhance the activity of specific brain functions without opening up the skull. We can gain a wealth of insights into brain connectivity and functionality in awake subjects and perhaps even treat diseases by counterbalancing deficits and overactivations or promoting existing processes of adaptation and recovery.

This thesis set itself the task to improve the effectiveness of a transcranial magnetic stimulation (TMS) protocol inducing positive motor cortex plasticity, i.e., increasing corticospinal excitability, by synchronizing the TMS pulses to certain brain states. Motor cortex plasticity is a decisive mechanism of clinical improvement in patients with paralysis due to e.g., ischemic (such as a stroke) or inflammatory motor cortex lesions. Thus, the enhancement of naturally occurring adaptive changes in brain connectivity has the potential to improve clinical outcome in a manner meaningful to patients' everyday lives. The main experiment described here seeks to increase the efficacy of a pre-existing plasticity-inducing TMS protocol by applying stimulation during brain states favorable to said neuroplasticity, which we hypothesize are brain states of excitation rather than inhibition. We target properties of oscillations observed in the surface EEG, namely of the 10 Hz μ-$alpha$ rhythm thought to reflect excitability within the sensorimotor cortex. TMS is applied in an EEG-triggered manner, more precisely triggered by intensity ('power') and phase of μ-$alpha$ oscillations. This protocol was preceded by a smaller-scale experiment, designed as a preliminary work to establish the relationship between the aforementioned μ-$alpha$ rhythm power and motor cortex excitability, in order to then transfer the resulting insights to the main experiment.

1.3 History of brain stimulation

I will begin with a brief account of the history of electric and magnetic brain stimulation and proceed to the methods used here, with a focus on EEG-triggered TMS. I will provide an overview of the underlying physical principles, mechanisms of action and fields of application and explain the presumed physiological role of the μ rhythm, leading up to the hypotheses of the experiments described in this thesis.

Very early on, humans have established the connection between electricity and the workings of nerves and brain. Electric torpedo fish were applied to the scalp to treat headaches as early as the first century AD, representing a primitive form of transcutaneous electrical nerve stimulation for pain relief. In 1780 Italian physician Luigi Galvani, eponymous of the term 'galvanization', pioneered research in electrical neurostimulation: He elicited muscle contractions in frogs' legs with a primitive copper-iron battery [Galvani, 1792]. Only about 20 years later, his nephew Giovanni Aldini rushed onward to propose electrical brain stimulation as a cure for what was at the time termed *"melancholy madness"* [Parent, 2004][1]. Interestingly, the current applications of electric and magnetic brain stimulation in psychiatry are largely identical at least in indication (major depression), if not method, to Aldini's work [Hoy and Fitzgerald, 2010].

Speaking of 19th century scientific advances, in 1831, Michael Faraday famously converted magnetic forces into electricity, harnessing a phenomenon he called 'electromagnetic induction' and paving the way for magnetic brain stimulation techniques. However, research in magnetic neuronal stimulation lagged behind electrical stimulation for the first one and a half centuries: it was largely limited to eliciting so-called 'magnetophospenes', i.e., the sensation of seeing light caused by magnetic stimulation of the retina and/or the occipital cortex, effected by participants placing their heads in big magnetic coils, first described in 1896 by French physicist-physician D'Arsonval [Lövsund et al., 1980].
This changed when, in the years 1976 to 1985, a team around English engineer Anthony T. Barker developed the first transcranial magnetic stimulator and demonstrated a targeted stimulation of the primary motor cortex (M1) resulting in a contralateral hand twitch, visible as spikes in the electromyogram (EMG) recording [Horvath et al., 2011]. At first, use of TMS was largely limited to diagnostic purposes, e.g., measuring motor conduction times. TMS research did not really

[1] It deserves mentioning that Aldini's attempt at reviving a recently hanged criminal by applying copious amounts of electricity to the corpse, leading to 'life-like' muscular convulsions, reportedly inspired Mary Shelley's famous character of Dr. Frankenstein [Parent, 2004]

take off until the 1990s, when physicians and neuroscientists began to develop TMS 'protocols' for a wide range of applications [Horvath et al., 2011].

1.4 Foundations of TMS: Physicist's perspective

To examine the foundations of TMS necessary to understand the experiments described thereafter, let us take a look at TMS from the assumed perspectives of three different specialists involved with its application:
First off, the physicist or engineer, who is perhaps primarily interested in *how TMS actually induces an electric current* in the brain, and more specifically its temporal and spatial resolution as compared to other methods of brain stimulation.
Next up, the neuroscientist contributes their neuroanatomical knowledge to deduce *where* the induced current travels within and beyond the human cortex with its various interconnected regions and their distinct functions. They also examine *how the current travels*, studying the physiology of propagated excitation on a neuronal and synaptic level.
Lastly, the clinical physician will pipe in and explore *possibilities of application* in their treatment of patients with neurological or psychiatric disorders. This will eventually lead us to a synopsis of TMS protocols in use today.

TMS is in effect a double detour towards electric currents in the cortex through magnetic induction: According to Faraday's law, an electric field that changes in strength or changes its location relative to a conductor will induce a magnetic field perpendicular to the electric one - and vice versa. Now within a TMS stimulator, the electric current running through metal coils is rapidly ramped up and down – constituting the aforementioned change over time - and thus induces an equally fluctuating magnetic field which in turn induces an electric field in a conducting material close to the coil, e.g., in the cortex. The induced magnetic field of about $1 - 4$ Tesla in strength lasts about 0.25 to 1 ms and causes in turn an electric field in the brain, which evades exact quantification due to the complex anatomy of different intracranial compartments and the cortex itself, requiring modeling and estimation. The technical details are described elsewhere at length [Wagner et al., 2007, Wagner et al., 2009].

But why take this complicated path when there is simple electric stimulation available? Unlike transcranial electric stimulation, TMS is a painless method capable of directly eliciting action potentials (APs, cf. 1.5), leading to a temporally specific, strong activation of cortical neurons. The ensuing path of propagated neuronal signaling culminates in a contralateral muscle twitch, an easily observable and quantifiable output which is influenced by the state of excitability in the cortex.

Transcranial electric stimulation (tES, which preceded TMS by about 30 years [Gualtierotti and Paterson, 1954], can equally produce APs, but at current magnitudes whose application is limited to mapping during neurosurgery due to the strong activation of scalp pain receptors.
Different forms of low-current tES, which differ mainly in current patterns (namely direct current = tDCS, alternating current = tACS and random noise stimulation = tRNS) are used in a number of stimulation protocols which aim at effects both performance-enhancing and treatment-oriented in nature [Yavari et al., 2018]. This stimulation, however, produces only a shift in the electric potential of neurons, making them either less or more likely to fire spontaneously, depending on the direction of the current. The resulting modulation of excitability can last up to several hours, allowing for distinct applications, but it lacks the directness and high temporal resolution of TMS. The current induced by a monophasic TMS pulse lasts only about 200 μs, allowing for a *"highly synchronous activation of neurons"* [Siebner et al., 2009] and permitting a higher pulse frequency.

The spatial resolution of TMS has been overstated in the past due to the use of very basic or rather simplified head models to estimate the brain area where effective current densities are induced. The difficulty of setting a threshold over which a current is deemed strong enough to activate a brain area adds further uncertainty to any such prediction. Modern realistic modeling approaches estimate the cortical area of influence (defined as being subject to a current density over 90% of the maximum) to be around 100-200 mm^2 [Wagner et al., 2009], which is still sufficiently accurate to allow for an FDA-approved use in cortical motor and language mapping prior to neurosurgery [Picht et al., 2011]. The propagation of the resulting effect through complex excitatory and inhibitory pathways throughout the rest of the brain is a necessary collateral to natural intracerebral connectivity.

1.5 Foundations of TMS: Neuroscientist's perspective

Despite this intrinsic 'effusion of excitation', focused or, at the very least, preferential targeting of distinct brain areas is one of the intriguing advantages of TMS. Having acquired a basic understanding of the physics of TMS, we should now follow the current induced by the stimulator on its path through the brain and beyond, to eventually make predictions as to its effects. First, a quick look at the spread of current as applied in the experiments to be described: Here, the 'hand knob' area, i.e., the motor representation of the hand within the primary motor cortex (M1), is stimulated, resulting in a twitching of the contralateral hand, which has the benefit of being an easily observable and quantifiable output (M1 being

one of the so-called ‘eloquent’ cortical areas) as well as being influenced by the state of excitability in the cortex, allowing us to draw conclusions as to the latter.

1.5.1 From pulse to twitch

Let us precede the following remarks on the path from pulse to twitch by a quick review of how neurons code information with their characteristic switch from a quantitative code to a qualitative ‘yes or no’ one: Collected excitatory and inhibitory synaptic inputs at the dendritic level quantitatively shift the resting membrane potential, i.e., the about -70 mV ‘default’ intracellular charge of the neuron, into one or the other direction. In total, they add up to either an excitatory (relative depolarization, i.e., less negative/more positive charge, EPSP) or inhibitory (hyperpolarization, i.e., more negative intracellular charge) postsynaptic potential (IPSP). External sources of electric currents, such as a TMS pulse, will influence opening or closing of voltage-gated channels, equally contributing shifts in the intracellular electric potential. The collected excitatory and inhibitory inputs shift the intracellular electric potential either closer to or further from AP threshold. Any supra-threshold stimulus, that is depolarization, will elicit an AP, i.e., a fixed sequence of rapid changes in intracellular charge largely driven by the opening of voltage-gated sodium channels, of the same ‘standard’ intensity. An AP is therefore an all-or-nothing response, like flicking a light switch on, i.e., a qualitative way of coding information.

In M1-TMS, the magnetically induced electric field in the brain depolarizes superficial cortical neurons sufficiently to elicit an AP. The excitation then synaptically spreads to other cortical regions, from there to subcortical and finally peripheral neurons. On its journey towards these muscles, the pulse passes through the following sites: APs are evoked (either directly or via intracortical interneurons, depending on coil orientation and stimulus intensity [Di Lazzaro and Ziemann, 2013]) in corticospinal neurons, which have a monosynaptic connection to spinal motoneurons, where EPSPs sum up until AP threshold is reached. The AP will then get transferred unto the neuromuscular synapse and elicit APs in the muscle fibers, visible in the surface EMG as a compound muscle action potential (CMAP, the sum of the APs of many motor units), termed MEP (occurring ca. 15-20 ms after the TMS pulse [Darling et al., 2006]). The path of excitation is depicted in Figure 14 on page 44. This multisynaptic course of signal propagation illustrates that MEP amplitudes are not only affected by cortical, but also by spinal and neuromuscular excitability. Numerous methods have been devised to control for changes in spinal excitability, but exceed the scope of this thesis. [Di Lazzaro et al., 2004] provide a synopsis of some pertinent studies.

1.5.2 Factors influencing current propagation

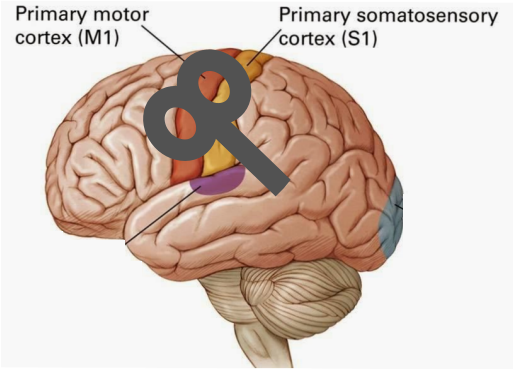

Figure 1: Figure-of-eight TMS coil in p.l.-a.m. position on motor hotspot, as seen from the side. Figure based on [Blausen.com staff, 2014].

In this particular pathway as in all TMS protocols, however, there are a vast number of factors to be taken into account that influence the path of the induced current, the magnitude and the nature of its impact. In the following section, the most important ones of those parameters will be divided into (i) properties of the stimulation, which are to some extent subject to the researcher's design, and (ii) properties of the stimulated brain:

(i) Influential properties of TMS stimulation

First, the shape of the coil directly impacts the shape of the induced electric field. With round coils, the maximum of field is set in a ring around the centre of the coil, ergo, there is no stimulation under the center of the coil. Figure-of-eight coils (also called double or butterfly coils) as used in the experiments described here consist of two adjacent round coils. The maximum of the electric field is located under the junction of the coils and, decisively, focused on a smaller area compared to round coils.

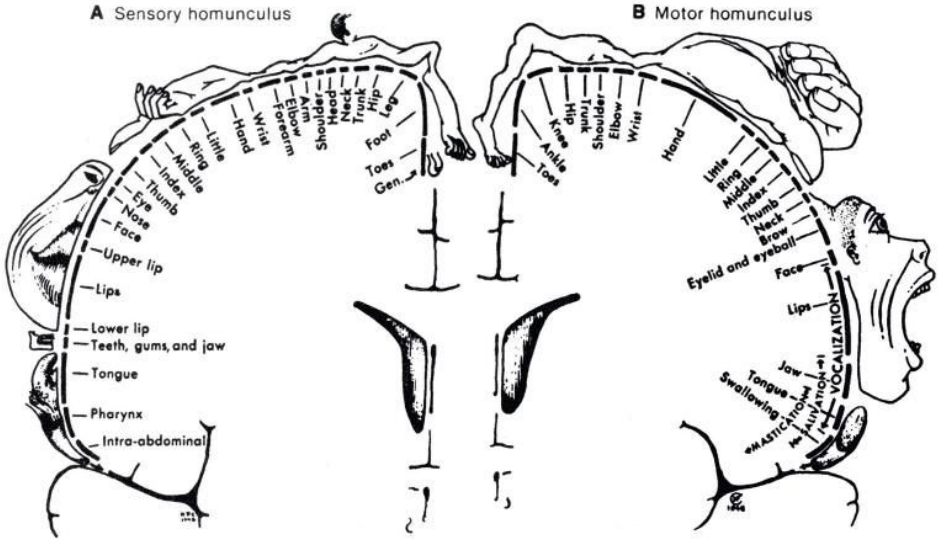

Figure 2: Canadian neurosurgeon Wilder Penfield was one of the first to perform systematic mapping, stimulating different parts of the primary sensory and motor cortex on the exposed cortex of his awake patients during epilepsy surgery. In 1951, he drew the results of his experiments in the form of a human body with the body parts distorted in size to represent the location and size of the corresponding brain areas and created the cortical 'homunculus', which continues to provide us with a vivid image of cortical anatomy, in this case specifically the easily accessible and 'outsized' motor hand representation. Figure adapted from [Penfield, 1950]

Second, every shift or tilt of coil position will result in an at least partially different set of neurons being preferentially stimulated. In motor cortex TMS protocols, the most commonly used coil positioning is posterolateral-to-anteromedial 45°, 'p.l.-a.m. 45°' (conventionally named after the direction of the current induced in the cortex), see Figure 1. This angle offers the lowest 'MEP threshold', i.e., elicits MEPs in the contralateral hand muscles at the lowest stimulation intensity [Mills et al., 1992]. The hand representation area of M1 is easily accessible to non-invasive stimulation both because of its size (cf. Figure 2) and prominent position on the lateral convexity of M1.

Within a certain coil shape and positioning, still the waveform of the TMS pulse exerts its influence through distribution of the induced current and response dynamics of (voltage-gated) ion channels in the neuronal membranes. Monophasic pulses, used here and depicted in Figure 3, are characterized by a strong directionality, as AP induction is largely effected by the fast initial increase of current (100 μs), the effect of the following slow (800 μs) decay of current being negligible due to its low speed (see above Faraday's Law). Monophasic pulses consume vast amounts of energy, as the energy of a pulse is not reused and thus completely transformed into heat. Consequently, only single pulses with a minimum inter-stimulus interval (ISI) of a couple of seconds are possible without overheating the coil.

In biphasic pulses, the induced current changes polarity in the course of the pulse. Here, up to 80% of the pulse energy returns to the capacitor and can be re-used for subsequent pulses. At low SIs, mainly the initial and steeper change in voltage takes effect, the reverse phase even counter-acting its effects and reducing efficiency, while at higher intensities, both current directions activate a distinct set of neurons each [Sommer et al., 2018].

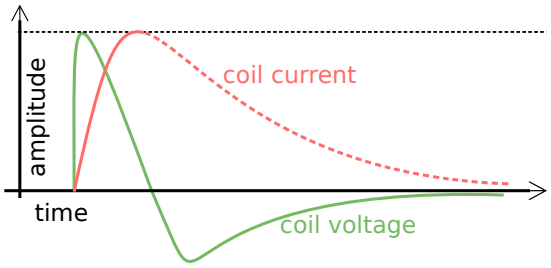

Figure 3: With monophasic pulses, the steep initial increase of current (continuous line) drives the stimulation effect

Perhaps most intuitively, the stimulation intensity also has a decisive influence on stimulation effects: SI is usually indicated in percent of MSO, i.e., maximum discharge voltage of the stimulator's capacitor. The discharge voltage is proportionate to the strength of the induced magnetic field and to the root of the energy of the pulse, according to basic physical capacitor laws. Without knowing the stimulator's maximum discharge voltage, SIs expressed in % MSO are therefore not directly comparable between different stimulator models.

In any case, SIs used in stimulation protocols of eloquent brain areas such as M1 are usually scaled to individual effect size: in this case, to the peak-to-peak amplitude of elicited MEPs (e.g., a mean size of 1 mV, or a percentage of the individual maximum MEP size – the latter requires measuring an individual input-output curve) or in relation to individual motor thresholds, namely

- Resting motor threshold (RMT): the SI at which 5 out of 10 pulses elicit an MEP of at least 0.05 mV peak-to-peak amplitude in the relaxed muscle
- Active motor threshold (AMT): the SI at which 5 out of 10 pulses elicit an MEP of at least 0.2 mV or at least 120% of background EMG amplitude in the tonically contracted muscle, usually at 10-20% of maximum isometric force

AMT is always lower than RMT: The intentional pre-activation of target muscles reduces both the threshold and the latency of MEPs because spinal motor neurons are already closer to AP threshold, requiring less incoming EPSPs to reach threshold. These motor effect references are often also used when stimulating 'non-eloquent' brain regions which lack a specific observable output.

(ii) Influential properties of the brain

While the aforementioned features of stimulation can be manipulated up to a point, the 'receiving end', namely the brain, also displays attributes to be taken into account when predicting TMS effects:

- the electrical conductivity of the tissues between the site of stimulation and the target area: The liquor cerebrospinalis possesses the highest conductivity, followed by the grey matter with the neuron somata and proximal axons and finally the white matter with the length of the axons contained. The conductivity of the pia mater, the layer of the meninges attached directly to the cortical surface, is still subject of discussion. When the pulse passes through regions of high conductivity, field strength is lost to those areas. An overview of conductivity studies is provided in [Koessler et al., 2017].
- the microanatomy of the stimulated cortex: The biggest change in membrane potential, i.e., the best chance of evoking an AP, is effected where cells bend relative to the direction of the induced electric field [Ilmoniemi et al., 1999]. Field strength furthermore decays with distance (see below). Length and orientation of axons impact the probability of AP induction by TMS. The complex folding of the human cortex into gyri and sulci means that the prevailing orientation of axons rotates with the curve of a gyrus and thus these neurons differ in their susceptibility to stimulation from a

certain position. Excitation may furthermore spread through a multitude of synapses. Consequently, predictions of which cells are affected by a TMS pulse are not easily made. The axons of different cortical cell layers make up different intracortical and corticospinal tracts. Even detailed computational TMS modelling ('in silico' stimulation) today still does not take fully into account axon morphology, differences in conductivity within one compartment ('anisotropic conductivity') and synaptic connections between the modeled cells.

- the distance from the site of stimulation: Like TES, TMS is limited in its areas of influence by the strong decay of current in the brain with distance from the site of stimulation – strong effects can only be expected in a depth of 2 – 3 cm [Deng et al., 2014]. With traditional coils, the current will have already decayed to 30% of its original strength at 4 cm distance from the scalp surface [Siebner et al., 2009]. Though some specialized coils for the targeting of brain areas 4 – 6 cm from the scalp have already been developed [Deng et al., 2014], focal deep brain stimulation nevertheless currently remains out of reach to NIBS techniques and a domain exclusive to neurosurgical DBS implants.

1.6 Foundations of TMS: Neurologist's perspective

Armed with knowledge about physical and neuroanatomical underpinnings and modification of stimulation parameters, let us take a fresh look at what we want to achieve.

1.6.1 Conceptual schema of TMS protocols

[Bergmann et al., 2016] have categorized TMS protocols first into those aiming at (i) 'online' effects, where results are measured during stimulation, and those aiming at (ii) 'offline' effects taking place after stimulation, see Figure 4.

(i) Online protocols can be further divided by effect into those aiming to quantify, interfere with or modulate the level or timing of neuronal activity.

- Quantify: Applying a (single) pulse and measuring the elicited changes in the EMG (MEPs) or EEG (TEPs)[2]
- Interfere: Using e.g. repetitive TMS (rTMS: pulses repeated at a frequency of usually 1 – 25 Hz) to set a so-called 'virtual lesion' by transiently disrupting a certain area's activity.

[2]TEPs = TMS-evoked EEG potentials: changes in EEG pattern directly affected by TMS pulses, investigated to assess cortical connectivity and physiology. TEPs are strongly intermingled with the sensory/auditory evoked potentials caused by the perception of the 'tap' and 'click' a TMS pulse generates [Conde et al., 2019], cf. 1.6.2.

- Modulate: through e.g. paired pulse protocols, where the first pulse influences the effect of the following one in an inhibitory or facilitatory manner depending on the time interval between the pulses. Pulses are either applied both over the same site or over opposite hemispheres or, in the case of afferent inhibition protocols (short-latency afferent inhibition = SAI and long-latency afferent-inhibition = LAI) a single pulse on M1 is preceded by contralateral electric peripheral nerve stimulation.

(ii) In offline protocols, the outcome is measured *after* stimulation. This is suitable for the observation of more gradual effects such as changes in synaptic strength, i.e., induction of plasticity. More on the principle of neuroplasticity and various protocols used to induce it will follow in 4.1.

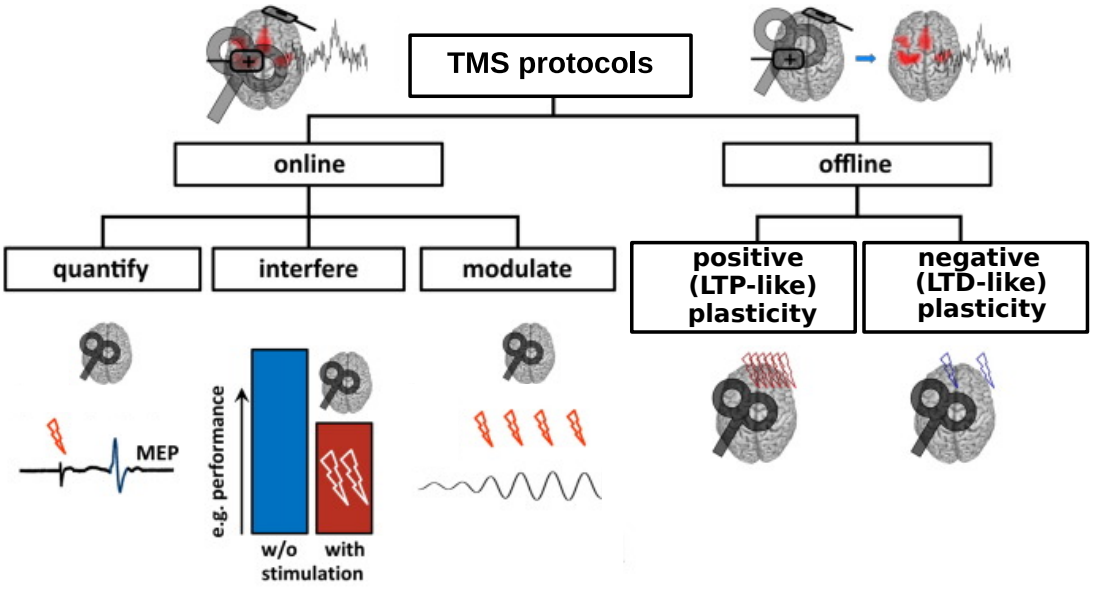

Figure 4: Conceptual schematic of TMS protocols. Figure adapted from [Bergmann et al., 2016]

1.6.2 Adverse Effects

While this wealth of possible applications is intriguing, the neurologist is a caring and seasoned clinician and routinely considers adverse effects as much as the desired ones. TMS is considered a very safe procedure with few side effects reported, which nonetheless deserve a closer look at this point:

A minor and self-limiting common side effect of TMS is a slight headache during or after stimulation. This could, however, plausibly be at least partially explained by the tight restriction in neck and head movement necessary to keep stimulus location constant (see 11.1) – no systematic investigations of headache as a side

effect of real or sham stimulation are known to this author. Another uncomfortable, but harmless effect reported on and observed during sessions are short twitches of scalp and facial muscles with every pulse, especially with higher SIs. While the former is due to direct stimulation of muscles, the latter is caused by stimulation of the Nervus facialis[3]. This can usually be easily avoided by a slight adjustment of coil position without compromising MEP effects. Due to the click emitted with every TMS pulse (explained by the Lorentz force) , increasing in volume with rising stimulation intensity, noise protection earplugs are recommended to avoid hearing damage.
Some rare cases of induced epileptic seizures without long-time effects have been reported, mostly when higher-frequency protocols such as rTMS were used. We consequently excluded subjects with an epileptic predisposition. Adverse effects among our participants will be reported in 3.5.1.

1.6.3 EEG-triggered TMS and EEG

Side effects are only one of many reasons why TMS protocols in general and offline ones in particular, like any treatment, should be effective and have predictable, powerful and durable effects with as little exposure as possible. It follows that the next issue to be tackled is how to make (offline) TMS protocols more efficient – by rendering them, as will be explained in the subsequent paragraphs, more specific to the individual brain. I will describe the method of EEG-triggered TMS and continue towards an introduction to EEG in general and the sensorimotor μ rhythm in particular.

Like other forms of non-invasive brain stimulation (NIBS), any effects which the relatively young field of TMS-based neuroscience has reported have always suffered from a large variability [Johnson et al., 2013], both between and within subjects, and poor replicability of results – a drawback which has been attributed to the disregard of stimulus timing to constantly changing brain states: Any area of the brain that we want to excite should ideally be at its most excitable at the time of stimulation. This idea has fuelled the development of a *closed-loop*, or rather *informed open-loop*, system in which the timing of stimulation is informed 'in real time' by fluctuating brain states. That is to say, TMS pulses are triggered by certain properties of the ongoing EEG measurement (see below in 1.6.3), such as are deemed to reflect brain states conducive to this protocol's aim. Section 2.3 contains a more detailed description of the EEG-triggered TMS system we used.

[3]The facial nerve is stimulated at the base of the skull due to electric vortex currents from under the coil spreading in the highly conductive liquor cerebrospinalis and the bunching of electrical density in the foramina because of the low conductivity of the surrounding bone. [Siebner and Ziemann, 2007]

A pre-determined TMS protocol is 'blind' to the state of the stimulated brain and thus constitutes an *open-loop* setup. *Informed open-loop* systems such as described here are informed by some of their output ('feedback' mechanism), but still require additional adjusting. In fully *closed-loop* systems, the output is integrated as input in a fully automated manner without external adjusting. For TMS, this output could be MEPs, TEPs, or a change in task performance. These data, acquired after every pulse, would in turn inform the stimulation parameters of the subsequent pulse such as SI, pulse pattern/frequency or coil placing. It can be argued that TMS already alters the EEG in such a way as to be a closed-loop system. For these experiments we are, however, assuming that the brain states that trigger magnetic pulses are ongoing and largely independent of prior stimuli, i.e., that we are observing an elicited output (EMG) without influencing the relevant input (EEG) by stimulation (see also [Bergmann, 2018]).
Where can we find information about brain states to identify targets for a TMS protocol? Since German psychiatrist Hans Berger recorded the first human electroencephalogram (EEG in 1924 [Berger, 1929], different frequencies of observed oscillations ('brain waves') have been categorized and investigated. Berger himself of course famously described occipital alpha oscillations and their response to visual stimuli (cf. section 1.6.4).
Before discussing the different EEG rhythms and their properties of power and phase, it is perhaps prudent to ask: What are we actually looking at when studying these electric waveforms measured on the surface of the skull? This signal is largely generated by groups of superficial cortical neurons displaying synchronized synaptic activity of a certain frequency. EPSPs (cf. 1.5.1) give rise to an electric dipole with a strong accumulation of extracellular negative charge. This charge shows up as a low point or trough in the EEG waves. The slower these waves, the stronger the synchronization of the changes in cellular charge between subsets of neurons. Akin to a code with less variation in symbols, less information is contained when the degree of synchronicity is higher. A simplified summary of the predominant EEG frequency increasing with rising alertness is shown below in Table 1.

The term *predominance* is key: Never do all neurons swing in the same frequency, any EEG signal is always a superposition of signals generated by subsets of neurons which keep distinct timings. Because there is never only one rhythm present, the intensity of a certain rhythm is quantified by a concept called 'power', a term used to describe the strength of a signal. The power of a rhythm is proportional to the squared amplitude of that oscillation over time. To represent the relative

power of a rhythm within a power spectrum, i.e., the contribution of a given frequency band to the overall power of the EEG signal, it is common to calculate the signal-to-noise ratio (SNR), i.e., the ratio of the power of the signal to the power of the 'noise' within a power spectrum of all oscillations contributing to the signal.

rhythm	frequency [Hz]	occurrence
Delta 	1–3	deep (non-REM) sleep
Theta 	4–7	drowsiness
Alpha 	8–14	relaxed awake state
Beta 	15–30	relaxed awake state, mental activity
Gamma 	30–100	active concentration, cognitive tasks

Table 1: Important EEG oscillations and when they occur preferentially

It is, however, a matter of definition where the signal ends and the noise begins: Researchers select a certain range of frequencies to be the subject of their attention and compare their power to an equally predefined band of adjacent frequencies of a chosen width. Depending on which frequencies are regarded as signal and how wide the band of noise is set, the 'noise' may thus be made up of neurons oscillating at other frequencies as much as it is made up of non-neuronal electric signals produced e.g. by contraction of scalp and jaw muscles. For a detailed explanation of how the power value of an EEG rhythm is calculated, refer to 3.3.

1.6.4 Alpha as Pulsed Inhibition

The Brain Networks and Plasticity (BNP) group in Tübingen, where the experiments summarized in this thesis have been conducted, focuses its research on the so-called μ rhythm, i.e., oscillations within the alpha frequency band (8-14 Hz) over the sensory and motor cortex. Strictly speaking, the term μ-rhythm encompasses also the beta frequency band (15-25 Hz) over the sensorimotor cortex, making it necessary to differentiate between μ-$alpha$ and μ-$beta$. For the purposes of this thesis, the term μ-rhythm shall refer to the 8-14 Hz range, i.e., μ-$alpha$, unless explicitly stated otherwise.

Why choose this particular rhythm? Experimental evidence points toward alpha oscillations in particular reflecting the delicate balance between excitation and

inhibition in the cortex, making this rhythm a measurable approximate for the states of brain excitability that we wish to target. In the following paragraphs, I will present some of the most important data supporting this hypothesis, will show where evidence is still missing and how our research fits into this gap.

Since Berger first characterized the now famous *Berger* or *alpha block effect* in the visual cortex, occipital alpha 'disappearing' or rather decreasing in power when eyes are opened [Berger, 1929], evidence has accumulated that establishes the alpha rhythm in several functional regions as having an active function rather than just reflecting 'cortical idling', i.e., cognitive inactivity. To wit, brain waves in the alpha frequency range have been implemented in selective neural processing driven by top-down control. Alpha is thought to focus cortical activity – in a spatial and temporal sense - and gate communication between areas by inhibiting currently irrelevant areas, excluding them both from activation and, consequently, from participation in interregional synaptic activity. [Klimesch et al., 2007] theorize that any temporary local reduction of alpha power represents a relinquishing of top-down (inhibitory) control over the area concerned, in order to allow it to be active and exercise its respective function. A strong alpha rhythm of high power occurs when a large number of neurons are oscillating in synchronicity, meaning only very large signals can stand out against this high level of noise [Mathewson et al., 2011]. As will be explained in the next paragraph, one can also state that during high alpha power, the net amount of inhibition is great.

Alpha waves seem to exert their top-down control by constraining the timing of neural firing in a rhythmic manner called 'pulsed inhibition': It assumes a generally inhibitory role with a maximum during the peaks [Klimesch et al., 2007, Jensen and Mazaheri, 2010, Mathewson et al., 2011] – thus, information about the extent of the inhibition effected by alpha oscillations can be found in both power and phase, as will be explained below. Several aspects can be regarded on how alpha effects this inhibition: The rhythm is thought to be generated by oscillating GABAergic interneurons which form inhibitory synapses with dendrites of pyramidal cells and induce synchronized periods of inhibition during the peaks [Mazaheri and Jensen, 2010]. The troughs[4] assume the role of *duty cycles*, allowing a window of heightened excitability. The heightened excitability during alpha troughs compared to peaks has been called 'phase effect' [VanRullen et al., 2011]. Regarded at the level of any single neuron, its probability of firing is subject to the dual influence of its intrinsic level of excitation and the strength of alpha

[4] also called 'negative peaks' by some authors. To avoid confusion, this thesis will reserve the term 'peaks' for the positive peaks

inhibiting it in a pulsed manner. It follows that neurons with a very high excitation level can override even higher levels of inhibition exercised by a strong alpha, and still fire rhythmically during the troughs - and vice versa during periods of low alpha power, even only slightly activated neurons will fire in the troughs, and very active neurons will even fire tonically [Klimesch et al., 2007]. Jensen and Mazaheri's theory of amplitude asymmetry [Mazaheri and Jensen, 2008] provides an intriguing synthesis of the concepts of power and phase: They propose that due to an asymmetric nature of alpha oscillations, only the alpha peaks are modulated in their amplitude by power, so that "the mean of the signal [over time is] biased by its magnitude" [Jensen and Mazaheri, 2010]. The less excitable peaks gain strength over the troughs when alpha power is high, shifting the balance towards relative inhibition. Conversely, during low alpha power the overall level of inhibition is so low that the difference in inhibition between peaks and troughs is hardly evident. While agreeing on the asymmetry of alpha, [Schalk, 2015]'s *function through biased oscillations* hypothesis argues for instantaneous amplitude of oscillations reflecting the degree of cortical excitability rather than a distinct function of peaks versus troughs.

Let us have a look at evidence supporting the pulsed inhibition hypothesis, with respect both to power and to phase, including observations of concurrence and of function. Starting with the visual cortex, where alpha oscillations have first been observed, then continuing to the μ rhythm, i.e., alpha frequency waves over the sensorimotor cortex. μ rhythm studies are further divided into those examining the sensory cortex (using attentional or tactile perception tasks) and those examining the motor cortex. The latter are thus direct 'predecessors' of the experiments we performed. Due to the focus of this thesis, the emphasis will lie on works using TMS stimulation over correlational evidence.

1.6.5 Alpha in the visual cortex

Researchers studying alpha in the occipital visual cortex, both with and without TMS, seem to conclusively report an inhibitory role of alpha power, with occipital alpha power decreasing during visual attention tasks [Thut et al., 2006, Herring et al., 2015] and detection rates of visual stimuli higher during periods of low alpha [Thut et al., 2006, van Dijk et al., 2008]. Whether this relationship between alpha power and excitability is linear is not clear, however, as most studies only compare low versus high alpha power in a relative manner or observe changes in this power. Only [Mathewson et al., 2009] reported a negative linear slope over four power quartiles.

As to the role of alpha phase, the same authors ([Mathewson et al., 2009]) found a decisive influence of phase on visual stimulus detection, and [Dugué et al., 2011] found a correlation with alpha phase on the probability of phosphene perception upon occipital TMS. Both of these studies however point to a lower perception rate when stimulus (presentation) coincided with an alpha trough. [Valera et al., 1981] reported a higher accuracy in stimulus detection at alpha troughs than peaks, but have not been able to replicate this effect in a later experiment [Gho and Valera, 1988]. [Osipova et al., 2008] describe a *phase-amplitude coupling* between posterior alpha phase and gamma activity, i.e., a temporary increase in gamma power for the duration of the alpha trough, providing evidence for the presumed *duty cycle* function of alpha troughs: Gamma oscillations are, as mentioned above in Table 1, associated with a more active brain state.

1.6.6 Alpha in the sensory cortex

Evidence collected so far points towards the sensorimotor μ rhythm being similar to visual alpha not only in frequency, but also in gating function. Akin to the visual cortex, shifts of attention as necessitated by tactile detection tasks seem to result in a weakening, i.e., decrease in power, of μ oscillations over task-relevant areas, accompanied by a simultaneous increase in power over task-irrelevant areas [Jones et al., 2010, Anderson and Ding, 2011]. Likewise mirroring occipital alpha, low sensory μ power has been associated with improved performance in a variety of detection and cognitive tasks [Jones et al., 2010]. In line with these findings, fMRI-BOLD studies have reported a reduced cortical perfusion with rising μ power at rest [Ritter et al., 2009, Laufs et al., 2003]. An exhaustive overview of pertinent studies can be found in the [Mathewson et al., 2011] review. If we agree to use perceptual threshold/performance in tactile detection tasks as a measure of somatosensory cortex excitability, we now know that lower μ power has been linked to higher detection rates, i.e., higher excitability. These data are however not sufficient to derive a linear-negative relationship between somatosensory cortical μ power and excitability. To obtain the precise nature of this relation, the slope of the curve, it is necessary to divide μ power into more conditions than just 'high' versus 'low'. Experiments doing just that have resulted in varied and apparently contradictory findings, with some studies reporting a negative linear (the lower the power, the better the performance) relationship [Jones et al., 2010, Schubert et al., 2009], but numerous other experiments suggesting an *inverted U* slope (best performance at medium μ powers, detection rates declining towards both ends of the power spectrum, cf. Figure 5). [Linkenkaer-Hansen et al., 2004, Ai and Ro, 2014, Zhang and Ding, 2010].

This *inverted U* relationship between μ activity and detection rates, which at first sight challenges the gating-by-inhibition hypothesis, has been explained with the Yerkes-Dodson law, which states that performance in complex tasks is at its optimum not during the highest, but medium levels of arousal [Yerkes et al., 1968]. [Rajagovindan and Ding, 2011] theorized that the *inverted U* is the derivative of the sigmoidal function which represents the neuronal firing rate in dependence of alpha power, inferring that sensory detection task performance depends on the speed of increase in firing rate. [Linkenkaer-Hansen et al., 2004] related the rising flank of the inverted U to the 'stochastic resonance' theory: In non-linear systems, a small amount of noise can improve the SNR by priming a sensory system or activating specific stimulus representations. Depletion of neurotransmitter vesicles in excitatory synapses and/or activation of a subset of surrounding GABAergic interneurons could be the explanation behind the falling flank of the U, as suggested by [Zhang and Ding, 2010]. On a cellular level, although performance in a tactile discrimination task improved slightly with decreasing μ power, neuronal firing rate in monkey S1 showed a type of 'upright-U' curve with minimum at medium power levels and maximum at high levels [Haegens et al., 2011].

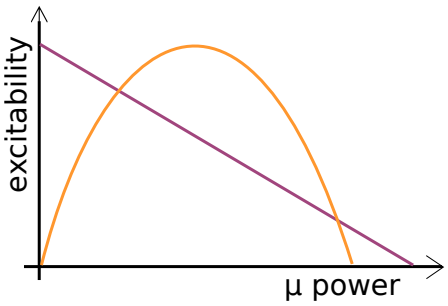

Figure 5: In the sensory cortex, different studies have either found a linear-negative (purple) or *inverted U* (orange) slope between μ power and excitability.

[Ai and Ro, 2014] also noted an effect of μ phase on tactile perception (trough > peak) for high μ powers and a trend for lower powers, which they explain as the high detection rate at optimal medium μ powers in the inverted U slope they found 'overriding' any difference in excitability between phases. In the same study mentioned before, firing rate in primate sensory increased during μ troughs compared to peaks [Haegens et al., 2011].

1.6.7 Alpha in the motor cortex:

While the effect of the power of the alpha rhythm in the visual cortex is well documented and data from tactile detection and attention tasks are copious, if contradictory, the analogous question for the motor cortex is a more recently approached problem. Motor cortex or rather corticospinal excitability (CSE) (cf. 1.5.1) can be comparatively easily measured in MEP amplitudes. At the time of conception of the experiments described here, studies investigating MEP amplitude in relation to pre-stimulus μ power had either shown lower amplitudes for higher power [Sauseng et al., 2009, Zarkowski et al., 2006], indicating an

inhibitory role of μ, or had not found a significant correlation at all [Maeki and Ilmoniemi, 2010, Berger et al., 2014, Iscan et al., 2016]. All of these works stimulated in an open-loop, uninformed manner and either simply searched for correlation, or sorted trials post-hoc into two 'bins' comparing small versus big MEP amplitudes – thus [Sauseng et al., 2009, Zarkowski et al., 2006]'s results are certainly reconcilable with, but in no way proof of, a linear-negative relationship between μ power and CSE. Returning to the often-cited primate study [Haegens et al., 2011], firing rate seemed to linearly decrease with rising μ power over M1 – only to increase again in the highest of five power bins.

Finally examining data on the impact of μ phase in motor cortex, [Yanagisawa et al., 2012] found a cross-frequency phase-amplitude coupling with pronounced gamma activity during μ troughs in intracranial electrocorticographic (ECoG) recordings[5]. [Triesch et al., 2015] reported a modulation of MEP amplitude by μ phase angle, with biggest MEPs achieved by stimulating at μ troughs. Like in the sensory cortical areas they studied, firing rates during μ troughs exceeded those during peaks in monkey M1 [Haegens et al., 2011].

1.6.8 Objectives of the experiments:

With the information of the preceding section in mind, let us reiterate the objectives of the experiments performed for this thesis: We strove to improve the reliability and effect size of a TMS protocol inducing positive plasticity by applying stimulation during brain states of high corticospinal excitability, as indexed by phase and power of the sensorimotor μ rhythm.

Our hypothesis in this approach was that states of high excitability are also states of high malleability, i.e., favoring induction of plasticity. Specifically, we expected an increased positive plasticity effect after a paired associative stimulation (PAS) intervention (more on this protocol in 4.1) triggered by μ troughs than after one triggered by μ peaks, thus an extension of the phase effect on excitability to the induction of positive plasticity. This main experiment was dubbed MUPAS (MU-rhythm and Paired Associative Stimulation).

In light of the particularly conflicting previous evidence regarding the function of μ power for CSE, we thought it advisable to first examine the direction and nature of the relation between pre-stimulation μ power and motor excitability in an EEG-triggered TMS setup including a systematic definition of power bins within an individual's power spectrum. Per our hypothesis, we anticipated a negative-linear correlation between μ power and MEP amplitude, i.e., the smallest MEPs

[5] Fascinatingly, they observed consistently high gamma during motor task execution, and rhythmic bursts of gamma entrained to μ troughs during a hold period > 2 s prior.

at the highest μ power, in line with the pulsed-inhibition theory. Following the schematic described above, MUPEX (MU-rhythm Power and motor EXcitability) would be classified as an online quantifying paradigm, and its results informed condition design for the main experiment.

2 Methods

The general methods and techniques employed in both experiments are described in the ensuing section. Divergent settings, methods only used in one of the experiments and other pertinent details will be specified in the respective experiment's methods subsections.

2.1 Participants

The study protocol conformed to the Declaration of Helsinki and was approved by the ethics committee of the University Hospital Tübingen (project number 144/2017BO1). All subjects completed a TMS-safety and, for MUPAS, also a MRI-safety questionnaire prior to being stimulated for the first time. They reported being in good health overall, having no history of neurological or psychiatric disease, and not having taken part in any experiments involving brain stimulation for at least 3 days prior to any session. To avoid any confounding by possible differences in excitability and plasticity between the dominant and non-dominant hemisphere, we included only subjects who were right-handed according to the Simplified Edinburgh Handedness Inventory [Oldfield, 1971] and stimulated only their dominant left hemisphere.

Subjects were recruited based on a strong μ power peak and a low motor threshold. More precisely, *inclusion criteria* were:

(i) a clear peaking of power in the μ frequency band (between 8 and 14 Hz) compared to other frequencies. The experimenter visually assessed the peak to have an amplitude of at least twice the background 1/f noise in the individual power spectrum (see Panel (1) in Figure 18 on page 52), which was estimated by a 3 s window Hanning tapered Fast Fourier Transform (FFT) from a 3-min eyes-open resting-state EEG which initiated each session. A 512 ms Hanning-windowed FFT was employed to extract the individual μ peak frequency. This criterion ensured a sufficient signal-to-noise ratio as inherent prerequisite for an adequate accuracy of the real-time power and phase targeting.

(ii) a 1 mV MEP threshold (MEP1mV) $\leq$ 80% MSO for APB (MUPAS) or either

FDI or APB (MUPEX) to enable sufficiently long stimulation periods without overheating of the TMS coil.

Additional criteria adopted for MUPAS will be described in section 4.2.

2.2 Recording and Stimulation

EEG: We used 64-channel EEG caps (EasyCap GmbH, Germany) with TMS-compatible Ag/AgCl sintered ring electrodes in the international 10-20 arrangement.

EMG: 2-channel surface EMG was recorded from the relaxed right abductor pollicis brevis (APB) and first dorsal interosseus (FDI) muscles in a standard belly-tendon montage.

EMG and EEG were recorded in DC mode with a 1000 Hz low-pass filter (for anti-aliasing purposes) and then digitized at 5000 Hz with a TMS-compatible amplifier (NeurOne Tesla with Digital Out Option, Bittium, Finland).

TMS: For the experiments presented in this thesis, only the hand area of the primary motor cortex (hereafter referred to as M1) was stimulated. TMS was applied with a 70 mm figure-of-eight coil, which was connected through a 4-into-1-module (Magstim, UK) to two Magstim 200^2 stimulators, to enable inter-trial intervals (ITI) below 4 s (recharge time). Coil position was *p.l.-a.m. 45°* over left M1 (see Figure 1), thus monophasic stimuli induced a posterolateral-to-anteromedial current in the brain. Coil placement was further adjusted from this position to elicit the biggest MEPs in the APB (for MUPEX: or FDI) muscle, and then maintained using neuronavigation (for details see 2.4). To inform stimulus intensity, individual resting motor threshold (RMT) and 1mV-MEP threshold (MEP1mV: SI eliciting an MEP with an average peak-to-peak amplitude of 1 mV) were determined using fully automated thresholding with a Simple Adaptive Parameter Estimation by Sequential Testing (SA-PEST) [Awiszus, 2003] integrated in the real-time system (described below in 2.3): SI of the next pulse was adjusted depending on the last MEP amplitude so that a fluctuating equilibrium was reached, where 50% of MEPs were smaller and 50% bigger than the target value of 0.05 mV for RMT and 1 mV for MEP1mV.

2.3 Real-time EEG-triggered TMS

In order to accurately target the different phases of the ~10 Hz μ rhythm, very fast processing of real-time EEG data, extrapolation of these data to predict the course of the oscillations and most of all triggering of the pulse with a reason-

ably short time lag is of essence. The Simulink-based 'Real-Time' system [Zrenner et al., 2018] triggers stimulators to deliver TMS pulses when certain predetermined EEG criteria are predicted to be met according to an extrapolation of EEG data acquired shortly before. To achieve this, the system processes the EEG and EMG data from a NeurOne amplifier, down-sampling it from that amplifier's sample rate of 5 kHz to 1 kHz and extracting data using the C3 Hjorth spatial filter, i.e., the EEG signal from the C3 electrode minus the mean of the signals from the diagonally adjacent electrodes: *C3 – mean (CP1, CP5, FC1, FC5)* [Hjorth, 1975], cf. Figure 6. This is a commonly used montage when extracting EEG data originating from left sensorimotor cortex. The real-time system was controlled by a custom-made Matlab script and achieved an overall technical delay of about 3ms, which is composed of conduction times in the cables, processing in the real-time system and a trigger-to-pulse delay within the stimulator. This delay was taken into account by the system to time triggers accordingly.

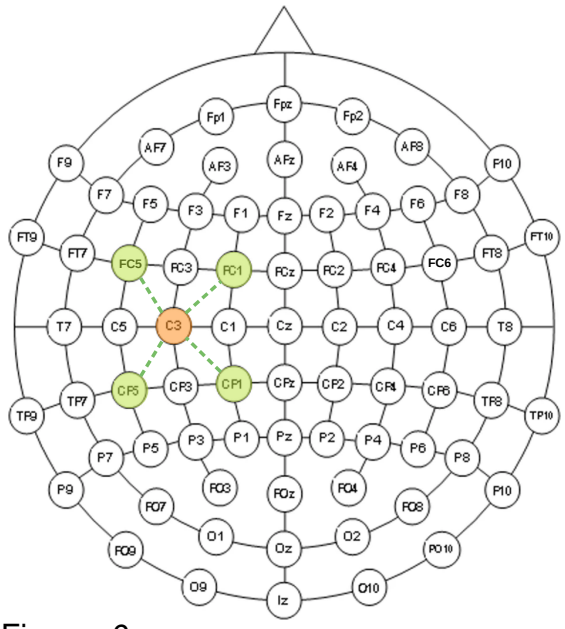

Figure 6: The C3 Hjorth montage marked on a schematic 64-electrode setup: the mean of the signals from the electrodes CP1, CP5, FC1 and FC5 (light green) is subtracted from the signal of the central electrode C3 (orange). Figure adapted from Fig. 5 in [Das et al., 2019]

Power targeting: The individual μ frequency bin (as determined from the 3 min resting-state EEG at the beginning of each session) was extracted from a continuously updated ('sliding') Hanning-windowed FFT of the last 512 ms of data. A sliding distribution of μ power values from the last 60 s of clean data (the 1.5 s after a TMS pulse were excluded to avoid the stimulation artifact) was updated every 10 ms to account for drifts in μ power over time. The real-time system then compared the current μ power value to the target bin of the ongoing trial, and triggered a TMS pulse if the power matched the correct bin. Additional methods applied only for MUPAS, namely electric peripheral nerve stimulation, magnetic-resonance imaging and real-time phase targeting, will be described in 4.2.

2.4 Neuronavigation

We used the frameless stereotactic neuronavigation system 'TMS-Navigator (Localite GmbH, Germany)', similar to those utilized in targeted neurosurgery, to register hotspot location and thus aid the experimenter in maintaining coil position

throughout a session (and in replicating it across the sessions of a participant in MUPAS). The system's navigation capabilities depend on an infrared camera that detects the position of 'trackers', i.e. reflectors for infrared light, relative to each other. One of those 'trackers' each is fixed to the subject's head, the coil and a pointer. Prior to the hotspot search, the latter is used to co-register landmarks on the subject's head to either

(i) for MUPEX and MUPAS screening: the three dimensional standard brain template, in essence an average of numerous MRI scans of healthy brains. It is named 'Montréal Neurological Institute' (MNI) for its place of creation.

(ii) for MUPAS main sessions: the 3D reconstruction of the subject's individual T1-weighted MRI scan.

Additionally for MUPAS, the position of all 64 electrodes was registered to make the EEG data recorded during the sessions available for future source-space reconstruction projects of the research group.

2.5 Statistical methods

Statistical analyses were performed with Matlab and the open-source statistics software JASP. Level of significance was set as $p \leq 0.05$ for all tests. Descriptive data are given as mean $\pm$ standard deviation. The following information about *significant* test results used will be provided in the relevant sections:

- Repeated measures Analyses of Variance (rmANOVAs):
  - F value$_{\text{degrees of freedom of numerator, and denominator}}$
  - p value

  We used the Greenhouse-Geisser adjustment to correct for violations of sphericity where necessary.
- Post-hoc student's t-tests:
  - t value$_{\text{degrees of freedom}}$
  - p value
- Correlations:
  - correlation coefficient r
  - t and p value of t-tests for correlation

3 Experiment: MUPEX

3.1 MUPEX. Introduction

In light of the varying results in previous studies linking motor excitability to M1 μ power, which have already been described in 1.6.7, the aim of the MUPEX experiments was to systematically examine the relation of μ power with motor excitability using real-time EEG-triggered stimulation, and thus to inform the design of MUPAS conditions. We evoked MEPs with μ-power-triggered spTMS of M1, and the target muscle was FDI (in 14 participants) or APB (in 2) depending on the best individual hotspot found. The dependent variable was MEP amplitude, the independent variable was pre-stimulation μ power. Trials were triggered by one of ten decile power bins dividing the individual μ power spectrum (1-10% trough 91-100%) in a pseudorandomly intermingled order. The power spectrum was repeatedly (every 10 ms) updated based on the last 60 s of clean EEG data (cf. 2.3). Our alternative hypothesis (H_1) was that CSE would significantly correlate with μ power. We specifically expected a negative linear correlation, with the biggest MEPs elicited during periods of lowest power, in line with the gating-by-inhibition hypothesis and previous motor cortex studies, rather than the inverted U slope sometimes found for detection rates of near-threshold sensory stimuli. The null hypothesis (H_0) stated that there is no correlation between μ power and MEP amplitude.

3.2 MUPEX. Session Design

Each participant underwent one session which was made up of 4 blocks, containing 250 trials, with short breaks between blocks for coil cooling (Figure 7).

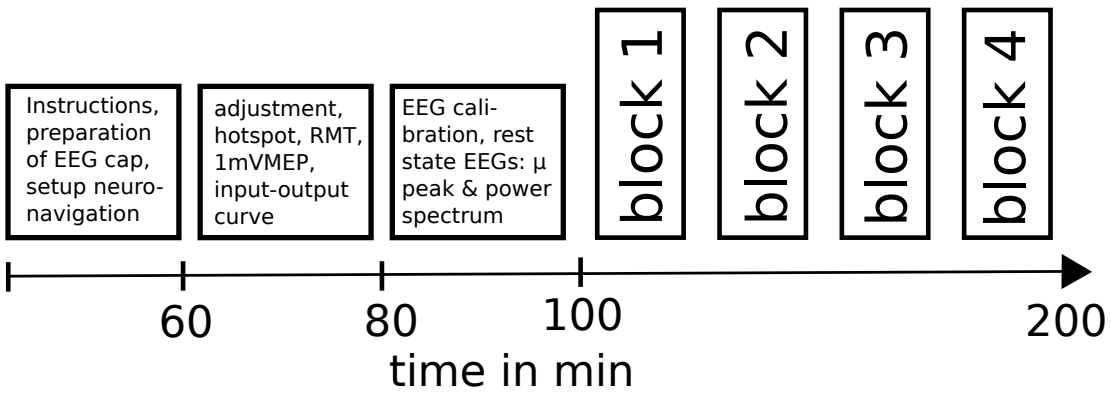

Figure 7: Schematic of MUPEX session design, timeline not to scale. Each of the 4 blocks contained 25 trials per power decile, adding up to 250 trials per block. Breaks between blocks were necessary to cool the coil.

The real-time system triggered a TMS pulse when

(i) a minimum ITI of 3 s had elapsed since the last pulse (to keep analyzed EEG periods free of stimulation artifacts, not to affect power estimation), *and*

(ii) current μ power over C3 Hjorth was within the decile bin selected for the next trial by a pseudorandomization algorithm. Each bin was targeted 25 times per block, thus 100 trials per power condition were recorded.

Stimulation intensity was set to elicit half of the maximum MEP amplitude as obtained from an individual input-output curve (IOC), testing SIs from 35% to 90% of MSO in 5% steps). 50% IOC SI was chosen as the steepest slope within the sigmoid IOC (cf. Figure 8) to make even small changes in excitability visible – as necessitated by the small power bin size compared to similar experiments. We had participants wear standard noise-protection earplugs during IOC stimulation to avoid hearing damage because of the high SIs used (cf. 1.6.2).

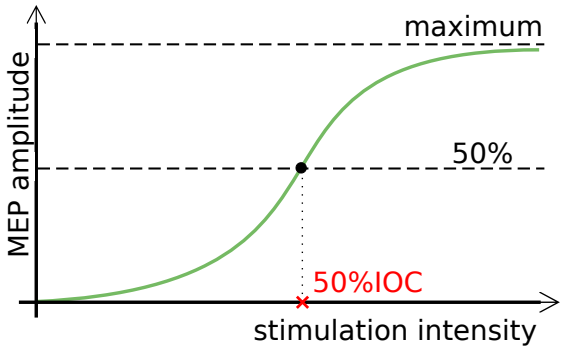

Figure 8: Illustration of input-output curve (IOC) with typical sigmoid shape, with SI = 50%IOC marked (red cross)

3.3 MUPEX. Data analysis

ITI stratification: There was a significant asymmetry in ITI distribution across power bins, with accumulation of longer ITIs in the 'marginal' power bins ($F_{9,135} = 11.8$, $p < 0.0001$). As ITI length is a known confounder for MEP amplitude [Vaseghi et al., 2015] (compare 3.5.2), we iteratively rejected the trial with the longest ITI from the bin with the longest average ITI until obtaining a significance level of $p \geq 0.2$ from the rmANOVA for ITI across conditions.

MEP amplitudes: MEP peak-to-peak amplitudes were normalized block-wise as percentage change from block average (across all power bins), and then averaged across blocks in order to account for slow changes in corticospinal excitability over time. A one-factorial repeated-measures ANOVA of the ten power bins was used to test differences in normalized MEP amplitude between bins. Pairs of neighboring bins were compared with post-hoc two-sided paired t-tests. Regression lines were individually fitted for each subject's MEP amplitudes per power bin, and their slopes (beta values) then tested for consistency across subjects with a two-sided one-sample t-test against zero.

EEG pre-processing: Post-hoc offline EEG analyses served only to validate the targeting of the correct power values by the EEG-triggered real-time system and thus the validity of the bins. Using the FieldTrip toolbox for Matlab [Oostenveld et al., 2011] and custom Matlab code, EEG data were segmented relative to TMS (-1000 to -20 ms), re-referenced to the common average of all EEG electrodes and zero-padded 1 second into the post-TMS interval to avoid corruption of power estimates by stimulation artifacts and TMS-evoked EEG potentials (TEPs). Time-frequency representations (TFR, cf. 12) were extracted by moving a sliding window (length of 3 cycles of the respective frequency) over the 500ms pre-TMS EEG data within a frequency range of 1 - 35Hz, performing a Hanning-windowed FFT every time. For time points close to time '0', i.e., the TMS pulse, the window necessarily included the TMS pulse and post-TMS interval, both of which were set to zero. For calculation of absolute pre-TMS μ power values (Figure 10), Hanning-windowed FFTs of 512 ms pre-TMS were performed and zero-padded to 1s to achieve a 1Hz resolution. Trials with EMG pre-innervation (> 50 μV baseline amplitude in EMG) or EEG artifacts (z-normalized signal in C3 Hjorth > 5 SDs) were rejected. Eye movements and muscle noise were identified and removed using independent component analysis (ICA), which identifies those artifacts based on their topography among electrodes, temporal profile within and across trials, and spectral profile. The temporal specificity of transient μ-$alpha$ power fluctuations was shown by calculating z-normalized time-frequency representations (TFRs) of the 0.5 s pre-TMS. The topographical distribution of pre-TMS μ-power (-300 to -100 ms before stimulation, z-normalized across power bins) between all electrodes was plotted.

3.4 MUPEX. Results

Participants: N = 18 participants were tested, 13 of whom had previously taken part in EEG-TMS experiment of the same research group. N = 2 of those (both individuals 'native' to EEG-TMS) could not complete measurements and thus did not enter analysis.

One of the exclusions was due to a MEP1mV threshold exceeding 80% MSO, the other candidate had to be excluded because we could not identify a single motor hotspot with consistent MEP amplitudes. The data of the remaining N = 16 subjects were analyzed.

The average age was 25.3 $\pm$ 3.6 years (ranging from 20 – 32 years), 12 participants were female.

Descriptive data: Individual μ peak frequency as determined before from the initial 3 min eyes-open resting-state EEG was 11.4 $\pm$ 0.9 Hz (10-13 Hz).
Mean RMT was 46.2 $\pm$ 7.3% MSO (range 37-59), 1mVMEPT was 55.8 $\pm$ 10.5% MSO (41-76 range) and thus on average 120% $\pm$ 8% of individual RMT. The 50% of individual IOC was on average 57.9 $\pm$ 11.4% MSO (range of 44-76% MSO), a mean 123% $\pm$ 10% of individual RMT. Values for 50% IOC and MEP1mV were thus quite similar: On average 50% IOC exceeded individual MEP1mV by 1.43% MSO $\pm$ 4.16. Per-subject differences ranged from 50% IOC exceeding MEP1mV by 9% MSO to MEP1mV exceeding 50% IOC by 5% MSO. In 5 out of 14 subjects, 50% IOC was lower than MEP1mV, showcasing inter-individual variance in maximal MEP amplitude. Two participants could not complete the IOC curve for technical reasons and reasons of personal comfort, respectively, and were stimulated with an SI of their individual MEP1mV instead. The values listed here are thus from the remaining 14 participants.
Session duration was 252.8 $\pm$ 40.7 min. One block lasted on average 20.5 $\pm$ 1.9 min, breaks lasted 9.5 $\pm$ 5.3 min.

ITI variability: Despite addressing this issue both in experiment design by implementing a sliding continuous power spectrum update and in post-hoc data cleaning (cf. 3.3), ITIs showed a considerable variability throughout the measurements. Before stratification, ITI across conditions was on average 4.7 $\pm$ 0.99 s. ITIs were shortest in the 41-50% power bin (towards the middle of the spectrum), 3.95 s on average. The 'extreme' power bins contained the highest average ITIs, with the 91-100% bin (7.33 s) exceeding the 1-10% bin (5.20 s). Power values 'passing through' medium values during spontaneous power fluctuations in both directions, i.e., periods of falling and rising power, could explain the tendency for shorter ITIs in the medium power bins.
Post-stratification, the average ITI across conditions was 3.8 $\pm$ 0.03 s, thus considerably shorter. The 41-50% bin again had the shortest overall ITIs of 3.79 s, but the differences to the 1-10% bin with 3.88 s and the 91-100% bin with 3.85 s were markedly reduced.

MEP amplitudes: Single-trial correlations were calculated per subject between pre-TMS μ-$alpha$ / μ-$beta$ power and MEP amplitude. The influence of the respective other frequency was controlled for by using partial correlations. These subject-wise correlation values were then tested with two-sided one-sample t-tests against zero for consistency across subjects. MEP amplitude was significantly dependent on pre-stimulus μ power bin (ANOVA: $F_{9,135} = 2.67$, $p = 0.007$),

but the differences in MEP amplitudes between directly adjacent power bins did not reach significance (all t-tests p > 0.05). Regression lines fitted subject-wise across all power-bins showed on average a positive linear slope (two-sided one-sample t-test against zero: t_{15} = 2.20, p < 0.05), i.e., increasing MEP amplitude with rising μ power (cf. Figure 9). This relationship with MEP amplitude was dependent on the 91-100% power bin and on ITI stratification in both analyses. Without either of these factors, p-values exceeded 0.1. It becomes evident from Table 2 that even after ITI stratification, the significant correlation between instantaneous μ power and MEP amplitude was still contingent on the per-subject block-wise normalization (cf. 3.3). The interindividual difference in MEP amplitude at 50%IOC and the variability of MEP size over time (between blocks within one subject) exceeds the extent of the influence of instantaneous μ power by far. This is illustrated by the almost identical absolute MEP amplitudes as averaged across participants across all power bins (row 1, Table 2).

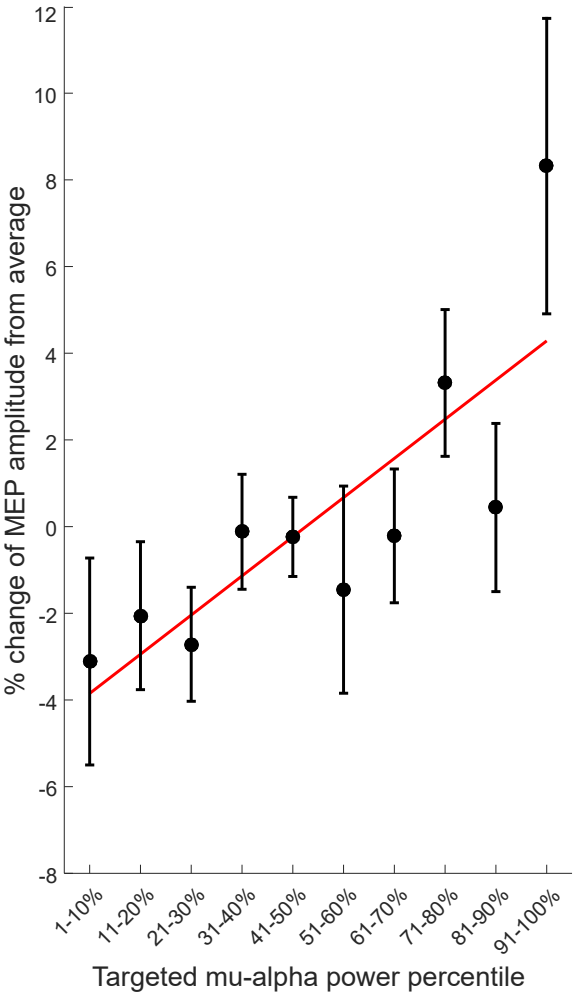

Figure 9: Positive linear regression line between μ power bin and normalized MEP amplitude. Black dots indicate group average of normalized MEP amplitudes, which were first normalized subjectwise to deviation from block averages and then averaged over blocks. Whiskers indicate ± standard error of the estimate. Figure from [Thies et al., 2018].

μ-$alpha$ versus μ-$beta$. Pre-TMS μ-$alpha$ (8-14 Hz) and μ-$beta$ (15-25 Hz) power were positively correlated with each other across trials (r_{avg} = 0.28, t_{15} = 7.44, p < 0.00001). The weak positive correlation of MEP amplitude with pre-stimulation power was only significant for μ-$alpha$ (r_{avg} = 0.05, t_{15} = 2.44, p = 0.028), but not μ-$beta$ (r_{avg} = 0.02, t_{15} = 1.60, p = 0.13).

Power targeting: Offline power analyses confirmed accurate targeting of μ power bins ($F_{9,135}$ = 748.0, p < 0.00001). Individual μ power values were significantly different between all power bins (all paired t-tests p < 0.000001; see figures 10

and 11). Temporal and topographical specificity was given: The real-time system had targeted a transient, locally specific power peak without contamination by occipital alpha, as shown in Figure 12.

These results were published in 2018 in *Brain Stimulation* [Thies et al., 2018].

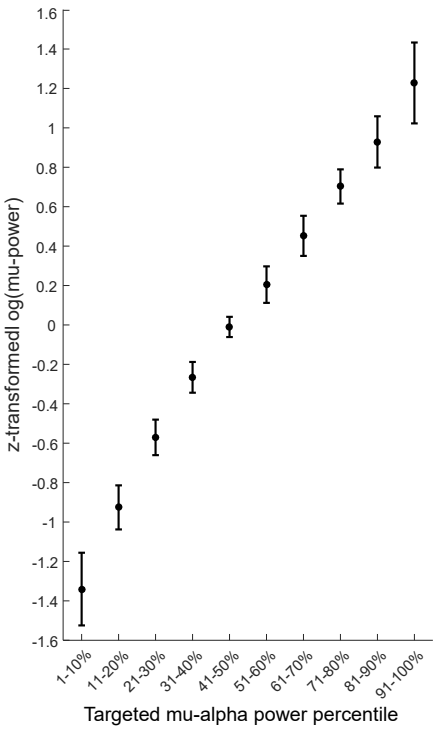

Figure 10: Dots = average z-normalized μ-power values 512ms pre-TMS for all power bins, calculated post-hoc. Whiskers = $\pm$ standard error of the estimate. Figure from [Thies et al., 2018].

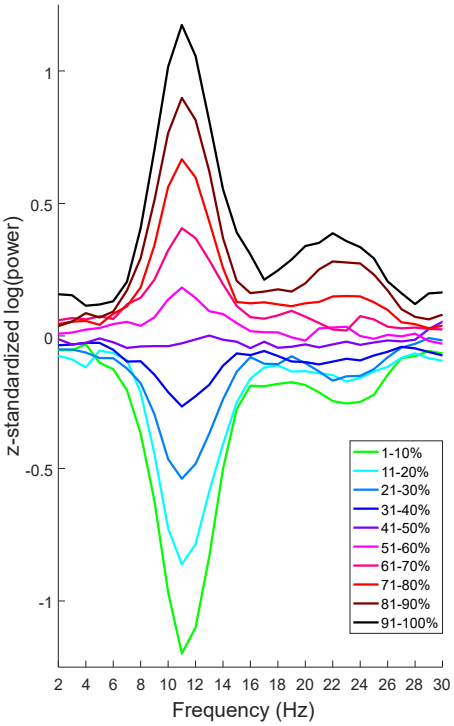

Figure 11: average z-normalized FFT power spectrum shows a parallel, but weaker modulation also of μ-$beta$ power between bins. The apparently weaker/nonexistent modulation in the medium bins results from the z-normalization. Figure from [Thies et al., 2018].

3.5 MUPEX. Discussion

This section contains a report of adverse effects among our participants, an interpretation of the results obtained in MUPEX, a comparison to those of similar experiments and a critical look at how this relates to the underlying hypotheses. Suggestions for future research, if and as far as they pertain to open questions and shortcomings of our experiments, will be included in the relevant sections.

3.5.1 Reported adverse effects

In the 144 stimulation sessions performed for the experiments described, only one case of post-stimulation headache and two cases of lightheadedness were reported to us by subjects:

1-10%	11-20%	21-30%	31-40%	41-50%	51-60%	61-70%	71-80%	81-90%	91-100%
2.2 mV $\pm$ 1.0	**2.3 mV**$\pm$ 1.0	**2.2 mV** $\pm$ 1.0	**2.3 mV** $\pm$ 1.0	**2.3 mV** $\pm$ 1.0	**2.3 mV** $\pm$ 1.1	**2.3 mV** $\pm$ 1.0	**2.4 mV** $\pm$ 1.0	**2.3 mV** $\pm$ 1.0	**2.4 mV** $\pm$ 1.1
-3.1% $\pm$ 9.5	**-2.1%** $\pm$ 6.8	**-2.7%** $\pm$ 5.3	**-0.1%** $\pm$ 5.3	**-0.2%** $\pm$ 3.7	**-1.5%** $\pm$ 9.6	**-0.2%** $\pm$ 6.2	**+3.3%** $\pm$ 6.8	**+0.4%** $\pm$ 7.8	**+8.3%** $\pm$ 13.7

Table 2: first row: absolute MEP values across participants in each power bin. Displayed is the mean $\pm$ SD [mV]. second row: across-subject average normalized MEP values in percent change [%]. Normalized block-wise as percent change from all of (across all power bins) block average and then averaged across blocks

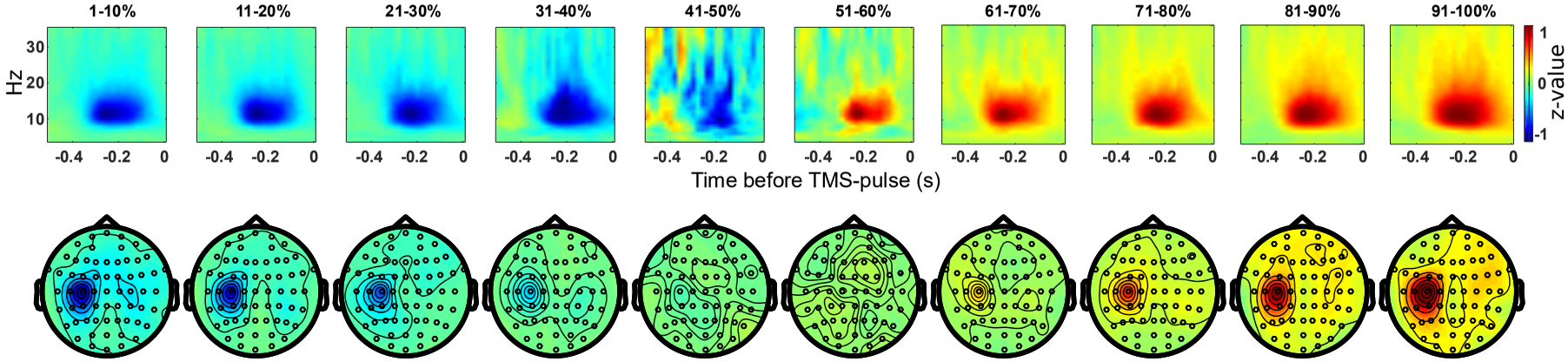

Figure 12: Upper row: Time-frequency representations of the 500ms pre-TMS, z-normalized: Yellow to red coloring shows values greater, green to blue lesser than the mean (= 0), see color gradient on the right of the figures. Close-to-zero values shortly before the TMS pulse at 0s are due to the zero-padding explained in 3.3. Note that meaningful transient power fluctuations take place only in the μ-$alpha$ frequency range.
Lower row: Topographical distribution of z-normalized pre-TMS μ-power (between 300 and 100ms pre-TMS). Local power fluctuations over the left sensorimotor cortex were targeted. This focality is not discernible in the medium (41-50% and 51-60%) power bins due to the z-normalization.
Figure from [Thies et al., 2018].

One subject had a mild headache lasting for a couple of hours after the session. They consequently refrained from taking part in further sessions.
Two subjects felt light-headed and nauseous during a session: In one case before stimulation had started, in the other case after about 5 single pulses. Both participants concerned recovered after a short break with a drink and a snack. One proceeded to take part in further sessions without any issues, the other subject preferred to end their participation. Both subjects concerned had contrary to our instructions attended the experiment on an empty stomach and attributed their symptoms to discomfort at the unfamiliar situation. In short, there is no valid reason to attribute the unspecific complaint of lightheadedness to any direct TMS effect.
One of the MUPEX subjects, who had been a regular participant in BNP experiments, reported having had a first epileptic seizure without close temporal association to any stimulation session. Unfortunately, this participant was not available for follow-up regarding the exact circumstances and specifics of the seizure or any long-term effects.

3.5.2 Interpretation of MUPEX results

Our finding that pre-stimulation μ power has a weak positive linear relationship with MEP size could point to a facilitatory rather than inhibitory role of the sensorimotor μ rhythm.
While this might seem, at first sight, contradictory to the pulsed inhibition hypothesis explained in the introduction of this thesis, some compelling theories have been put forward as to why we and other groups have recently found a positive linear relationship rather than the expected negative one.

Three prominent explanations for positive power-MEP amplitude slopes such as we found in MUPEX are:

(1) a facilitatory rather than inhibitory role of sensorimotor μ-$alpha$
(2) an inhibitory role, but a S1 origin of μ-$alpha$ (such as picked up by surface montages)
(3) different effects of μ power depending on stimulation intensity

A more detailed look at each of those is to follow.

(1) Facilitatory:
Hussain et al. 2018: variation of trough-specific facilitation
Stimulating with 120%RMT (roughly equivalent to MEP1mV according to our and other data) and comparatively long fixed ITIs of 20 s, [Hussain et al., 2018]'s post-hoc sorting did not find a significant effect of pre-stimulus μ power or phase on

MEP amplitude. They did, however, report a Phase x Power interaction: Within trials coinciding with a μ trough, there was a positive linear relationship between μ power and MEP size. For peak trials, the MEP amplitude did not appear to vary in dependence of power. The authors provide a tentative explanation for this phenomenon: μ peaks could correspond to a neutral state of excitability not impacted by *"synchronized excitatory thalamocortical input to pyramidal cells"* [Hussain et al., 2018], an alternative theory as to the origin of the μ-$alpha$ rhythm. This controverts Jensen and Mazaheri's theory of amplitude asymmetry explained in 1.6.4, which states that only peaks are modulated by power.

Allowing for varying effect sizes between studies depending on setup, the weak positive slope relating μ power and MEP amplitude we found in MUPEX with an open-phase or rather 'phase-blind' stimulation could be in agreement with Hussain et al.'s results, arising from a superposition of the positive linear relationship they found for trough trials and the zero slope curve for peak trials.

Bergmann et al. 2019: pulsed facilitation

[Bergmann et al., 2019], using a very similar setup to MUPEX (and a possibly overlapping subject pool), also observed a positive slope when comparing MEPs evoked during low (1-20%) versus high (81-100%) of the repetitively updated individual μ power spectrum. They reported an additionally facilitating effect of troughs and rising flanks[6] , but found no effect of power or phase on GABAergic short-latency intracortical inhibition (SICI) and derive from this a possible role of μ as a pulsed facilitation rather than pulsed inhibition.

In light of the sizable number of experiments supporting an inhibitory role of alpha-frequency rhythms in visual and sensory cortical areas (including evidence on a cellular and functional (perfusion and metabolic) level (cf. 1.6.5 and 1.6.6), it is at most feasible to question the *universality* of the inhibitory role of alpha-frequency rhythms.

The following approaches therefore continue to assume a principally inhibitory nature of the μ rhythm:

(2) S1 origin of μ-$alpha$:

What if the rhythm we target is in fact inhibitory, but not originating from the motor cortex we stimulate? Evidence supporting this theory includes data from both extracranial and intracranial (ECoG) EEG studies, which propose the existence of

[6] Using a high power 'pre-condition' for all phase-targeted trials, mean MEP amplitudes were ranked as follows: *troughs* and *rising flanks* > *peaks* and *falling flanks* > *low power, open-phase*. This incidentally challenges [Schalk, 2015]'s *function through biased oscillations* theory of mere instantaneous voltage amplitude modulating corticospinal excitability through the difference in excitability between falling and rising flanks.

two distinct μ rhythms within the sensori-motor cortex with distinct topographies and functions within those topographies, namely a postcentral (S1) anatomical source of the μ-$alpha$ rhythm that we focus on and a precentral (M1) μ-$beta$ rhythm (15-25 Hz) [Salmelin and Hari, 1994, Ritter et al., 2009, Stolk et al., 2019], as illustrated in Figure 13. These studies also found some evidence for a similarly inhibitory, but motor cortex-focused role of this μ-$beta$ rhythm, which was suppressed during contralateral motor task execution [Salmelin and Hari, 1994] or motor imagery [Stolk et al., 2019] and inversely correlated with fMRI-BOLD signal over the motor cortex [Ritter et al., 2009].

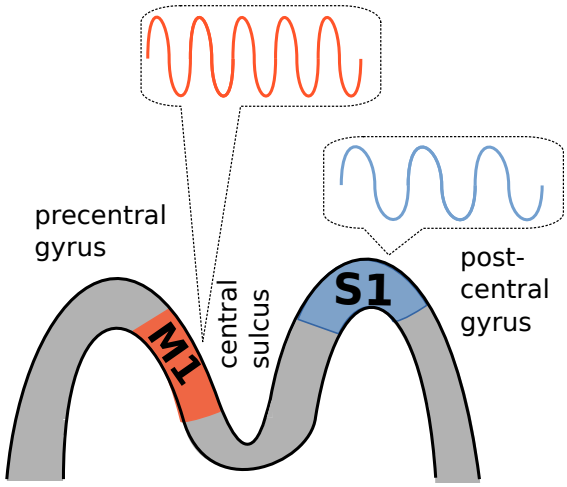

Figure 13: Rough illustration of the proposed postcentral origin of μ-$alpha$, corresponding to the location of S1 (blue) on the crown of postcentral gyrus and M1 (red) on the anterior bank of the central sulcus

Moreover, electric stimulation of the electrodes with most strongly expressed μ-$beta$ was more likely to generate a motor response (muscle twitches) – with somatosensory responses for stimulation of precentral μ-$alpha$ electrodes – in neurosurgical epilepsy patients with implanted diagnostic electrode arrays [Stolk et al., 2019]. Two TMS experiments [Keil et al., 2014, Schulz et al., 2014] furthermore found bigger MEPs with lower μ-$beta$ power. In MUPEX, by contrast, μ-$beta$ frequencies co-varied with μ-$alpha$ between power bins in MUPEX, but did not correlate significantly with MEP amplitude. This observation may be explained by both a 20 Hz harmonic of the 10 Hz μ-$alpha$ [Salmelin and Hari, 1994] or/and a natural co-variation of two independently generated rhythms [Jones et al., 2009]. [Bergmann et al., 2019] and [Ogata et al., 2019] have attempted to reconcile the pulsed inhibition hypothesis and the apparently facilitatory nature of μ-$alpha$ in their experiments by assuming a pulsed inhibition effected by μ-$alpha$ in S1 that results in a 'pulsed dis-inhibition' or rather pulsed release from the strong S1-to-M1 feedforward inhibition [Murray and Keller, 2011], leading to a reversal in previously expected power effects on M1 excitability. [Ogata et al., 2019] specifically suggest that the phenomenon of opposite-in-sign power effects between S1 and M1 comes into play more when higher SIs are used, in which case TMS would also directly stimulate S1, increasing the S1 to M1 feedforward inhibition.

More evidence is needed to support these deductions, specifically stimulation experiments isolating the role of μ for S1 excitability. Therefore, I will briefly present

some ideas for future research, giving the putative studies names encompassing the main experimental question, analogous to MUPEX and MUPAS:
Post-hoc sorting has revealed an *inverted U* relationship between pre-stimulus μ power and the N1 (140 ms) component of sensory evoked potentials (SEPs) [Zhang and Ding, 2010], mirroring the inverted U relationship found between μ power and performance in a tactile detection task [Linkenkaer-Hansen et al., 2004, Ai and Ro, 2014] (cf. 1.6.6). If and how μ phase influences SEPs, specifically the amplitude of the N1 peak, remains to be investigated. In MUSSEP, intermingled stimulated (MNS applied N20 before C3 Hjorth phase condition is predicted to be met) and unstimulated trials would be applied, each of these 'pairs' time-locked to the same phase so that phase-specific characteristics of EEG 'at rest' will not contaminate SSEPs. A setup of this kind would have the advantage of isolating the somatosensory cortex without involving the motor one. The results could then inform a power- and phase-triggered short-latency afferent inhibition (SAI) (see 1.6.1) protocol as a proxy for S1 to M1 feedforward inhibition: MUSAI. This essentially uses the same protocol as paired associative stimulation, but online rather than offline effects are analyzed: An afferent sensory signal, e.g. elicited by peripheral nerve stimulation, arriving in M1 just prior to a TMS pulse will inhibit the output of M1 in such a manner as to reduce the amplitude of the elicited MEP compared to an MEP elicited by the same TMS SI without a preceding afferent stimulus (by about 20 to 75% depending on the exact parameters used, [Turco et al., 2018]). Following the pulsed inhibition hypothesis and assuming an S1 origin of μ-$alpha$ rhythm, S1 excitability and thus the strength of its inhibitory effects on M1, i.e., the extent of SAI, should be greater if MNS were triggered N20 before a trough or triggered by low μ power compared to the relevant opposite conditions. Regrettably, such an experiment would again suffer from the same confounding property of having more than one cortical area involved.

Additionally, it remains unclear whether S1 to M1 inhibition is really the decisive or rather a modulating factor on SAI, which could be effected mainly through direct projections from the thalamus to M1, bypassing S1 [Turco et al., 2018] – in which case M1 would be actually the main cortical factor, reducing SAI extent when M1 excitability is high. Results from MUSSEP could help differentiate between S1 and M1 components. Double pulses (eliciting SAI) and single pulses (triggered by the respective same EEG condition) for comparison should be intermingled to avoid the effect of slow power drifts over time on corticospinal excitability - something that is inherently not accounted for in studies employing post-hoc trial sorting rather than EEG triggering. For the same reason, 'MUSAI' unfortunately eludes post-hoc analysis from MUPAS as double (during the PAS intervention) and single pulses were applied at different times during the experiment.

A filtered view – the facet of montage: [Karabanov et al., 2021] introduce the perspective of EEG montage used to filter μ power and phase as further indication of an S1 source of μ-$alpha$. Comparing the highest and lowest quartile of the individual μ-$alpha$ power spectrum, they found a positive slope (as we did in MUPEX) only when applying a Laplacian surface montage (like the one we used), which they state is located rather postcentrally, but not when resampling to a radial source projection with a more precentral focus - despite the fact that both montages should be sensitive mostly to radially oriented sources. These presumed topographical differences in EEG signals picked up by different montages relate back to the S1 theory just mentioned, as in addition to the μ-$alpha$ vs μ-$beta$ conundrum, Laplacian montages might be more sensitive to EEG signals originating postcentrally in S1.
Montage is surely an important aspect and more publications should include a re-sampling of data to different montages to validify results. However, a second group has recently published evidence for either a positive or no significant correlation of μ power and MEP amplitude: Despite using the same (Laplacian) montage both times, [Ogata et al., 2019]'s results varied in dependence of the SI used:

(3) stimulus-dependent μ function:
A second theory brought forward in the same publication [Karabanov et al., 2021] also assumes a principally inhibitory nature of μ, but drawing on a neuronal modeling study [Matthews, 1999], proposes differing effects of μ power on corticospinal output depending on stimulus intensity: For a weak brief external stimulus, the response (synaptic output) of the model neuron grew with increasing

intrinsic tonic firing rate – the opposite is true for a strong stimulus, which elicited the biggest response at a low firing rate. If one equates a high intrinsic firing rate to low μ power ([Haegens et al., 2011] reported evidence for this in monkey sensorimotor cortex, see 1.6.6 and 1.6.7) and vice versa, one would expect a negative μ power-CSE slope for low, near-threshold SIs (as found e.g. by [Sauseng et al., 2009, Zarkowski et al., 2006]) and a positive slope for higher SIs [Bergmann et al., 2019, Thies et al., 2018, Karabanov et al., 2021]. Interestingly, data collected within the same research group as MUPEX and MUPAS [Schaworonkow et al., 2018b] point to an influence on SI also on the phase effect, see 4.7.2. This intriguing approach of an SI-dependent power slope is largely supported by a comparison of results of numerous M1-stimulation experiments with differing SIs, displayed in Table 3. Most importantly, [Ogata et al., 2019] found a difference in μ power effect when stimulating with two different SIs within the same experiment: a positive slope when using MEP1mV and no significant correlation when using RMT. [Madsen et al., 2019]'s results appear to be an exception to this observation, as they reported a negative slope despite using a relatively high SI (120%RMT). However, all of their trials were triggered within the highest quartile of the individual μ power spectrum - taking into consideration the comparatively weak influence of μ power on MEP size with a big underlying variability of MEP amplitudes within each power bin/condition found in most studies (more on this in the following section), considering only such a narrow range of μ powers might well skew results.

Power 'categories' for comparison are an important but little-mentioned factor in μ power studies: They range from 2 categories on either extreme end of the spectrum [Bergmann et al., 2019, Karabanov et al., 2021, Ogata et al., 2019] to several bins [Thies et al., 2018] or even a continuous range [Hussain et al., 2018] – some researchers decided to approach the correlation from the EMG rather than the EEG side and sort trials into low or high MEP amplitudes [Ogata et al., 2019, Maeki and Ilmoniemi, 2010] (compare also Table 3).

study	montage	SI	ITI (& effect)	power cal.	power bins	power effect	phase effect
Hussain et al. 2018 post-hoc	C4 Hjorth	120 % RMT	20s	abs. values & comp. lowest and highest 10% of MEPs	continuous spectrum	interaction w. phase	troughs: pos. power slope peaks: no power effect
Bergmann et al. 2019 EEG-tr.	C3 Hjorth	MEP1mV	irreg., min. 3s (strat. post-hoc)	16 subj: rep. 3 min rest EEG, 7 subj: sliding update of 60s	1–20% vs. 81 – 100%	pos. slope	troughs/ rising flank: bigger MEPs
Madsen et al. 2019 phase: EEG-tr., power: post-hoc	radial	MEP1mV	irregular: avg 11.9 s (weak pos. slope)	rest EEG before stimulation	only within highest power quartile (76-100%)	very weak neg. slope	no
Ogata et al. 2019 **Exp. 3** EEG-triggered	C3 Hjorth	MEP1mV	not reported	rep. updated ind. power spectrum	lowest 10% vs highest 90%	pos slope	not assessed
Ogata et al. 2019 **Exp. 2** post-hoc	C3 Hjorth	MEP1mV vs. RMT	5-7s	none	comp. high vs low MEP ampl. trials	MEP1mV: pos slope RMT: none	not assessed
Karabanov et al. 2020 both	radial (EEG-tr.) vs Laplacian, (post-hoc)	MEP1mV	avg 10.3-60s (weak pos slope)	5 min rest EEG bef. stim.	highest vs lowest quartile	none (radial), pos (Laplacian)	no (post-hoc)
Thies et al. 2018 EEG-triggered	C3 Hjorth	50% IOC	3.79-3.85 (post-strat)	sliding update of 60s	10 bins, 10% each	weak pos slope	not assessed
Sauseng et al. 2009 post-hoc	C3, Fz, CP6	RMT	4-6s		sub- vs supra-threshold (50μV)	neg slope	not assessed
Zarkowski et al. 2006 post-hoc	C3	RMT	10s	correlating abs. power and MEP amplitude		neg slope	not assessed
Berger et al. 2014 post-hoc	source reconstruction	RMT	4-6s	correlating abs. EEG amplitude 500ms pre-TMS		none	yes, but at interind. different phase angles
Maeki et al. 2010 post-hoc	4 channels over M1	RMT	2-3s	1/3 biggest vs 1/3 smallest MEP trials		none, but neg slope for μ-$beta$	none
Iscan et al. 2016 post-hoc	for each electrode	110% RMT	3-10s	correlation betw. power and MEP	tested for each electrode	none	not assessed

Table 3: Comparison of some TMS experiments studying corticospinal excitability at rest in dependence of pre-stimulation μ power, including evidence published after measurements for MUPEX and MUPAS had been completed. power cal. = base for power calculation.

All that being said, the power and phase effects that are of such interest to neuroscientists are in fact rather weak when compared to the 'intrinsic' variability in MEP sizes, which are further confounded by the influence of ITI for which there is consistent evidence:

The impossibility of keeping ITIs constant is a 'built-in' shortcoming of EEG-triggered TMS, as the naturally occurring brain states that trigger pulses do not always coincide with the current trigger condition. The minimum ITI set to elapse after a given pulse (see 3.2) further distorts intervals between pulses. This constitutes an important confounder for our dependent variable, as the time passing between one pulse and the next influences MEP amplitude decisively [Vaseghi et al., 2015, Thies et al., 2018, Hassanzahraee et al., 2019]: Longer ITIs have the tendency to result in larger MEPs. This has been attributed to the transient reduction in blood flow effected by supra-threshold TMS in stimulated brain areas, after which it takes up to 15 seconds for all affected neurons to return to maximum 'performance' upon renewed excitation [Mochizuki et al., 2006, Thomson et al., 2011, Thomson et al., 2012]. Any ensuing pulse after an interval of less than 15 seconds would act upon less than optimally excitable cortical neurons, resulting in a smaller MEP. In fact, in MUPEX, the effect of ITIs on MEP size was so large as to a priori obscure any effect of μ power on MEP size and to skew statistical differences between power bins because of an accumulation of longer ITI trials in the more extreme power values, which necessitated a specific post-hoc stratification (see 3.3 and 3.4).
In summary, ITI influence on MEP amplitude is an important confounding factor in EEG-triggered TMS that needs conscientious reporting and accounting for – either in data analysis or in study design, e.g. by including a dummy pulse irrespective of condition in online protocols after a certain maximum ITI has been reached. It is worth noting at this point that [Hassanzahraee et al., 2019]'s data point to an increase not only in amplitude, but also in 'reliability' (i.e., decreased variability) of MEP amplitude when using larger ITIs ($\geq$15 s). This observation, which is incidentally in concordance with [Mochizuki et al., 2006]'s data of near-infrared spectroscopy (NIRS)-assessed hemoglobin levels returning to pre-pulse levels after about 15 seconds, could justify setting a minimum ITI to about that value rather than implementing a maximum ITI through a dummy pulse to reduce confounding influence of intervals on CSE. Systematic evidence on change in effect with even longer ITIs than that is lacking, but extrapolating from the observations about temporarily decreased blood flow, a sort of 'ceiling effect' of a certain ITI is to be expected, when all neurons will have returned to pre-pulse perfusion

and thus performance. Practicalities are to be considered nonetheless, as experiment duration escalates with longer inter-trial-intervals. Conversely, [Vaseghi et al., 2015] found no difference in reliability with longer ITIs.

The relation between different ITI lengths and MEP amplitude as well as a mixed effects analysis between SI, pre-stimulation μ power and ITIs on MEP size certainly warrants further investigation as it impacts the validity of countless TMS studies investigating CSE. Therefore, an experiment relating a wide range of ITIs (including >20 s) to MEP amplitude at different SIs each (requiring a sizable number of participants and trials per condition due to the number of factors investigated) is called for, investigating questions such as 'What is the minimal difference in ITI inducing a relevant effect on MEP size?' and 'Is the effect (size) of ITI on MEP amplitude influenced by SI?'. This would add valuable insight into variables potentially confounding CSE and thus both inform design of future studies and aid interpretation of previous experiments. Subsequent studies could introduce the components of EEG properties such as power and phase into the 'mix' – there is already data [Schaworonkow et al., 2018b] showing an influence of SI on extent of phase effect, and recently an influence of SI on power effects has also been suggested, as discussed in the previous section.

3.6 MUPEX. Conclusion

Looking back at the hypothesis or research question that gave rise to MUPEX, we expected a linear-negative (or *inverted U*) slope between μ-$alpha$ power and CSE. However, our data suggest a weak positive linear relationship. In light of the variable findings of numerous similar studies, this result should be assessed with caution before extrapolating to neuroscientific underpinnings or refuting the gating-by-inhibition theory, considering the vast amount of evidence backing it. Most findings in support of this concept however studied cortical processing of sensory input (visual or attentional/tactile detection tasks), involving primarily the sensory part of the sensorimotor cortex. There is some evidence pointing to μ-$beta$ as the predominant rhythm of the precentral motor cortex reflecting CSE rather than the μ-$alpha$ rhythm that we targeted. Through feedforward inhibition we might still be able to observe a M1 excitability effect of μ-$alpha$, 'reverse in sign' to S1. However, in [Ogata et al., 2019] and [Thies et al., 2018], no significant correlation between μ-$beta$ and CSE was found.

It must be acknowledged that despite the wealth of studies with detailed description of methods, no fully stringent difference in study design or data analysis appears to conclusively explain differing results or rather divide evidence supporting

an apparently facilitatory versus inhibitory role of μ-$alpha$ for CSE. This calls for more experiments which, like [Karabanov et al., 2021] and [Ogata et al., 2019], deliberately vary certain specifics suspected to influence results (like spatial filtering and stimulation intensity) within the same setup and subject pool to compare data. Juxtaposing the same stimulation protocol time-locked to power and phase of μ-$alpha$ versus μ-$beta$ would be particularly interesting.
In contrast to occipital alpha oscillations, the role of the sensorimotor μ-rhythm for corticospinal excitability thus remains imperfectly understood despite the constantly growing number of studies investigating it, and hence warrants further research.

4 Experiment: MUPAS

4.1 MUPAS. Introduction

Easily the most fascinating property of that endlessly fascinating organ, the human brain, is its potential for the modification of existing connections and the creation of new ones throughout adult life – enabling adaptation, learning, development and regeneration after damage, the extent of which continues to astound researchers and physicians alike.
Initially plegic body parts in stroke patients can regain most of their movement over time, and this functional recovery is reflected by cortical reorganization: new connections (synapses) between neurons are formed. Synaptogenesis and thus the extent of recuperation can be amplified through targeted training of the affected limbs, i.e., physiotherapy: in animal models, (task-specific) physical exercise seems to incite the unaffected parts of the motor cortex to grow new connections and functionally take over for the irreversibly damaged areas [Carmichael, 2006, Biernaskie and Corbett, 2001, Jones et al., 1999].
Still, as already mentioned in 1.2, about a third of stroke survivors are subject to moderate to severe disability and consequently dependent on help with their daily activities at 3-months follow-up according to the German Stroke Registry [Grau et al., 2001], a portion consistent with data from other developed countries [Kelly-Hayes et al., 2003].
What if we were able to directly trigger the plasticity processes that we know the brain to be capable of? It is tempting to harness the brain's aptitude for adaptation and attempt to amplify existing processes of plasticity.

To do this, one first has to understand how plasticity works. What kind of changes take place in the neural networks to make us learn, remember, adapt? Plasticity

can be categorized into intrinsic (mainly effected by density and activity of voltage-gated ion channels in a neuron, contributing to AP generation) and synaptic plasticity, the latter subdivided further into structural (synaptogenesis, i.e., formation of new synapses) versus functional plasticity (changes in synaptic efficiency). Functional synaptic plasticity, i.e., strengthening and weakening of existent synapses, constitutes the main mechanism of learning and memory formation according to current neuroscientific knowledge. First off, a brief explanation of terminology:
One of the key terms in this context is *Hebbian learning*. As early as 1949, Canadian psychologist Donald Hebb theorized that *"When an axon of cell A is near enough to excite a cell B and repeatedly or persistently takes part in firing it, some growth process or metabolic change takes place in one or both cells such that A's efficiency, as one of the cells firing B, is increased."* [Hebb, 1949]. This statement is often synopsized in the catchy phrase 'Neurons that fire together, wire together'. The theory of synaptic plasticity has since been expanded to accommodate also negative plasticity, the weakening of synapses.
The terms of 'long-term potentiation' (LTP) and 'long-term depression' (LTD) are used to describe, in the broadest sense, a change in output outlasting the transient input that caused it. More specifically, they mean the synaptic strengthening or weakening, by extension the overall increase or decrease in postsynaptic effect of a neuron, that results from a certain pattern of activation. In some cases, the firing sequence of synaptically connected neurons determines the direction of plasticity, which is then termed 'spike-timing dependent plasticity' (STDP) or 'Hebbian plasticity': If the presynaptic neuron is repeatedly activated shortly before the postsynaptic one, the synapse connecting these two neurons is strengthened. Correspondingly, a reverse order of events with the postsynaptic neuron firing before the presynaptic one will eventually weaken the synapse. These processes were first experimentally induced by [Bi and Poo, 1998] in dissociated rat hippocampal neurons.
Among the molecular mechanisms underlying LTP, the NMDA-receptor-dependent type has perhaps been most exhaustively studied: The NMDA subtype of ionotropic glutamate receptors serve as 'molecular coincidence detectors', only opening when both the presynaptic neuron (releasing glutamate into the synaptic gap) and the postsynaptic neuron (depolarized sufficiently to displace the Mg^{2+} ion blocking the channel opening) are active. The increased calcium influx into the neuron through NMDA channels spurs intricate processes of protein synthesis and gene transcription culminating in an ultimately long-term strengthening of synaptic efficacy [Bliss and Collingridge, 1993].

Both LTP-like and LTD-like plasticity have been induced in-vivo with TMS. Table 4 contains a brief synopsis of relevant TMS protocols. The references provided are exemplary in nature, as these techniques have been abundantly replicated over the years. Inter-stimulus interval (ISI) denotes the time lag between two stimuli within one specific stimulus pattern, inter-trial interval (ITI) describes the delay between two such patterns, i.e., the inverse of the repetition rate.

	Positive (LTP) 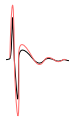	**Negative** (LTD) 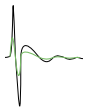
PAS	ISI 20/21.5/25/N20/N20+2ms [Stefan et al., 2000, Wolters et al., 2003] 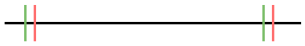	ISI 10 ms [Wolters et al., 2003] 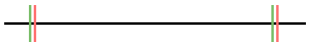
rTMS	5 Hz rTMS [Peinemann et al., 2004] 	1 Hz rTMS [Chen et al., 1997] 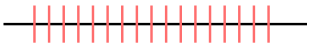
dp-rTMS	ISI = 1.5 ms , rep. rate 0.2 Hz (ITI = 5 s) [Thickbroom et al., 2006] 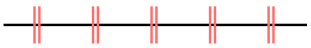	ISI = 3 ms, rep. rate 0.6 Hz (ITI = 1.67 s) [Khedr et al., 2004] 
TBS	Intermittent (iTBS) (2s stim, 8s pause) [Huang et al., 2005] 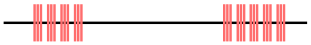	Continuous (cTBS) [Huang et al., 2005] 

Table 4: Schematic of TMS protocols inducing LTP-like and LTD-like plasticity. Stimulation patterns are for illustrative only and not true to time scale. Black horizontal lines = time, red vertical lines = TMS pulses.
References are exemplary only.
PAS = paired associative stimulation, green lines = peripheral electric nerve stimulation. rTMS = repetitive TMS. dp-rTMS = double-pulse repetitive TMS. TBS = theta burst stimulation: triplet pulses with ISI = 20 ms (f=50 Hz) and ITI = 200 ms.

In our experiment we modified a protocol called Paired Associative Stimulation (PAS), first developed by [Stefan et al., 2000]. PAS is, broadly speaking, a combination of two stimuli whose courses of excitation convene in a certain cortical area. If these signals arrive shortly after one another, changes in the excitability of said area outlasting the intervention can be observed. The direction of change (increasing or decreasing excitability, subsequently also termed positive or negative plasticity) is determined by the sequence in which the stimuli arrive in the cortical target area, following the principles of STDP.
MUPAS was based on the classical variant of PAS, combining electrical stimulation to the right median nerve at the wrist with TMS of the left M1 hand knob:

The signal from the right median nerve travels through the spinal cord over the thalamus either directly to M1 or via the left primary sensory cortex (S1) in about 20 ms and is transmitted from there to M1, cf. Figure 14. Single-pulse TMS of the left M1 probed APB MEP amplitudes before and after the intervention to assess changes in excitability.
PAS-induced plasticity shares the following properties with LTP/LTD induced on a cellular level in brain cells/brain slices [Müller-Dahlhaus et al., 2010]:

Cortical process: The absence of change in F-wave[7] amplitude and brainstem-evoked MEPs after a PAS intervention suggests that the plasticity processes are indeed taking place in the cortex [Stefan et al., 2000].

Spike-timing dependency: PAS-induced plasticity can be bidirectionally modulated depending on the order in which stimuli arrive in the primary motor cortex: If the sensory signals reach M1 first (as is the case with ISIs of 21.5 ms [Weise et al., 2006], 25 ms [Stefan et al., 2000], the individual N20 latency [Ziemann et al., 2004], and N20+2 ms [Müller et al., 2007], M1 excitability is typically increased (positive plasticity) and vice versa (negative plasticity at ISIs of 10 ms [Wolters et al., 2003] or N20-5 ms [Ziemann et al., 2004, Müller et al., 2007]. If the stimuli are too far apart (e.g. ISIs of 100 ms and more), no plasticity effect is obtained [Stefan et al., 2000]. These patterns are in good accordance with STDP induced in hippocampal cells, where postsynaptic spiking within 20 ms after presynaptic activation produced LTP, postsynaptic spiking within 20 ms before presynaptic activation resulted in LTD, and longer delays between pre- and postsynaptic activation in either direction did not produce a plasticity effect [Bi and Poo, 1998].

Input specificity: The effects of STDP experimentally induced in neurons are limited to the cell or rather synapse that was activated ([Zilberter et al., 2009] discusses different mechanisms in play). In mammals, the S1-to-M1 projections are in part topographically homologous: corresponding sensory and motor areas/parts of the 'homunculi' are connected, and receive equally topographically specific peripheral input [Rosen and Asanuma, 1972, Caria et al., 1997].

[7] An F-wave is a characteristic 'late' deflection observed in electroneurography after supramaximal stimulation of a peripheral nerve. The signal first travels in 'antidromic' direction retrogradely along the axon of the motoneuron to its cell body in the anterior horn of the spinal cord, where some of the motoneurons 'backfire', causing a wave of excitation travelling in 'orthodromic' direction, i.e., corresponding to the physiological direction of excitation along the motoneuron back to the muscle. Thus, changes in F-wave amplitude, pattern or latency isolate spinal excitability without involving the cortex.

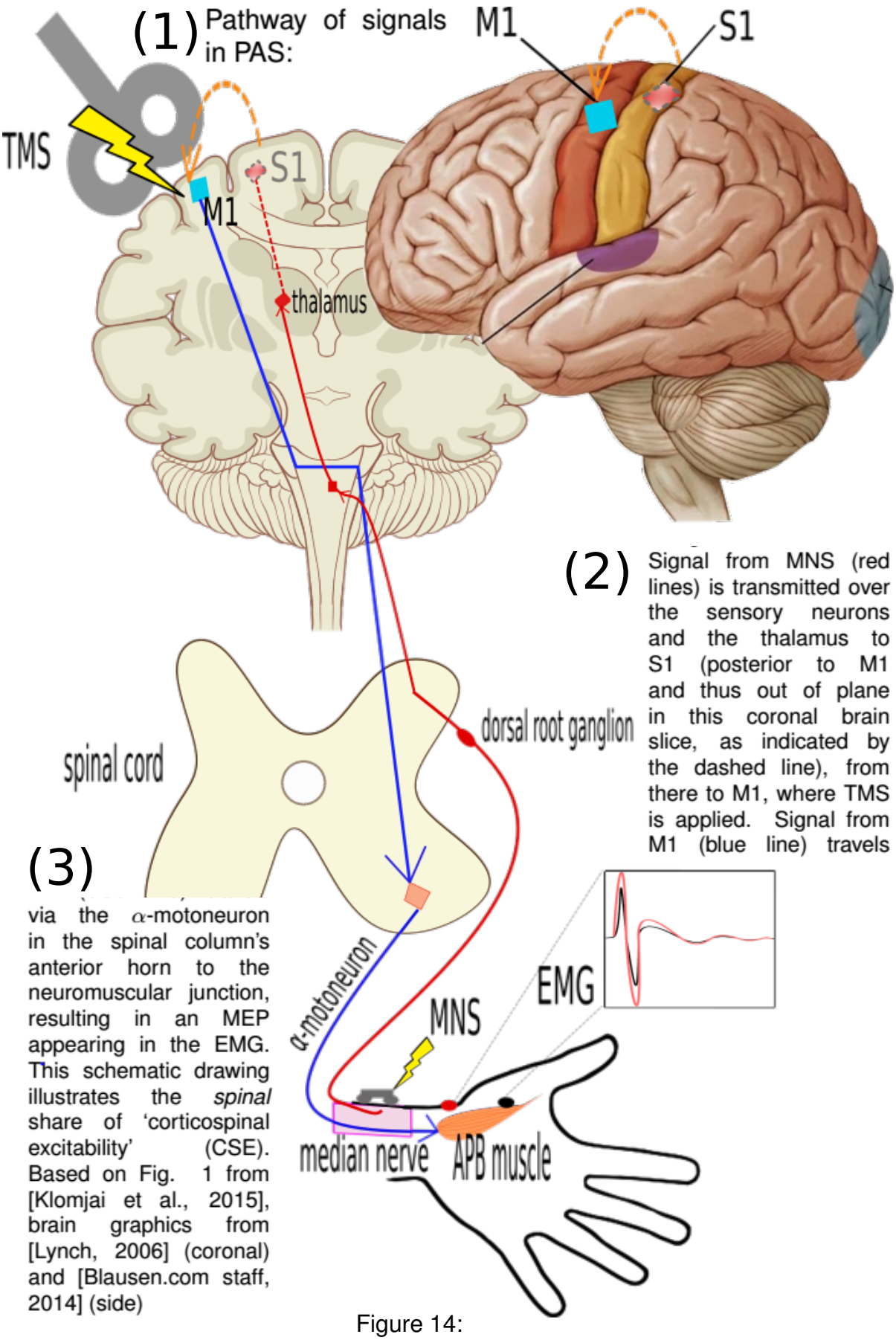
(1) Pathway of signals in PAS:
M1
S1
TMS
S1
M1
thalamus
(2) Signal from MNS (red lines) is transmitted over the sensory neurons and the thalamus to S1 (posterior to M1 and thus out of plane in this coronal brain slice, as indicated by the dashed line), from there to M1, where TMS is applied. Signal from M1 (blue line) travels
dorsal root ganglion
spinal cord
(3)
via the α-motoneuron in the spinal column's anterior horn to the neuromuscular junction, resulting in an MEP appearing in the EMG. This schematic drawing illustrates the *spinal* share of 'corticospinal excitability' (CSE). Based on Fig. 1 from [Klomjai et al., 2015], brain graphics from [Lynch, 2006] (coronal) and [Blausen.com staff, 2014] (side)
α-motoneuron
MNS
EMG
median nerve
APB muscle

Figure 14:

Plasticity after PAS application seems to share this spatial specificity, only muscle representations in M1 that received the coupled double input being strengthened in output: [Stefan et al., 2000, Wolters et al., 2003, Weise et al., 2006] have shown that MNS-PAS increases MEPs in APB (innervated by N. medianus) more than in Abductor digit minimi (supplied by N. ulnaris).

Homeostatic plasticity is a complementary type of plasticity to prevent overly strong plasticity effects. Underlying mechanisms include synaptic scaling (modification of all synaptic entries on a neuron to keep the sum of incoming activation constant, happening over a time scale of hours to days), intrinsic neuronal plasticity (modulation of ion channels), and synaptic metaplasticity: According to the 'Bienenstock-Cooper-Munro theory of bidirectional plasticity', the threshold for inducing positive (LTP-like) or negative (LTD-like) plasticity moves dependent on the prior level of postsynaptic activity - after a period of strong postsynaptic activation, LTD becomes more probable and vice versa [Watt and Desai, 2010]. This last, fast-acting mechanism seems to also apply to PAS-induced plasticity, which is decisively influenced by prior LTP or LTD processes: Motor learning involving the target muscles less than six hours prior to stimulation prevents the induction of LTP-like plasticity [Stefan et al., 2006, Ziemann et al., 2004] and augments LTD-like plasticity [Ziemann et al., 2004], and vice-versa with PAS-induced LTP suppressing practice-dependent plasticity [Kang et al., 2010][8]. Interestingly enough, this keeping of balance seems to be in place also across cortical representations: heteronymous muscles show LTP after LTD-PAS [Weise et al., 2006].

NMDA dependence: The role of NMDA receptors for LTP has been discussed earlier in this section. Pharmaceutical interventions with NMDA receptor blocking substances impede LTP-PAS effects [Stefan et al., 2002].

To conclude, the evidence points towards PAS-induced plasticity working through very similar if not identical processes and cortical pathways as LTP/LTD, which is why the changes in excitability caused by such protocols are termed 'LTP/LTD-like plasticity'. Unfortunately, PAS protocols are afflicted by a striking variability, both between participants of a study and between studies, in extent and even direction of the effect obtained. Responder rates, if reported at all, vary between 52% [Müller-Dahlhaus et al., 2008] and 78% [Fratello et al., 2006]. Furthermore, in [Müller-Dahlhaus et al., 2008] the remaining 48% showed a significant decrease in excitability following a LTP-PAS protocol. Several nil findings [Kujirai et al.,

[8] worth noting: even though MEP amplitudes were not significantly different from baseline after PAS in this study

2006, Kang et al., 2010, Meder et al., 2021] have also been reported despite the use of established protocols. Another crucial flaw is the short duration of PAS effects, lasting from 30 [Stefan et al., 2000] to 120 minutes [Grundey et al., 2012], which thus far limits clinically meaningful applications, e.g. in stroke recovery.
These shortcomings motivated us to develop a modified LTP-PAS version with paired pulses time-locked to more excitable brain states. Assuming a favoring of induction of LTP-like plasticity during periods of high M1 excitability, we intended to improve reliability and possibly persistence of effect.

4.2 MUPAS. Methods

In addition to the methods described in 2, the following techniques were used for MUPAS:

Magnetic resonance imaging: For more accurate neuronavigation, particularly pertaining to hotspot consistency between sessions, as well as availability for future source space analysis [9], we acquired (n = 9 of included subjects) or used pre-existing (n = 7) individual T1-weighted (T1 3D MPRAGE sequence, scanner was Siemens PRISMA 3T) MRI brain scans of participants.

Real-time phase targeting: After performing the downsampling and spatial filtering of EEG data already detailed in 2.3, a frequency band containing the individual $\mu\text{-}alpha$ frequency $\pm$2 Hz was extracted from the sliding last 512 ms of C3 Hjorth raw signal using a two-pass zero-phase finite impulse response (FIR) filter. Filter ripple artifacts at the borders of the 512 ms sliding window (64 ms on each side) were removed. Based on the remaining 384 ms, a Yule-Walker autoregressive model forward-predicted the signal of the removed 64 ms until time 0 ('now') and 64 ms into the future. Signal at time 0 was then defined as either a high (peak) or low turning point (trough).
At the start of each session, a visual appraisal of the accuracy of this process was performed by the experimenter with stimulators turned off to view uncorrupted EEG (cf. 4.4).

Peripheral nerve stimulation: For electric median nerve stimulation (MNS), we used a Digitimer DS7A Current Stimulator with 50 mm spacing between cathode and distally placed anode, with felt tip electrodes which were soaked in 0.9% saline solution prior to use. The stimulator was set to produce rectangle pulses with a width of 200 μs.

[9] use of EEG data to estimate the origin of a certain rhythm or signal in the brain

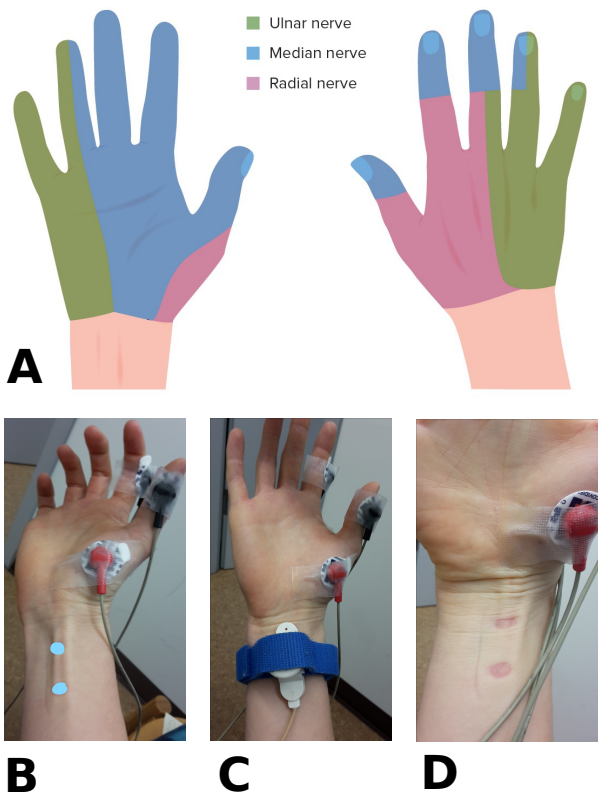

Figure 15: A: The sensory innervation of the hand. In this case, the median nerve (blue) was stimulated. From [Lecturio Staff, 2020].
B: Tendons of the flexor digitorum superficialis (left) and flexor carpi radialis (right) with the intended position of the electrodes marked in light blue.
C: Nerve stimulator *in situ*, blue Velcro band for fixation.
D: Imprints left after stimulation, used to achieve stimulation site consistency in MUPAS.

The median nerve runs most superficially in the distal forearm and wrist, shortly proximal to and in the carpal tunnel, between the tendons of the flexor digitorum superficialis and flexor carpi radialis. Initially (during the screening), the electrode holder was placed at the mid of the palmar side of the wrist and subsequently varied the position to find the spot with the lowest perceptional threshold. Subjects were shown a colored illustration of the sensory innervation areas of the hand (cf. Figure 15, Panel A) to instruct them on where to expect a tingling sensation and thus avoid confounding by accidental ulnar nerve stimulation. Once the location with the lowest sensory threshold was found, the electrode holder was fixed to the subject's arm using the bracelet attached (cf. Figure 15, Panel B-D).

4.3 MUPAS. Session Design

With MUPAS, the dependent variable was the change in MEP size from baseline after the LTP-PAS intervention, as measured at 7 time points after said intervention. The independent variable was the EEG condition that triggered PAS. The initial experiment design included 5 main sessions with the PAS intervention being triggered by μ troughs, peaks, low and high μ power, respectively, plus one open-loop condition. Between the only very slight influence of μ power on M1 excitability that MUPEX found and the conflicting previous evidence on μ power and CSE (see 1.6.7), we decided instead to only compare 4 conditions: two phase conditions and one open-phase condition, all of which were subject to an additional μ power range requirement for triggering, as well as an open-loop condition for reference (illustrated in 16, Panel B). Session design is outlined in Figure 16, Panel A. The 'open-loop' session was realized as a *Replay* of the individual subject's first session's ITIs (ensuring a symmetric distribution between *Power*,

Peak and *Trough* sessions as template). Sequence of conditions was randomly assigned to each subject, while assuring a balanced placement of conditions to first/second etc. session to minimize potential time effects accumulating with increasing number of PAS sessions per subject. The replay session could by nature never be a participant's first session.

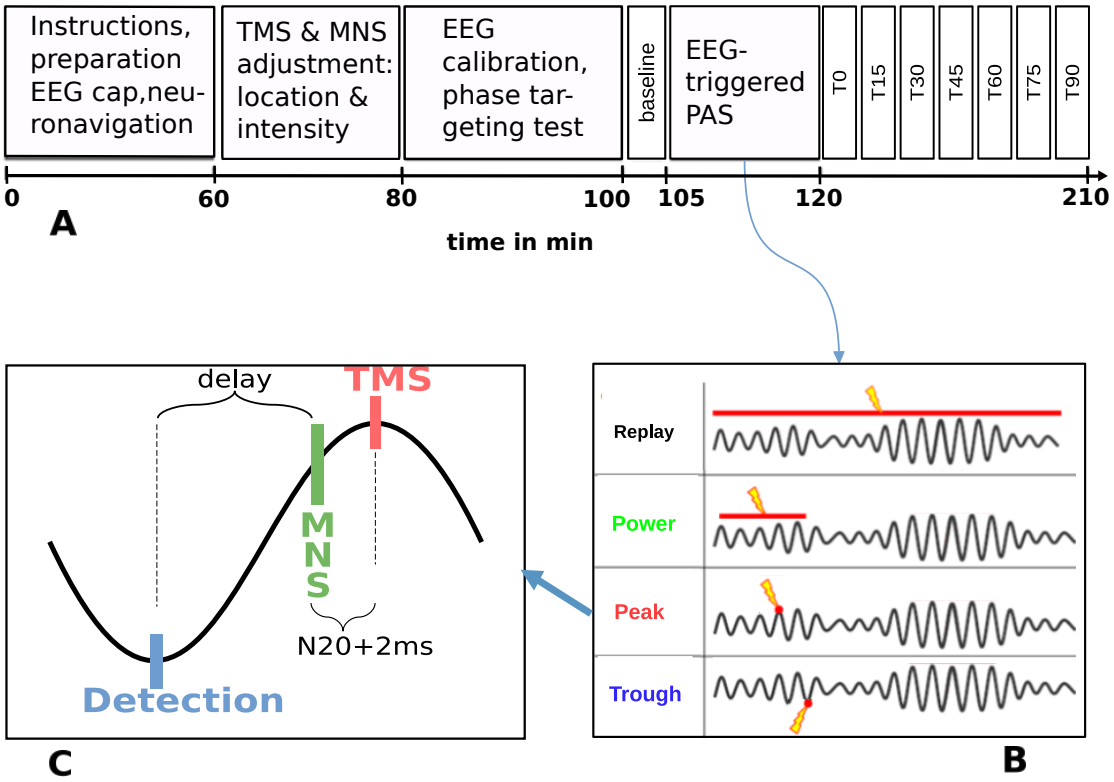

Figure 16: Panel A: Session design, timeline not true to scale.
Panel B: Visualization of EEG conditions for the PAS intervention: 'medium' μ-alpha power range (25.75% of individual spectrum) applied to *Power*, *Peak* and *Trough* conditions.
Panel C: Phase targeting during PAS: TMS was applied when an occurrence of a peak or a trough was predicted, MNS N20+2ms before.

SI for MNS was set to three times the perceptual threshold, as established in most PAS protocols ([Stefan et al., 2000, Müller-Dahlhaus et al., 2008, Wolters et al., 2003, Ziemann et al., 2004] to name just a few).
ISI between MNS stimulus and TMS pulse was fixed to the individual N20 latency plus 2 ms. Conduction time from stimulus to S1 activation is estimated at 20 ms (e.g. TMS to S1 is most efficient at blocking the perception of a cutaneous stimulus at 20 ms delay to the stimulus [Hannula et al., 2005]), reflected as the N20 peak (occurring around 20 ms after stimulus, hence the name) in somatosensory evoked potentials (SSEPs). We opted for measuring the individual N20 latency within median nerve-SSEP (see 18) to account for interindividual differences in arm length and conduction time. The additional 2 ms constitute the customary

estimate for S1-to-M1 transit time (N20+2 ms was used as ISI for instance by [Müller-Dahlhaus et al., 2008, Müller et al., 2007]).
SI for TMS was titrated to MEP1mV at baseline, an intensity successfully used in several previous PAS studies (e.g. [Stefan et al., 2000, Müller et al., 2007, Müller-Dahlhaus et al., 2008, Ziemann et al., 2004].
During the EEG-triggered sessions, MNS was triggered N20+2 ms before the respective conditions listed below were predicted to be fulfilled, followed by a single TMS pulse after N20+2 ms (cf. Figure 16, Panel C).

Open-phase, power-triggered condition (Power):

(i) a minimum ITI of 3 s had elapsed since the last TMS pulse
(ii) current μ-$alpha$ power is within 25-75% of the individual, repeatedly updated μ-$alpha$ power spectrum (refer to 2.3 for a detailed explanation)

Phase-triggered conditions (Peak and Trough):

(i) minimum ITI of 3 s
(ii) current μ power within 25-75% of the individual spectrum
(iii) phase matching the current condition

Our reasons for setting the aforementioned power range also for the phase-triggered conditions were twofold:

(1) we wanted to exclude low μ powers at which phase targeting has been shown to be extremely inaccurate. This could be due to insufficient SNR for the algorithm to reliably extract the waves of the relevant rhythm and predict their course. Low powers in a band-pass filtered signal could also conceivably just reflect filtered 1/f noise, even in the complete absence of a meaningful neuronal oscillation.
(2) we furthermore wished to avoid extreme μ powers on either end of the spectrum in order to keep any supposed influence of extreme power values on excitability (as suggested by numerous studies comparing higher versus lower power and finding a difference in excitability, see 1.6.7) thus inducibility of plasticity to a minimum. In particular, average excitability at low μ powers might be so high as to render phase differences irrelevant [Klimesch et al., 2007].

Our alternative hypothesis (H_1) was that the LTP-PAS intervention would result in the biggest and most robust plasticity effect in the *Trough* condition and the least or even no effect when triggered by *Peaks*. The *Power* and *Replay* conditions served in essence as two control conditions due to the change in session design

(see above). Figure 17 contains an idealized version of expected outcomes.
The null hypothesis (H_0) supported no improvement in LTP induction when PAS was triggered by μ-$alpha$ troughs compared to peaks, by extension either an equal or a smaller effect for the *Trough* compared to *Peak* condition.

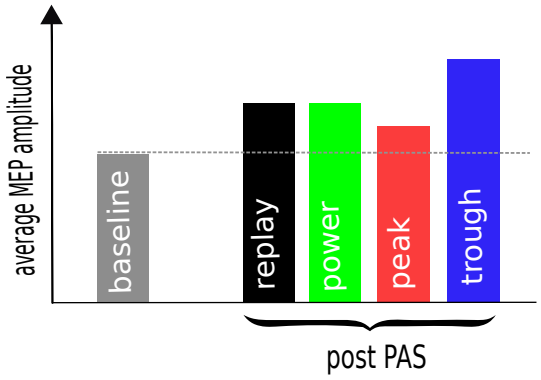

Figure 17: On the left: the mean MEP amplitude at baseline (grey bar), on the right expected mean post-PAS MEP amplitudes per condition. We expected the strongest plasticity effect for trough-triggered PAS (blue bar), followed by the open-phase control conditions *Replay* (black) and *Power* (green). We expected the weakest LTP-like effect after peak-triggered PAS (red bar).

Main sessions involved a baseline MEP measurement (after adjusting the individual SI from the MEP1mV acquired in the screening session if needed) of 80 trials and about 6 min duration, followed by the intervention of 225 pairs of MNS and TMS pulses and 7 follow-up MEP measurements of 40 trials each at 0, 15, 30, 45, 60, 75 and 90 min after intervention (compare Figure 16, Panel A). Both the baseline and the post-intervention MEP measurements were open-loop, but with a minimum ITI set to 3 s to keep ITI lengths within a comparable range, reducing a confounding influence of ITI on MEP size (see 3.5.2). During the breaks, subjects were instructed to keep their right hand relaxed and not move it, which was verified by visual control of the EMG signal by the experimenter. Session duration was about 4 h 30 min including setup preparation (for a detailed description of an exemplary measuring session, cf. 11.1).

4.4 MUPAS. Screening

The screening session preceded the four main sessions, and served both as confirmation of subject inclusion criteria and for acquisition of the individual N20 latency in MNS-evoked SSEPs. The sequence of a screening session with examples from included and excluded participants' data is depicted in Figure 18 on the following full page.
Inclusion criteria are listed in order of testing (any participant failing on one of these was immediately excluded and the following criteria were not tested anymore). As criteria *(i)* and *(ii)* were in place also for MUPEX, a detailed description of those can be found in 2.1.

(i) strong μ-$alpha$ peak
(ii) reliable APB hotspot with MEP1mV $\leq$80% MSO (unlike for MUPEX, FDI could not be target muscle due to the proposed input specificity of PAS

effects described above)

(iii) sufficiently accurate phase targeting according to the experimenter's visual appraisal. This was implemented as a 6 min resting state EEG with triggering conditions set to peaks or troughs in an intermingled sequence, but stimulators turned off. In this way the trigger times could be displayed superimposed on uncorrupted EEG data. This step ensured adequate precision of the phase-targeting algorithm, which probably differed between participants only because of μ-$alpha$ rhythm SNR and thus acted like a more rigorous extension of criterion (i).

Sequence of a screening session:

- only the C3 Hjorth electrodes (Fz, Cz, Ref, Ground, C3, CP1, CP3, CP5, FC1, FC5) were prepared
- neuronavigation was based on a rough co-registration of the scalp surface using the MNI template brain
- 3 min resting state EEG to confirm sufficient μ rhythm peak
- automatic thresholding of RMT and MEP1mV (see2.2)
- 6 min resting state EEG as a 'phase targeting test' (20 pulses per condition)
- MNS 'hotspot' search and determination of perceptual threshold
- SSEPs were evoked using an SI of 300% perceptual threshold and 500 pulses at a frequency of 3 - 5 Hz in a Fz-CP3 bipolar electrode montage. N20 latency was measured by an automated Matlab script and adjusted manually when necessary
- phase effect testing: Initially, the existence of a 'phase effect' (cf. 1.6.4) was set as one of the inclusion criteria, because we considered it to be a prerequisite for the hypothesis of PAS efficiency being influenced by phase at time of application. The existence of a phase effect was defined here as the average MEP amplitude of trough-triggered trials exceeding that of peak-triggered trials on visual inspection of overlapping plots averaging 200 trials per condition at MEP1mV SI. When inclusion rates were too low (see 4.6.1), however, this criterion was dropped and the phase effect only tested to be able to subdivide the participants' results for further analysis. In fact, no participant was excluded based on this criterion. As data from the same group [Schaworonkow et al., 2018b] suggested a higher phase effect 'responder rate' at lower SIs and with more trials (cf. 4.7.2), we adapted this section of screening to include 400 pulses per condition at 110%RMT.

One such session lasted on average about 2 hours.

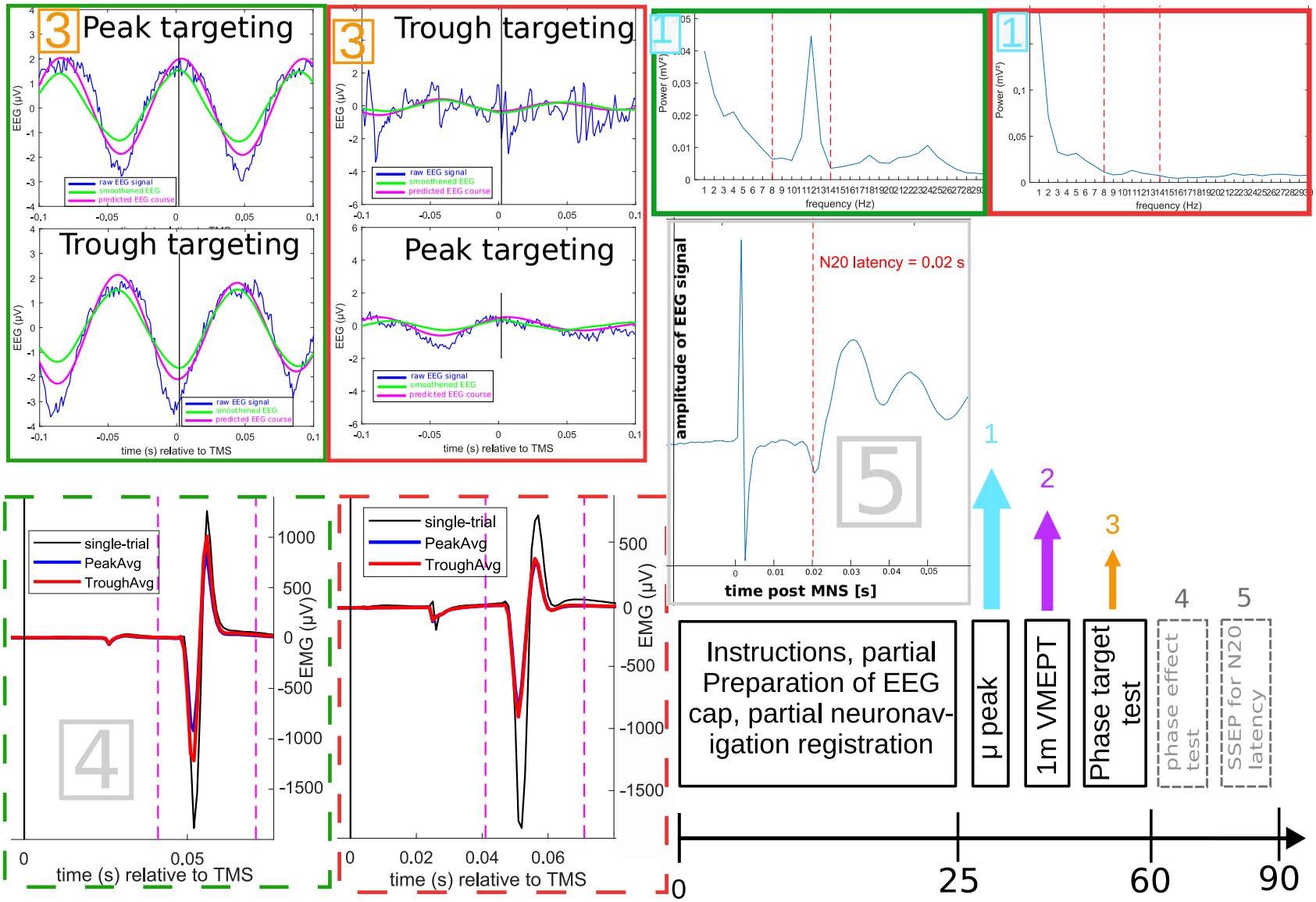

Figure 18: Lower right: sequence of a screening session with arrows indicating 'exit points' where participants could be excluded in order of application. For exclusion criterion (1) (insufficient μ peak) and (3) (inaccurate phase targeting in preview) Matlab figures from exemplary participants are included, each featuring a suitable, included candidate's data on the left, framed in green, and an excluded candidate's data on the right, framed in red. In the left panel of (1), the individual μ peak frequency extracted was 12 Hz. (4) shows an exemplary phase effect responder (green frame) and non-responder (red frame). These frames are dashed to illustrate that existence of a phase effect was not applied as an exclusion criterion. (5) is an exemplary SSEP with an individual N20 latency of 20ms.

4.5 MUPAS. Consistency Strategy

With MUPAS, we faced the challenge of keeping the manifold parameters of stimulation described thus far as consistent between sessions within one subject as possible in order to minimize confounding influences on M1 excitability or plasticity induction (influences other than the intended independent variable, i.e., the triggering condition for the PAS intervention).
The following measures were applied in each of the four sessions:

(i) μ rhythm SNR, peak frequency and accuracy of phase targeting was reconfirmed before commencing stimulation in each session to ascertain quality of power- and phase-targeting

(ii) we measured MEP size using the previous MEP1mV as SI on a stimulation site matching the previous hotspot(s) as registered in Localite. SI and/or stimulation site were adjusted where required

(iii) site of stimulation for MNS was recreated based on a photograph of the imprint left by the electrodes on the individual subject's forearm, taken after the first of four main sessions (see Figure 15). Perceptual threshold was verified and re-acquired if needed.

This was by necessity a tradeoff between reproducing the exact *stimulation parameters/input* (SI of TMS and MNS and site of stimulation for MNS and TMS as compared to the skin imprint or the saved hotspot, respectively) and recreating the *effect/output* (i.e., MEP size, MNS at 3x the sensory threshold). We decided to err in favor of recreating the output on the one side, as we had titrated these parameters based on the elicited effect rather than the input from the beginning, and in favor of faithful SI rather than hotspot recreation, because we assumed the latter to be rather more sensitive to small inaccuracies in cap positioning and Localite registration.
To reduce the impact of (probably cortisol-level mediated [Sale et al., 2008]) circadian rhythm on plasticity induction [Sale et al., 2007], we scheduled sessions within one subject on the same time of day as far as possible and tried to keep at least 3 full days between sessions to reduce carry-over effects between sessions.

4.6 MUPAS. Results

4.6.1 Screening results

All in all, 50 individuals were screened, 15 of whom had already participated in experiments of the same group and were thus pre-selected for a strong μ peak in C3 Hjorth and a sufficiently low resting motor threshold. The average age of

screening participants was 24.54 $\pm$ 5.09 years (range of 18 - 50 years), 31 were female.
Among the 27 excluded subjects, in order of application of criterion,

(1) 13 failed because of an insufficient μ peak (1 of those from the group's 'subject pool')
(2) 6 because of an APB-MEP1mV exceeding 80% MSO (1 of those from the subject pool)
(3) 8 because of inaccurate phase targeting as esteemed in the 'pre-view' section despite an apparently sufficiently clear μ peak (4 of those from the pool)

Hence, 23 out of 50 screening participants fulfilled the inclusion criteria.

As to the phase effect which was initially planned as a further inclusion criterion: Out of the 25 subjects (10 of them pool subjects) where this was tested[10], 13 (52%) displayed the phase effect according to visual appraisal. Among preselected participants from our group's 'subject pool', 8 out of 10 displayed a phase effect, resulting in a phase effect responder rate of 33% among participants 'native' to EEG-TMS versus 80% among individuals that had previously already passed validation for μ rhythm SNR and motor thresholds.
After adapting SI and trial number for phase effect testing (see 4.3), we saw a vast improvement in responder rate (6 out of 8 = 75%). From only our data, we can hardly assume a relevant influence of stimulation parameters on this improvement (see 4.7.2), as all of those 8 subjects were 'pool subjects' and had thus previously already passed validation for μ rhythm SNR, motor thresholds and, in some cases, phase effect.

4.6.2 Main Sessions

Performance of the real-time system:

Phase targeting. Post-hoc analysis of the C3 Hjorth EEG signal prior to the TMS pulse artifact confirmed phase targeting to be largely accurate, as shown in Figure 21 on page 58.
Power targeting. μ power profile FFT showed on average a satisfactory μ peak for all EEG-triggered conditions (see Figure 22 on page 58). Phase and power targeting visualization of individual subjects can be found in the attachments (27 and 28 on pages 98 and 99). However, there were big within-subject variations in absolute μ power during PAS intervention between conditions (cf. tables 7 and 8), which will be discussed with other possible confounders further on in this section.

[10] gaps between numbers are due to technical issues or changes in screening design

Descriptive data:

Participants. Of the 23 subjects fulfilling all inclusion criteria in the screening, 18 proceeded to take part in the main experiment. Two subjects had to be excluded after 2 and 3 sessions, respectively, because of a decline of μ rhythm SNR that rendered the phase triggering ineffective. The remaining 16 participants completed the experiment and entered analysis. Among those 16, the average age was 24.5 $\pm$ 7.3 years (ranging from 19 to 50 years). 10 were female, 11 (about 69%) had displayed a phase effect during screening.

Repetition sessions. Due to technical difficulties, some of the ITI replay sessions used overly large ITIs, resulting in a longer duration of the PAS intervention than in the template first session which of course defeated the purpose of a replay session. Additionally, the same coding error led to overly long ITIs during PAS in some early sessions. Using an updated Matlab script, the sessions concerned were repeated with all subjects available for a re-measurement (4 out of 5 subjects concerned, 7 out of 9 sessions). We decided to include the remaining two sessions with lengthy ITIs in analysis in order to obtain 16 full sets of data and not compromise statistical validity.

Scheduling. Owing to scheduling constraints of our participants, we managed to only perform 43 out of 64 analyzed sessions in the afternoon. 9 subjects had sessions only in the afternoon and would thus be expected to have highest PAS efficiency [Sale et al., 2007, Sale et al., 2008] due to low cortisol levels, but did not perform better (see subgroup analyses further on in this section). As to within-subject constancy of session timing, we managed to keep sessions within 3 hours of each other in 14 out of 16 subjects. 10 of those had sessions within 2 hours of each other, and 9 of those even within one hour of each other. 3 full days were kept in between sessions in all but one case where it was only 2 full days.

Values only acquired in each subject's first session:

- Mean RMT from SA-PEST was 48.4 $\pm$ 6.2% MSO (range 33 - 61% MSO)
- MEP1mV from SA-PEST was on average 60.1 $\pm$ 9.4% MSO (42 - 74% MSO), thus 124 $\pm$ 8% of individual RMT
- MNS perceptual threshold was 2.80 $\pm$ 0.38 mA (1.90 - 3.30 mA). MNS intensity changed between sessions in one subject
- N20 latency as measured from the SSEPs in the screening session: 19. 6 $\pm$ 1.6 ms (18 - 23 ms)

Plasticity effect:

A quick reminder: MEP amplitudes measured at 8 timepoints (baseline pre-PAS and T0, T15, T30, T45, T60, T75, T90 post-intervention) were the dependent variable. They entered analysis either as absolute values or 'baseline-corrected', i.e., subtracting the individual session's average baseline MEP amplitude from the mean at any of the later measurements.

PAS condition ((i) ITI *Replay* as open-loop condition, (ii) *Power*-triggered (open-phase), (iii) *Peak*- and (iv) *Trough*-triggered) was the independent variable.

In summary, the PAS intervention appeared to not result in any changes from baseline for any condition at any of the measurement times (compare Figures 19 and 20). Let us still take a detailed look at the statistic tests we performed:

Two-way repeated-measures 4x8 rmANOVA did not reveal any significant change in MEP amplitude dependent on

- condition: $p > 0.9$
- time: $p > 0.7$
- interaction analysis (IA): $p > 0.6$

The changes of MEP amplitude change from baseline value, as assessed with a 4x7 rmANOVA of baseline-corrected MEPs, equally did not reach significance:

- main effect condition: $p > 0.8$
- main effect time: $p > 0.7$
- IA: $p > 0.1$

Separate one-way 1x8 rmANOVA of MEPs across time points for each PAS condition resulted in the following p values:

- replay condition: $p > 0.8$
- power-triggered condition: $p > 0.5$
- peak-triggered condition: $p > 0.1$
- trough-triggered condition: $p > 0.3$

1x7 rmANOVA of baseline-corrected MEPs for each condition did not reveal any significant results, either:

- replay condition: $p > 0.3$
- power-triggered condition: $p > 0.6$
- peak-triggered condition: $p > 0.1$
- trough-triggered condition: $p > 0.3$

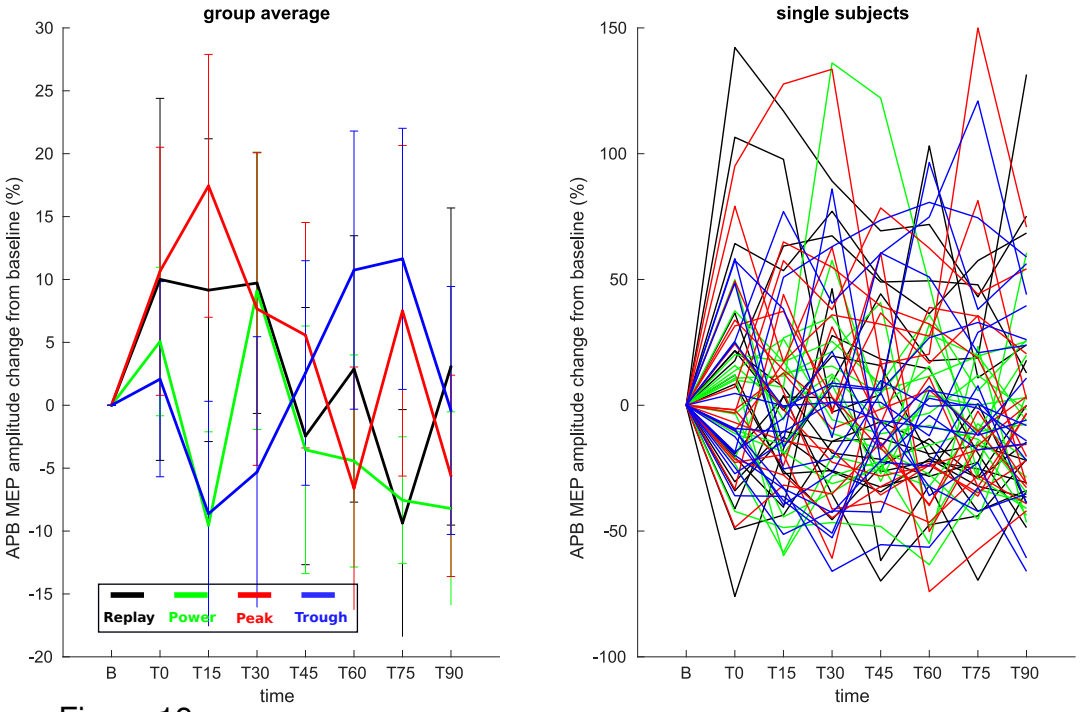

Figure 19: Left panel: group-average MEP amplitudes relative to baseline (mean amplitude at any time-point across all subjects minus mean baseline amplitude).
Right panel: all single subject plots overlayed to showcase the great inter- and intraindividual variability in changes from baseline

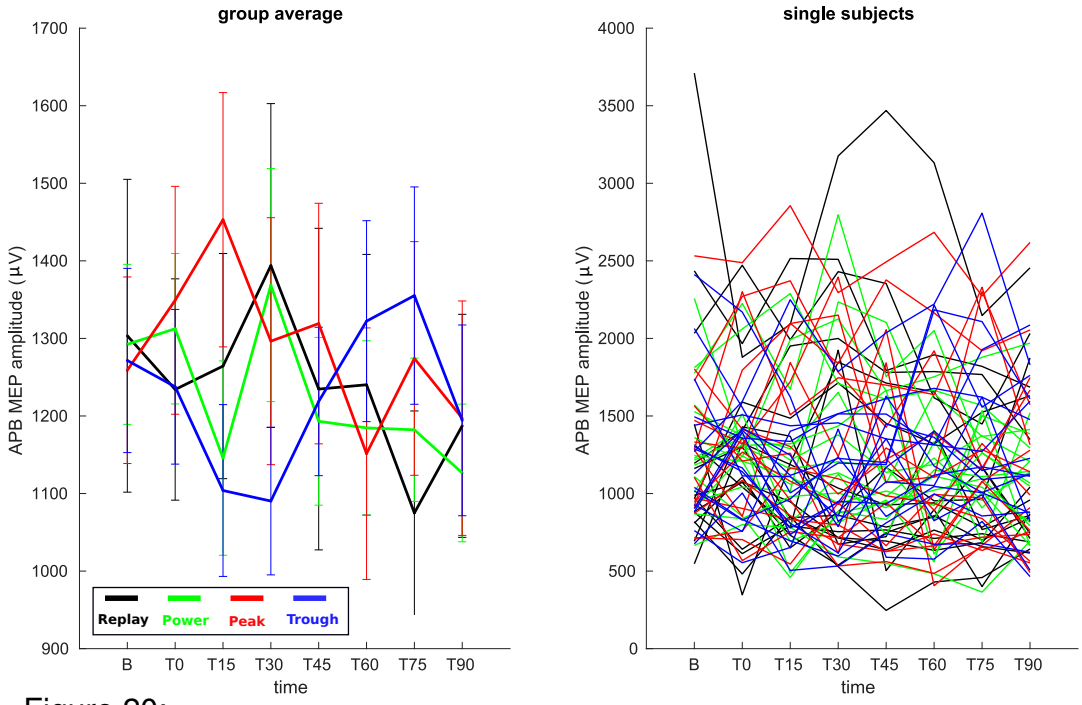

Figure 20: : Left panel: group-average absolute MEP amplitudes across all time-points.
Right panel: all single subject plots overlayed to illustrate the inter- and intraindividual variability in absolute MEP amplitudes in all measurements

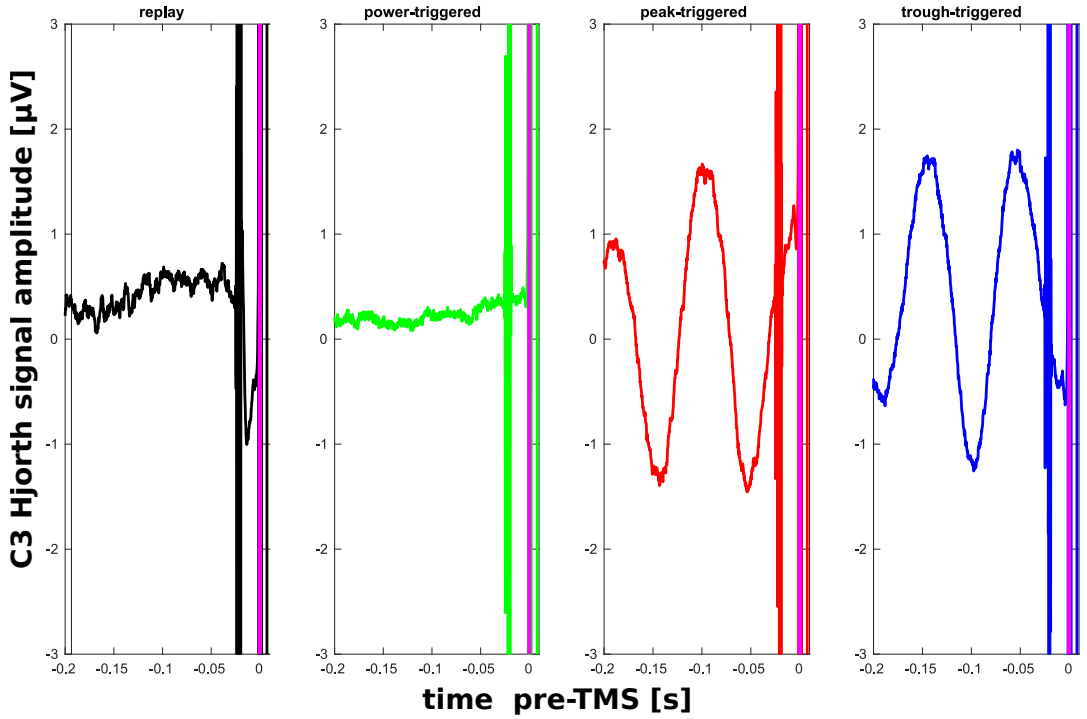

Figure 21: C3 Hjorth signal (amplitude in µV on the y-axis) time-locked relative to delivery of TMS (time '0' on the x-axis) per condition, averaged across all participants. As intended, no oscillations are visible for the open-phase *Replay* and *Power* conditions as all phase angles were 'hit' by TMS equally, resulting in all trials averaging out to zero.

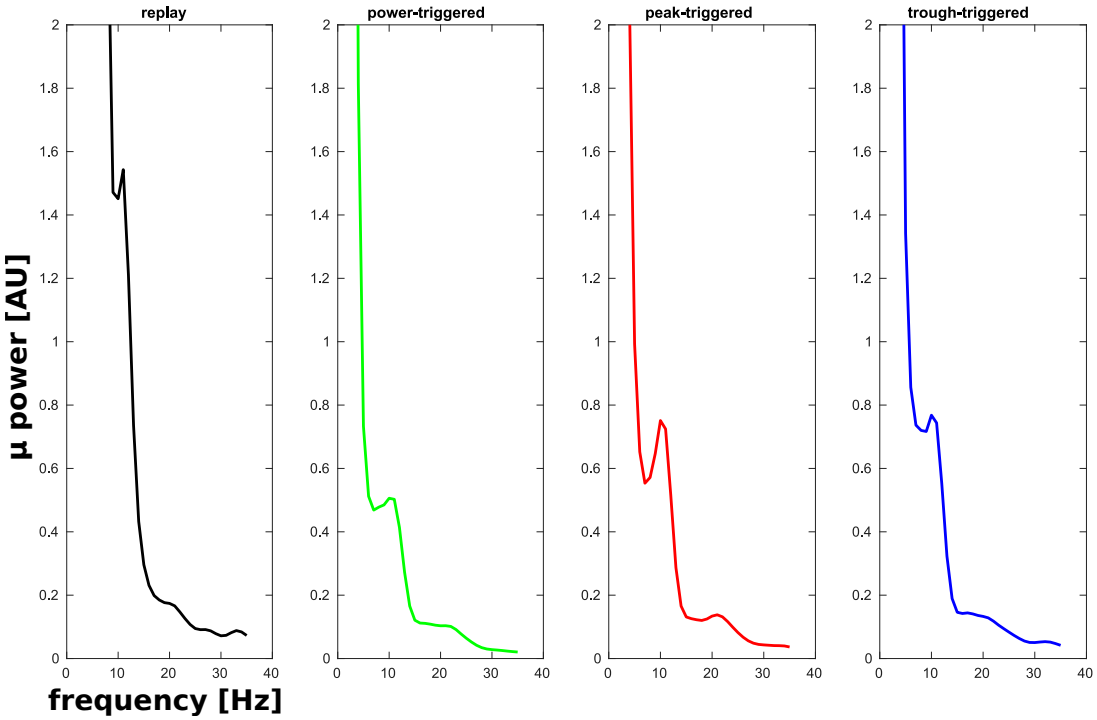

Figure 22: FFT-calculated pre-TMS C3 Hjorth signal power spectra. The *Replay* condition as the only condition without a power trigger requirement shows no distinct μ-$alpha$ peak.

Accordingly, one-sample t-tests against 0 (H1 > 0) for all baseline-corrected MEP measurements across all conditions did not show a significant increase in MEPs from baseline for any time point (all p > 0.1) apart from an isolated significant result for T15 in the peak-triggered condition (t15 = 1.846, p = 0.042). *Peak vs. trough.* In light of the apparently weak effects, we decided to compare only peak- and trough-triggered conditions, as per our hypotheses we expected the biggest difference in effect between these brain states.

2x8 rmANOVA for MEPs did equally not reach level of significance:

- Condition: p > 0.5
- Time: p > 0.7
- IA: p > 0.3

Finally we performed a 2x7 rmANOVA for baseline-corrected MEP amplitudes:

- Condition: p > 0.8
- Time: p > 0.7
- IA: $F_{6,90}$ = 2.350. p = 0.037

Thus, the only comparison that reached statistical significance between MEP time courses for peak- and trough-triggered PAS.
Post-hoc tests (one-sided paired t-tests) were however not able to show any significant difference supporting our hypothesis (more LTP in trough- than peak-condition) in baseline-corrected MEPs at any of the 7 post-intervention time-points (all p $\geq$ 0.1).

From inspection of plotted MEP timelines (group average in Figure 19 on page 57), these non-significant differences in MEP changes between peak- and trough-triggered sessions seem to follow a direction contrary to our hypotheses: the data favor a slight initial increase of MEP amplitudes for peak-triggered and a slight initial decrease for trough-triggered PAS sessions until about 45 minutes after intervention. After this the amplitudes seem to undergo a brief counterdirectional deviation from baseline before ending up at a level at or slightly below baseline amplitude.

The underlying MEP data are subject to great inter- and intraindividual variability (cf. subjectwise plots in the attachments on page 100) and apart from T15 in the peak-triggered sessions (see above), at no single time point in any of the conditions did one-sample t-tests against 0 (H_1 > 0) for baseline-corrected MEPs reach significance (all p > 0.1).

Neither the power-triggered nor the replay condition revealed any discernible trends or significant changes in the time course of MEP amplitudes.

Subgroup analyses. We considered it plausible that a relevant difference between peak- and trough-triggered PAS would appear only or more strongly in individuals who had displayed a discernible phase effect on excitability during screening. A sub-group analysis of only the 11 subjects with a phase effect during screening did not yield any significant results for MEPs over time or difference between conditions using the same tests as described above (also when comparing only peak- and trough-triggered sessions) (all $p > 0.1$).
In view of the wildly fluctuating MEP amplitudes at baseline, we additionally analyzed only participants with baseline MEPs 'close to target' in all four sessions (between 0.7 and 1.5 mV, n = 6). This did not yield any significant outcomes. A subgroup of subjects that had only had sessions in the afternoon (n = 9) did not display enlightening results, either.

Possible confounders:
We observed a remarkable variability of MEP amplitude at baseline and absolute μ power during PAS both between and within subjects. Therefore, we performed additional statistical analyses (4x1 rmANOVA) to verify that each of these factors did not vary in correlation with either EEG condition or sequence of sessions (accumulating over time) within one subject and thus did not confound results. We also opted to enter PAS duration and ITIs within PAS, stimulation intensity, and μ frequency into these analyses, as they changed – albeit moderately – between sessions, too.

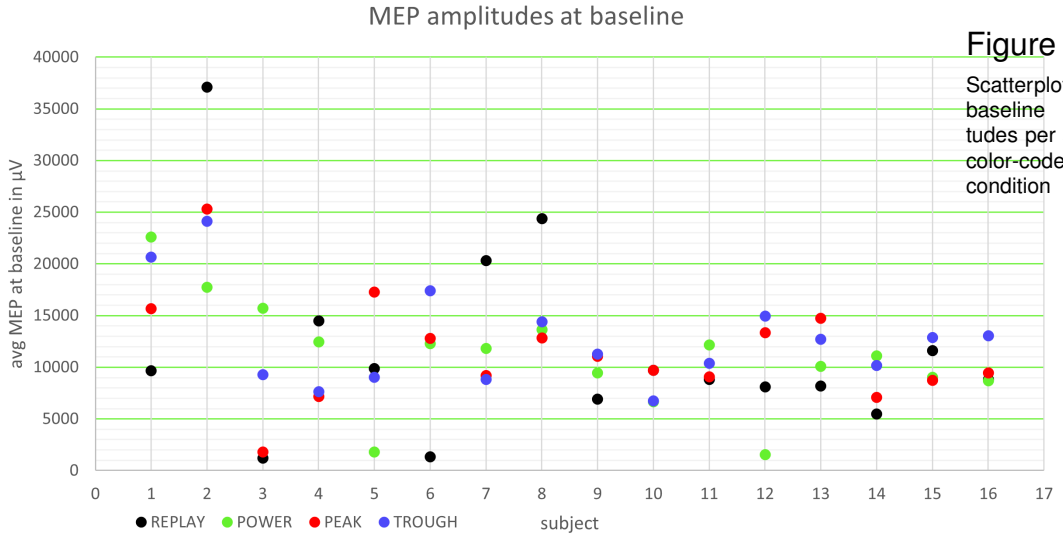

Figure 23: Scatterplot of baseline amplitudes per subject, color-coded per condition

MEP amplitude at baseline varied between subjects and between sessions within a subject, as can be seen in Figure 23, a phenomenon that extended to the post-PAS measurements, cf. Figure 20 on page 57. Again, single-subject plots can be found attached on page 97. A one-way rm-ANOVA test revealed, however, that the average amplitude at baseline did not depend in a statistically significant manner ($p > 0.7$) on the condition or number of session ($p > 0.9$).

Absolute power values during PAS (mean of all 500 ms pre-TMS powers during the PAS intervention) changed by up to 695 AU (arbitrary units) between conditions within one subject, depicted in figures 24 and 25. 4x1 rmANOVA yielded non-significant trends for both condition and session number (both $p = 0.085$), so we followed up with post-hoc tests. Two-sided paired t-tests for the absolute power values between any combination of conditions or sessions did not reach significance level, however (all $p > 0.2$).

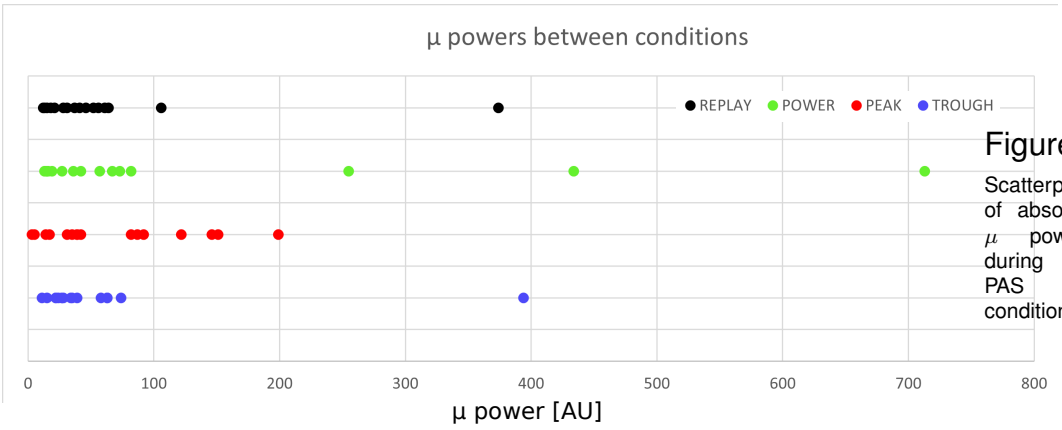

Figure 24: Scatterplot of absolute μ powers during PAS per condition

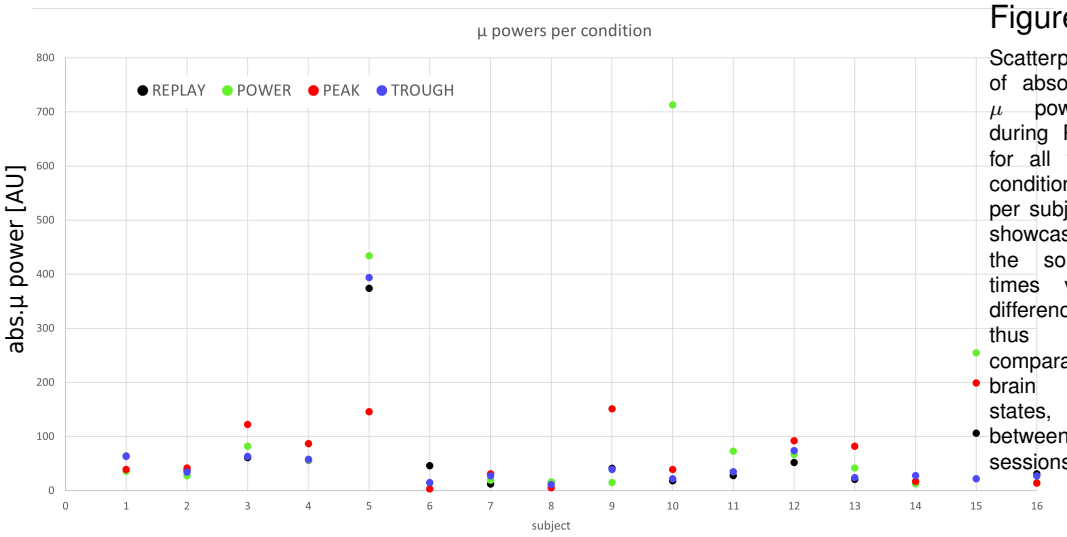

Figure 25: Scatterplot of absolute μ powers during PAS for all four conditions per subject, showcasing the sometimes vast differences, thus not comparable brain states, between sessions.

Stimulation intensity changed between sessions in 8 out of 16 subjects, by a maximum of 16% MSO in one subject. A one way rmANOVA (4x1) did not point to a significant influence of condition (p = 0.1) or session (p = 0.2).

μ *peak frequency* changed in 10 out of 16 subjects between sessions, by a maximum of 2 Hz within one subject. Condition (p > 0.2) or session (p > 0.5) did not significantly affect peak frequency.

PAS durations varied from 9.1 to 21.0 min, with a mean of 11.9 $\pm$ 1.3 min and a tendency for longer duration in the Replay session (cf. Figure 26 and Table 7). There was no significant difference in PAS duration between sessions (p > 0.4). Comparison between conditions approached significance (p = 0.089), but two-sided paired t-tests between conditions were not significant.

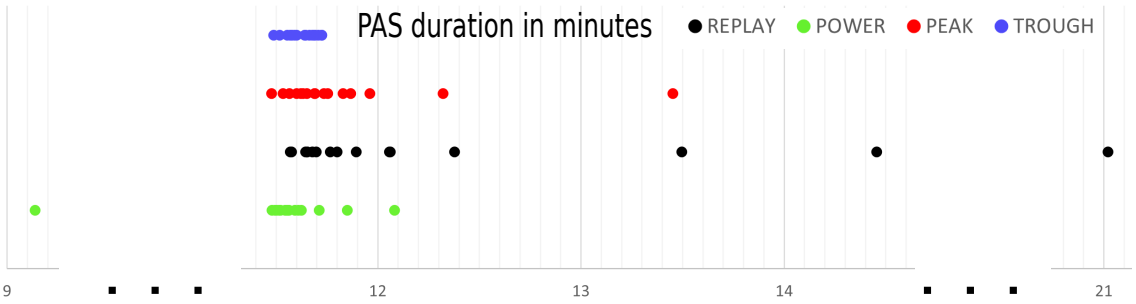

Figure 26: Scatterplot of the durations of the PAS interventions per condition

ITIs naturally followed PAS durations, with the longest inter-trial intervals in the Replay condition (mean 3.45 s vs. 3.12 s in Trough), but equally without a *significant* difference between conditions (p = 0.074 in 4x1rmANOVA, all p > 0.07 in post-hoc tests).

Within one subject, *MEP amplitudes* between sessions and within one time-point were also very unstable, as visualized by the standard deviations in tables 5 and 6.

To illustrate within- and between-subject variability, μ peak frequency, SI, PAS duration and absolute μ power during PAS (of sessions entering analysis, i.e., including repeated sessions) are depicted as average across all sessions, differences over time (first through fourth session per subject) and between conditions in tables 7 and 8.

4.7 MUPAS. Discussion

The following section is comprised of a statement of specific limitations, and possible explanations for the nil results we obtained. I will subsequently touch on how the decision to apply EEG-triggered TMS impacted experimental design and subject pool, which is of course partially relevant for MUPEX, too. Finally I will go beyond the findings from this specific experiment and analyze the 'real-life' applicability of TMS plasticity protocols in general and PAS in particular.

4.7.1 Limitation: Influences on plasticity induction not accounted for

Hormones: In order to enable recruitment of a sufficient number of suitable subjects (keeping in mind the already quite selective screening process owing to our inclusion criteria listed in 2.1) within a reasonable time frame, we decided not to exclude female participants, even those not on hormonal contraception. In-vivo evidence for influences of the female cycle on TMS-assessed cortical excitability remain scarce - possibly due to the same reasons. However, some TMS studies [Smith et al., 1999, Smith et al., 2002, Inghilleri et al., 2004] reported evidence that cortical excitability is reduced during periods of high progesterone levels (such as the luteal phase, i.e., the second half of the female cycle) and increased when estrogen is high (such as prior to ovulation in the late follicular phase).
This has been explained by the allosteric GABA-A-receptor agonism of progesterone metabolites (a function similar to benzodiazepines) [Lan and Gee, 1994] and by the increase of glutamate-mediated neuronal excitability by estrogen [Woolley et al., 1997]. Plasticity studies focusing on menstrual cycle changes are even more few and far in between: [Tecchio et al., 2008] observed a reduction in LTP-PAS effects with age only in postmenopausal women and attributed this to the low estrogen levels after menopause. In essence, differing hormone levels within and between female subjects during their sessions could plausibly have introduced a further measure of variance in plasticity induction.

Nicotine has been shown to influence (PAS-mediated) cortical plasticity, its most relevant property for our experiments being a blocking of facilitatory plasticity in smokers during nicotine withdrawal [Grundey et al., 2012], a subject factor not accounted for.

Physical activity: [Cirillo et al., 2009] were able to induce LTP-PAS only in physically highly active subjects (>150 min of exercise per day) and not in sedentary participants (<20 min of exercise per day on at most 3 days per week), pointing to physical activity as an important modulator for neuroplasticity.

Table 5: Absolute MEP values across participants at each time-point. Displayed is the mean ± SD [mV]

	BL	T0	T15	T30	T45	T60	T75	T90
Replay	**1.16** ± 0.90	**1.23** ± 0.57	**1.13** ± 0.70	**1.24** ± 0.92	**1.23** ± 0.83	**1.16** ± 0.74	**1.04** ± 0.58	**1.14** ± 0.63
Power	**1.10** ± 0.53	**1.23** ± 0.51	**1.02** ± 0.45	**1.30** ± 0.68	**1.08** ± 0.57	**1.06** ± 0.58	**1.02** ± 0.49	**1.01** ± 0.50
Peak	**1.16** ± 0.53	**1.28** ± 0.66	**1.34** ± 0.70	**1.01** ± 0.76	**1.20** ± 0.65	**1.15** ± 0.65	**1.24** ± 0.66	**1.05** ± 0.52
Trough	**1.27** ± 0.48	**1.19** ± 0.48	**1.00** ± 0.56	**1.04** ± 0.46	**0.95** ± 0.61	**1.22** ± 0.66	**1.06** ± 0.66	**1.14** ± 0.57

Table 6: Difference from baseline across participants at each time-point. Displayed is the mean ± SD [mV].

	T0	T15	T30	T45	T60	T75	T90
Replay	**0.10** ± 0.58	**0.06** ± 0.47	**0.10** ± 0.41	**-0.02** ± 0.41	**-0.03** ± 0.33	**-0.09** ± 0.36	**0.03** ± 0.50
Power	**0.05** ± 0.23	**-0.06** ± 0.27	**0.03** ± 0.24	**0.00** ± 0.38	**-0.07** ± 0.31	**-0.07** ± 0.20	**-0.03** ± 0.27
Peak	**0.11** ± 0.39	**0.19** ± 0.41	**0.06** ± 0.49	**0.06** ± 0.36	**-0.06** ± 0.37	**0.11** ± 0.50	**-0.04** ± 0.31
Trough	**0.02** ± 0.31	**-0.05** ± 0.35	**-0.01** ± 0.40	**0.06** ± 0.33	**0.11** ± 0.44	**0.13** ± 0.41	**0.04** ± 0.28

Table 7: Consistency of parameters across MUPAS conditions. Displayed is the mean ± SD.

	replay	power	peak	trough
μ **peak [Hz]**	**10.9** ± 0.9	**11.2** ± 1.0	**11.0** ± 0.7	**11.3** ± 0.9
SI [% MSO]	**59.4** ± 9.8	**59.7** ± 9.0	**60.5** ± 10.2	**58.4** ± 9.2
PAS duration [min]	**12.7** ± 2.4	**11.5** ± 0.6	**11.8** ± 0.5	**11.6** ± 0.1
μ **power [AR]**	**60.9** ± 87.0	**117.4** ± 194.3	**69.0** ± 59.3	**58.5** ± 91.4

Table 8: Consistency of parameters across MUPAS sessions (in per-subject order). Displayed is the mean ± SD.

	All sessions	S1	S2	S3	S4
μ **peak [Hz]**	**11.1** ± 0.8	**11.2** ± 0.8	**11.1** ± 0.8	**10.9** ± 0.9	**11.1** ± 1.0
SI [% MSO]	**59.5** ± 9.3	**58.8** ± 9.3	**60.2** ± 9.7	**60.1** ± 9.2	**59.1** ± 10.0
PAS duration [min]	**11.9** ± 1.3	**11.7** ± 0.2	**11.7** ± 0.1	**11.6** ± 0.8	**12.5** ± 2.4
μ **power [AR]**	**76.5** ± 119.2	**135.6** ± 189.3	**47.3** ± 37.1	**66.4** ± 94.0	**56.4** ± 91.8

While we did not collect these data from our subjects, it is to be assumed that most would engage in physical activity at a level in-between these somewhat extreme groups. However, it appears highly unlikely that LTP-PAS responders over numerous studies, in the absence of specific recruitment for this characteristic, regularly perform this extraordinarily high amount of exercise.

4.7.2 Interpretation of MUPAS results

We were not able to induce any plasticity effect with our PAS protocol. Also, differences between conditions were not significant and the experiment suffered from a large inter- and intra-subject variability in MEP amplitude and absolute μ power during the PAS intervention.

Despite the high variability in PAS effects that inspired the conception of MUPAS in the first place and that has been extensively discussed previously in this thesis, PAS is by and large a well-established plasticity-inducing NIBS protocol with manifold studies reporting evidence as to its efficacy (as evident from the extensive reviews [Wischnewski and Schutter, 2016, Suppa et al., 2017]).
Our concept, intended to reduce variability of PAS results, might have achieved the opposite and decreased reliability further: We could conceivably have artificially dispersed and diluted these weak effects by splitting them into several EEG conditions with their own respective effects rather than condensing a stronger and more reliable effect with specific triggering conditions as intended. Consistency over four sessions per subject equally constitutes a complicating aspect, crucial for valid comparisons between conditions.
We will proceed now to look at some of the factors that could have impeded plasticity induction and differences between sessions in this specific case.

Phase effect in screening and main experiment:

As described in 4.6.1, we had a phase effect responder rate of 52% in participants that had previously passed validation for strong μ-$alpha$ peak, MEP1mV of maximum 80% and accurate phase targeting 'pre-view'. This rate is inconsistent with measurements conducted about the same time within the same group which used the same real-time system as well as similar setup and inclusion criteria: [Schaworonkow et al., 2018b] reported the existence of a phase effect in 13 out of 15 participants [Zrenner et al., 2018] in 11 out of 12 and 9 out of 11, respectively. This apparently lower prevalence among our participants deserves critical examination, as we originally considered the existence of a phase effect on excitability to be a prerequisite for our hypothesis of an analogue effect on plasticity (see 4.3).

Reasons for our poor phase effect responder rate can be sought

(1) in stimulation parameters, as the aforementioned experiment [Schaworonkow et al., 2018b] points at a higher probability of finding a phase effect when using lower SIs. The authors recommend 20% of individual IOC, data from MUPEX point to our MEP1mV being closer to 50% IOC. On the other hand, the same study found the biggest absolute phase effect, which was essentially what we were identifying with the plotted average, at about 50% IOC. To wit, [Bergmann et al., 2019] reported a significant phase effect stimulating with MEP1mV.
Schaworonkow et al.'s second recommendation of at least 150 number of trials per condition has already been amply fulfilled by our original 200 pulses per condition.
A possible explanation for the phenomenon of SI-modulated variation of phase effect is a 'saturation' of neuronal response: Very strong stimuli elicit a response close to the maximum, lessening an influence of phase that is more apparent with weaker pulses. Considering the bias towards larger MEPs in our results, we could well have missed a potential difference in PAS inducibility between phases that might have been detectable with lower SI.

(2) in calculation of phase effect: As described in 4.4, we determined the existence of a phase effect through visual appraisal of overlapping curves showing MEP sizes for peak- and trough-triggered trials averaged over all pulses for the respective condition. When reviewing evidence on a μ-$alpha$ phase effect on corticospinal excitability, one is struck by considerable dissimilarities in the calculation and cut-off for declaring the existence of this effect and by extension the rate of participants displaying it ('phase effect responder rate'): [Zrenner et al., 2018] likewise plotted the average MEP amplitude of trough- versus peak-triggered trials, but normalized to the individual mean. The same authors mentioned multiple times before have, in a different publication, reported multiple calculation approaches [Schaworonkow et al., 2018a], which have a pairwise comparison of subsequent trials in common (the ith peak-triggered MEP with the ith trough-triggered MEP), both in a yes-or-no manner (percentage of trial pairs per participant for which the trough-triggered MEP is larger in amplitude than the peak-triggered MEP) and for the N/P-fraction, by which they intend to *"reduce the impact of slow time effects on MEP size"* [Schaworonkow et al., 2018a]. Across participants still only about 60% of trials showed any phase effect in the expected direction. Considering the very low probability of two subsequent trials having the exact same amplitude due to the large variability of MEPs as mentioned several

times before, it can be inferred that also a considerable fraction of trial pairs in those experiments displayed in essence an (albeit perhaps small) 'reverse phase effect', calling into question the universal physiological meaning of any effect of μ phase on excitability. In the study cited before, [Schaworonkow et al., 2018b], phase effect was calculated using the ratios of median MEP amplitudes per condition, thereby reducing the impact of extreme outlier MEP values.
In contrast, [Madsen et al., 2019] regarded mean MEP amplitudes per phase condition (averaged over all participants and trials) and reported no statistically significant influence of phase on MEP amplitude.
For future experiments, a generally accepted standard on both the stimulation parameters used to study phase effect, and a definition (and thus standard method of calculation) of what constitutes an existent phase effect and therefore separates 'responders' from 'non-responders' would greatly aid comparison and interpretation of reported results.

Plasticity induction:
(1) Even though MNS threshold itself appears to not impact LTP-PAS efficiency [Müller-Dahlhaus et al., 2008], in our participants the *intensity of median nerve stimulation* of three times the perceptual threshold was sometimes supramotor (elicited APB muscle contractions visible to the naked eye). Thus the target muscle had in some cases been peripherally activated shortly prior to the contraction elicited by the TMS pulse, a possible confounding influence on CSE:
LTD-rTMS is more efficient when supramotor than submotor [Lang et al., 2006] peripheral nerve stimulation is applied. In fact, supramotor repetitive peripheral nerve stimulation (rENS) alone is able to induce input-specific cortical LTP- (intermittent 10 Hz trains with 500 ms on-500 ms off stimulation over 2 hours [Ridding et al., 2000, Charlton et al., 2003]), or LTD-like plasticity (continuous 1 Hz stimulation over 15 min [Lang et al., 2006]). Direction of plasticity seems to depend either on frequency (akin to classical rTMS protocols) or continuous versus intermittent pattern of stimulation (akin to TBS) – in any case pointing to a 'global' effect of input pattern, whether in the form of direct TMS of motor cortex or via re-afferent input to M1 via rENS-induced muscle twitches. In our case, peripheral nerve stimulation was delivered irregularly at about 0.31 Hz on average, a pattern that has not been tested for rENS alone.
Although most PAS studies titrate MNS SI to 3 times the perceptual threshold (like we did in MUPAS), often without reporting relation to motor thresholds – and LTP-PAS has also been successfully performed using the motor threshold as SI of MNS [Kamke et al., 2012], the variability of MNS motor threshold to 300% of

perceptual threshold we observed both within and between subjects might well have distorted plasticity induction.

Another issue with peripheral nerve stimulation is that the sensation eventually surpasses discomfort and develops into pain – the threshold and its relation to the individual perceptual threshold of course subject to high interindividual variability. Pain has been shown to reduce MEP amplitudes during application of the painful stimulus [Suppa et al., 2013, Larsen et al., 2018]. However, one study has shown successful cortical LTP induction through 'pain-PAS', i.e., using an intentionally painful peripheral stimulus as the first of the paired pulses (notably, no plasticity effect was observed when applying only the painful stimuli without TMS) [Suppa et al., 2013]. Similarly, induced local pain has not impeded training-induced motor plasticity as assessed by TMS [Ingham et al., 2011].
All in all, these characteristics of peripheral nerve stimulation, if detrimental at all, will apply to all studies employing paired associative stimulation. As with the other confounding factors that will be discussed in the following sections, in the case of a multi-session experiment like MUPAS, inadvertent inconsistencies between sessions could have obscured meaningful differences in target effect (plasticity) between conditions.

(2) We employed an *EEG-triggered 'two-region protocol'*: Exceeding the already complex mixed excitatory and inhibitory synaptic connections between different cortical regions that influence TMS effects even when we focus direct stimulation on one cortical area (see 3.5.2), paired associative stimulation involves both an indirect stimulation of S1 through MNS as well as direct TMS of M1. Thus two functionally distinct cortical regions with possibly their own respective rhythms (μ-$alpha$ and μ-$beta$), perhaps connected μ timelines[11], multiple interconnections of facilitatory and inhibitory nature are involved, making it rather more difficult to identify any one brain state favoring positive plasticity induced by this protocol.
It can be argued that a more excitable S1 will have a stronger input to M1, which while inhibitory on the single trial level (cf. SAI) over time presumably contributes to the induction of positive plasticity, i.e., an increase of corticospinal excitability, if followed by stimulation of M1 (cf. 4.1) - but an M1 inhibited by an excitable S1 at the same point in time could arguably weaken plasticity induction.
In contrast, a different method of inducing LTP-like plasticity applied in the same lab, using 100 Hz triple pulses at a 1 Hz repetition rate applied only over M1,

[11] The 'travelling wave theory' with some evidence of fixed phase shifts within one frequency between neighboring regions [Schaworonkow et al., 2018a] is a fascinating observation the details of which however exceed the scope of this dissertation.

has shown a clear phase dependency: triplets applied during μ troughs resulted in LTP whereas the peak-triggered condition showed no plasticity effect [Zrenner et al., 2018]. In line with these findings, Baur et al. [Baur et al., 2020] from the same group reported an LTD effect of 1 Hz rTMS only at μ peaks.

(3) Consistency of parameters other than our independent variable (EEG trigger of PAS intervention) is a crucial aspect in this. Despite the measures in place (described in 4.5), there was a considerable degree of inhomogeneity both between sessions within one subject and between subjects (section 4.6.2) regarding MEP amplitudes at baseline, absolute μ powers, and in some cases hotspot locations compared to the previous stimulation sites saved in Localite (although the latter, apparent deviations between hotspots across sessions within one subject, were most likely due to slight inaccuracies in cap positioning and scalp surface registration).

Most PAS experiments target a *baseline MEP amplitude* of at most 1mV. We observed in our baselines a bias towards larger (up to an average baseline of 3.7 mV in one session) MEPs, which could assumably prevent any significant further increase through plasticity induction due to a 'saturation effect' of neuronal response analogous to the IOCs of spontaneous excitability (as acquired e.g. in MUPEX). Higher MEP values are closer to the plateau of the IO-curve where MEPs do not grow further with increasing stimulation intensity. In the few publications acquiring IOCs pre- and post-intervention in plasticity protocols (however still using MEP1mV as SI of the conditioning stimulus during PAS), a steepening of the right side of the IOC [Cirillo et al., 2009, Kumpulainen et al., 2012] is reported – none of these curves really explore the right-most, plateau part of the IOCs, however. Assuming a steepening of the IOC post-intervention, but with an unchanged maximal amplitude, plasticity could only be induced up to a certain MEP size. Conversely, LTD-inducing rTMS protocols have proven to be more efficient when applying higher SIs. [Fitzgerald et al., 2006, Bagnato et al., 2005] could only increase SICI with a 1 Hz rTMS protocol if pre-intervention SICI was not already too pronounced, hinting at regulating mechanisms akin to homeostatic metaplasticity (compare 4.1). Still, even in the MUPAS sessions with on-target or smaller baseline MEP amplitudes no significant plasticity effect could be induced (see 4.6.2) and baseline amplitude did not depend significantly on condition.

Absolute μ-$alpha$ *power* fluctuated strongly between sessions within one subject, differing by up to 695 AU between conditions, but not depending significantly on the condition. Hence, brain states were ultimately not comparable between

sessions, which could have concealed a meaningful difference between conditions. On the other hand, had we not implemented a running power spectrum update but kept our trigger thresholds based on each subject's first session's calibration EEG, the PAS interventions would have suffered from cripplingly long inter-trial intervals, an issue discussed in section (ITI) further on.

(4) The principle of *homeostatic metaplasticity* and how it shapes interactions between temporally associated plasticity processes, be they induced by NIBS or through motor learning, has been extensively described in 4.1 and is clearly of particular poignancy in a multi-session plasticity experiment such as ours. Carry-over effects from previous PAS sessions are however unlikely in this case as we managed to keep a minimum of 3 full days between sessions in all but one case in accordance with NIBS guidelines, which far exceeds any duration of effect observed after a single PAS session.
We did furthermore discourage subjects from pursuing activities involving motor learning in the days prior to a session, but of course these processes can never be fully avoided or accounted for. It is therefore possible that differences in current LTP thresholds between subjects and between sessions of one subject have blurred the effects of the PAS intervention and differences between conditions.

(5) Attention influences PAS effects, with increasing grades of attention on the target muscle area increasing efficiency of LTP-inducing protocols [Stefan et al., 2004]. On the other hand, solving (complex) cognitive tasks during PAS can block the effect completely [Stefan et al., 2004, Kamke et al., 2012].
We instructed our subjects to keep their attention fixed on the crosshair and did not specifically tell them to concentrate on the perception of the MNS and TMS pulses during the intervention so as not to skew the μ power range, as we were aiming to study the effect of μ oscillations at rest. Many other PAS experiments either direct participants to focus visual and tactile attention on the targeted hand [Fratello et al., 2006], set them a targeted attentional task such as counting MNS stimuli [Müller-Dahlhaus et al., 2008], or employ visuo-auditory EMG feedback [Stefan et al., 2000, Wolters et al., 2003, Ziemann et al., 2004].
All of those methods – whether intended to explicitly increase efficiency, or keep μ power stable or reduce the amount of trials with EMG pre-innervation – will focus participants' attention on the targeted hand to a higher extent than just asking them to relax the hand as we did. Hence the absence of attentional focus on the targeted right hand could have discouraged LTP-like plasticity.

(6) Last but perhaps most decisively, our EEG-triggered PAS interventions had *irregular ITIs* by necessity (see also 3.5.2). Although the need for a stable trial frequency in PAS interventions is at first perhaps less apparent than in analyzing MEP amplitude as an online dependent variable, the lack of a fixed ITI between the paired stimuli is what really sets our approach apart from the vast majority of PAS studies, which employ a set frequency for the paired pulses, with 0.05 to 0.2 Hz appearing most efficient [Wischnewski and Schutter, 2016]. In this case, the length of the PAS intervention was on average 11.9 ± 1.3 min with mean ITI within a session varying from 3.1 to 5.6 s, thus mean frequencies per session of 0.18 to 0.32Hz. Decisively, ITI length varied within one session, too. To the knowledge of this author, no other PAS studies with strongly varying ITIs have been published so far - a single study [Bergmann et al., 2008] had slightly jittered ITIs between 5.1 and 6.9 s. The absence of a fixed frequency for the paired pulses could well have impeded plasticity induction, although overall duration of intervention varied very little and neither duration of the PAS segment nor mean ITIs depended significantly on conditions.
The average frequency of PAS paired stimuli across all sessions was about 0.31 Hz, which exceeds the recommendation from Wischnewski's review [Wischnewski and Schutter, 2016]. However, also high-frequency PAS protocols up to 5 Hz have yielded good plasticity results [Quartarone et al., 2006, Tsang et al., 2015] with [Quartarone et al., 2006] even reporting a plasticity effect lasting 6 hours after stimulation, therefore outperforming classical PAS, after 2 minutes of 5 Hz PAS (600 paired stimuli).

In summary, all of the factors mentioned in the preceding sections might have skewed results in directions varying between subjects and sessions, preventing plasticity induction and obscuring any difference between conditions.
Regardless of our nil results in plasticity induction, we also proposed to find meaning in EEG oscillations about brain states, e.g. in MUPEX. Our hypotheses, particularly pertaining to the so-called phase effect, are partially based on results from the same research group. It is therefore vital to critically inspect the way our lab selects the participants for its experiments. I will continue from this examination of applicability of our group's findings towards the corresponding question for TMS plasticity protocols, touching on why they are promising for clinical application and why they are not ready for it yet, and finally - after our failed attempt at improvement by EEG-triggering – what other modifications could make them so.

4.7.3 Applicability

More efficient or efficient for more?

While it is fairly easy to understand the technical necessity of our subject criteria such as μ peak and motor thresholds (cf. 2.1), both these requirements and our recruiting environment unquestionably introduce bias, including factors known to influence cortical functions. These aspects arguably lessen the applicability of our findings to the general population, especially the patient population with neurological diseases that we want to apply our plasticity protocols on.

It is presently still unclear why in all screenings thus far conducted in the BNP lab, a considerable portion of volunteers do not display a μ rhythm with an SNR sufficient for accurate EEG-triggered stimulation. We assume, after all, a general physiological role of the properties of this rhythm. Possibly this is due to natural interindividual variability in cortical anatomy [Zilles et al., 1997] rather than a difference in physiology – a slight shift of the shape and position of gyri and sulci would make an individual's sensorimotor μ harder to pick up with a standard montage.

[Schaworonkow et al., 2018a] compared the standard C3 Hjorth montage with electrode filters individually computed to maximise μ-SNR with participants from the BNP subject pool. They did not find any significant difference in phase targeting and resulting phase effect. However, the subject pool consisted of individuals already pre-selected for their high μ-SNR in the standard C3 Hjorth montage, which might in their case be of comparable accuracy to the individual filters. It remains to be seen whether individuals usually excluded from our experiments due to insufficient μ-SNR might benefit from those or other individual filters based on anatomically guided source-level reconstruction, possibly opening up efficient phase-triggered TMS for a wider range of participants.

Recruitment of previous BNP subjects follows more or less 'naturally' from these low inclusion rates, leading to overlapping subject pools which further lessen the generalizability and statistic validity of our findings.

To find volunteers in the first place, we sent a circular mail to all student accounts of the University of Tübingen advertising our experiments. This leads to our volunteers being predominantly quite young and generally healthy (surpassing the TMS-safety requirement for absence of neurological and psychiatric disorders) as well as university students. Most other publications applying NIBS in healthy individuals have a very similar sampling bias. I will elaborate on the discrepancy between subjects and intended population in the following section.

Applicability of NIBS plasticity protocols:

a) Population

There is an obvious and striking difference between the participants in most experiments studying PAS and other plasticity-inducing NIBS protocols and the intended patient population in future applications: Most stroke patients are 65 years or older, and the risk for persisting functionally relevant (motor) deficits requiring the kind of intensive rehabilitation that would call for NIBS-enhanced strategies further increases with age [Roy-O'Reilly and McCullough, 2018]. Numerous comorbidities further distinguish stroke patients from the average study participants, but let us focus on the organ directly affected by NIBS: the brain. Post-stroke patients are at a considerably higher risk of epileptic seizures (about 11% risk within the first 5 years after stroke [Burn et al., 1997]) which adds a safety concern to TMS application: TMS can in rare cases elicit seizures, more so for higher-frequency rTMS protocols (cf. 1.6.2) which are also in use in plasticity induction. In clinical application, this risk is often alleviated by opting to treat the contralesional hemisphere with inhibitory/LTD-inducing protocols (physiological reasoning for this below) rather than activating/facilitating the ipsilesional one. Most studies employing rTMS or PAS in post-stroke patients will still either explicitly exclude patients with post-stroke seizures [Kwon et al., 2014, Kim et al., 2006, Chang et al., 2010, Takeuchi et al., 2008] or state that they applied exclusion criteria according to common TMS safety guidelines/contraindications [Palmer et al., 2018, Tarri et al., 2018], implying an exclusion of (post-stroke) seizure patients – in the studies mentioned, no adverse effects of stimulation were reported.

Pertaining specifically to EEG-triggered plasticity protocols, it is conceivable that at least with large cortical infarctions, μ rhythm SNR would be declined, rendering power and phase triggering massively inaccurate to the point of impracticality.

b) Relevance

Aside from safety concerns, it is of course vital to ascertain if enhancement in motor cortex excitability, being the target achievement of plasticity-inducing NIBS protocols, actually translates to improved motor function relevant for 'activities of daily living' (ADL), such as the ability to take care of personal hygiene, (device-assisted) mobility, preparation and eating of meals [Brach and VanSwearingen, 2002] – in short, degree of independence from caregiving.

Let me precede the following paragraph by stating that there is still a definite lack of studies assessing long-term functional effects of plasticity-enhancing protocols, more so for PAS than for rTMS. Experiments recruiting stroke patients rather than healthy participants are even more few and far between. Due to the scarcity of

PAS application studies, I will be incorporating some evidence from rTMS experiments.

First off, ipsilesional M1 does show decreased excitability, stemming not only from reduced excitatory corticospinal output (particularly in the acute early days after stroke [Swayne et al., 2008]), but also from increased interhemispheric inhibition [Murase et al., 2004] to the extent of maladaptivity: A reduced inhibition of the contralesional hemisphere by the ipsilesional one causes a shift in balance among the reciprocal inhibitory interhemispheric connections. This phenomenon has been transduced to the development of contralesional inhibiting protocols - which might, however, be more adequate to smaller strokes, where residual ipsilesional function is not realized fully due to interhemispheric inhibition, whereas in bigger lesions, the contralesional hemisphere is relevantly implied in processes of 'vicariation', i.e., taking over function of infarcted areas [Di Pino et al., 2014].

Second, there is some evidence for a correlation of improvement in motor cortex excitability with functional improvement: [Koski et al., 2004] reported a correlation between short-term CSE-increasing effects of occupational therapy (including increased MEP amplitudes such as achieved by PAS in other studies, but also, relating back to the interhemispheric imbalance just discussed, reduced discrepancy between MEPs between hemispheres) and long-term functional motor improvement. [Frantseva et al., 2008] showed that LTP-PAS effects were correlated with successful motor learning in healthy and schizophrenic participants.

By contrast, [Player et al., 2012, Palmer et al., 2018] did not find a correlation between PAS effects and motor learning despite achieving a significant increase in MEP amplitudes post-intervention.

c) Effect duration

Effects of classical PAS and other plasticity-inducing TMS protocols in healthy individuals generally last an hour at most, with some studies reporting a duration of up to two hours [Grundey et al., 2012] – a period of time hardly relevant for stroke recovery. Several adaptations of protocols have been developed to amend this issue:

There is some evidence that repeated sessions ([Chang et al., 2010] ipsilesional 10 Hz rTMS on 10 consecutive days induced effects lasting up to 3 months) or coupling NIBS with established rehabilitation methods such as physiotherapy [Avenanti et al., 2012] could consolidate and prolong plasticity effects.

This last concept and its relation to another adaptation intended to boost plasticity deserve a closer look: As discussed several times before, PAS-mediated plasticity interacts with other NIBS plasticity protocols and motor learning following the

principle of homeostatic metaplasticity (cf. 4.1 and 4.7.2), an observation that has been utilized in 'priming', also termed 'pre-conditioning', an NIBS plasticity protocol by preceding it with one promoting plasticity in the opposite direction, both within one modality ([Müller et al., 2007]: PAS and [Todd et al., 2010]: rtMS) and across modalities ([Siebner et al., 2004] : tDCS primes rTMS) to enhance the efficiency of the primed protocol. Given this effect, it appears contradictory that coupling LTP-PAS in a close temporal manner with physiotherapy, which conceivably involves motor learning, should increase rather than block LTP effects. [Opie et al., 2020] accordingly reported an increased retention of training-acquired motor skills a week after LTD-PAS intervention in older adults.
However, some apparent exceptions to this rule have been observed and thus provide some support for the idea of coupling LTP-PAS with physiotherapy:
In healthy participants, [Singh et al., 2014] showed improved LTP-PAS efficiency when the intervention is preceded by physical exercise. [Nitsche et al., 2007] reported that when anodal, usually facilitating tDCS precedes LTP-PAS, effects are enhanced – when tDCS and PAS are applied simultaneously, however, LTP is blocked as predicted by homeostatic metaplasticity. [Rosenkranz et al., 2007] evoked reduction rather than facilitation of CSE when performing LTP-PAS one day after motor training – five days after training, LTP-PAS led to facilitation again. As mentioned by [Ridding and Ziemann, 2010], the temporal offset between two plasticity-modulating interventions may thus indicate the direction of their interaction – a consideration which surely warrants further investigation.
Clinical enthusiasm for NIBS in stroke rehabilitation remains tampered not only because of the paucity of clinical trials, but also because of several nil findings among them, even when one or several of the modifications just described were applied: [Tarri et al., 2018] could not induce significant effects when applying (sham-controlled) ipsilesional LTP-PAS and physiotherapy on five consecutive days. Interestingly, a subgroup of patients with very low CSE at baseline (i.e., high RMT, low MEP amplitudes) showed more of a PAS effect – in contrast to [Müller-Dahlhaus et al., 2008] who reported a correlation of low RMT with better PAS response in healthy individuals. This could point to a preferential benefit of LTP-augmenting protocols for patients with a strongly affected CSE, which is of course the direct target parameter of plasticity interventions. As the variability of plasticity effects, or the absence thereof, appears to be proportionate or even increased in stroke patients compared to healthy participants, calls are being made for 'lesion-specific', individualized protocols. Data suggest that the stage of recovery [Tarri et al., 2018], subcortical or cortical infarction [Ameli et al., 2009]

and degree of disability [Di Pino et al., 2014] should inform adapted stimulation 'recipes'.
Extensive further research is most certainly needed, as routine translation into clinical practice requires a minimum effect size and reliability, especially considering the immense technical and personnel effort involved – and the tight staffing ratios in rehabilitation clinics.

4.8 MUPAS. Conclusion

Calling to mind the intention to improve LTP-PAS efficiency by applying it during more excitable brain states, we must admit failure. Unfortunately, we have not been able to identify brain states conducive to PAS-plasticity induction, not least because we have not managed to induce any plasticity at all, irrespective of EEG condition. Possible reasons for our nil findings have been discussed at length in the previous sections.
However, between conduction and publication of these experiments, data from the same group have emerged describing increased efficiency of an LTP-inducing rTMS protocol when synchronized to high-excitability μ-$alpha$ troughs [Zrenner et al., 2018], and vice versa for LTD-inducing rTMS at low-excitability [Baur et al., 2020]. I would thus tentatively answer the question I posed in the introduction about whether an excitable brain is also a more 'malleable' one in the affirmative.

5 Conclusion

So how do we go on from here? Rather than admitting defeat, we should strive to improve the EEG-triggered approach to TMS in order to obtain steadier results.
Though replication of nil results with varying ITIs is necessary, the apparent necessity for a fixed frequency application might limit PAS eligibility for EEG-TMS. rTMS protocols in contrast seem to fulfil the requirement of constant repetition within an rTMS train, which due to its higher temporal resolution can be replied as a repetitive train during peak or trough.
Impressive as the technical achievement of the highly precise and low-delay real-time system may be, two principals concerns remain to be resolved for EEG-triggered TMS to graduate to a valid routine treatment tool: First and foremost, it is time to focus some of our energy on developing the technology and setup necessary to make accurate EEG targeting available for all. Not until then can we confidently establish the functional role of brain waves as expression of brain states. This necessarily encompasses identifying an optimal (calculation of an individual) EEG montage to act as the truest possible 'lens' through which to view said oscillations. We can then proceed to gain a higher degree of certainty about which oscillations and which of their features we should be targeting for maximum efficiency - a question which is, despite decades of TMS research, still not conclusively answered today, as reviewed in 3.5.2. Is μ-$alpha$ or μ-$beta$ the rhythm to look out for when studying corticospinal excitability – and does higher power signify more or less excitability? How relevant is μ phase? For instance, another group [Madsen et al., 2019] has not been able to replicate a significant phase effect despite using a very similar setup.
Which brings us to a decisive principle in all of research: replication of results, using as identical setups as possible, before inferring physiological meaning from the oftentimes 'weak' (in terms of effect size or level of significance) results, intellectually intriguing conjectures aside.
A ready and humble admission to our methods' limitations, critical interpretation of any findings and scrupulous reporting of methods to enable exact replication are of the essence in order not to create overblown expectations.
That being said, EEG-triggered TMS remains a very promising tool both for neuroscience and neurology, capable of revealing insights into the 'secretive' workings of the brain mentioned at the beginning of this thesis as well as translating these insights into innovative treatments. TMS is currently already recognized as a treatment method for a range of psychiatric and neurological indications such

as depression [Eldaief et al., 2013], migraine [Lan et al., 2017] and for mapping motor and language regions prior to neurosurgery [Eldaief et al., 2013].
EEG-TMS can also play an important role as preparatory research informing the design of brain-computer interfaces (BCI). BCIs bypass the peripheral nervous system, creating a direct connection from brain signals to control of neuroprosthetics, enabling passive movement of paralyzed limbs. EEG-TMS can identify 'eloquent' oscillatory patterns relevant to specific movements, e.g. event-related desynchronization (ERD) in sensorimotor μ rhythm during (intended/imagined) movement.

Farther along the path, research could be moving towards fully closed-loop EEG-TMS: in addition to the informed open-loop system has already been achieved with brain waves triggering stimulation, the effects that stimulation exerts on a number of outcome parameters (e.g. MEP size, SSEP component amplitude, task performance) could then in turn inform the ongoing stimulation (e.g. pulse strength, timing, coil positioning) to achieve maximum effect size. Spatial resolution could be improved by using overlapping coils of different shapes and modifying the relative SIs. Real-time source-space modeling could predict the current magnitude, focality and depth for any combination of position and SI distribution between coils. The experimenter would only have to define a target area and intended current density at target. A wealth of applications still remains to be discovered, among them enhancement of neuroplasticity remains as the most auspicious form of application. Future developments will ensure a permanent place for TMS and specifically EEG-TMS not only in research, but also as a highly efficient treatment tool in neurorehabilitation.

6 Summary

This thesis presents two experiments employing real-time EEG-triggered transcranial magnetic stimulation (TMS) on healthy volunteers to investigate the role of sensorimotor 8-14Hz μ rhythm in EEG at rest on corticospinal excitability and induction of positive plasticity. We intended to identify brain states favorable to induction of positive plasticity to inform development of more efficient TMS protocols for clinical application e.g. in stroke patients.

Applying TMS triggered by pre-determined EEG brain states in real time (opposed to *open-loop* TMS with post-hoc trial sorting) offers not only more precise research into the role of certain brain waves, but also translation into more efficient therapies. The membrane potential of superficial cortical neurons fluctuates rhythmically, visible as oscillations in surface EEG. Different brain areas seem to communicate through these synchronized fluctuations. 'Brain waves' therefore convey valuable information about the excitability of said areas.

Oscillations in the alpha frequency range (8-14Hz) play a crucial role in this, gating information by inhibiting brain areas irrelevant to the current task. According to an influential hypothesis, this function is exerted as an 'asymmetric pulsed inhibition', with a maximum of inhibition during the peaks and during high alpha power ($\sim$ amplitude). Sensorimotor alpha frequency waves (μ rhythm) play a similar role as the well-researched occipital alpha does for the visual cortex. The primary motor cortex (M1) provides a quantifiable measure of (corticospinal) excitability, the amplitude of TMS-elicited contralateral muscle twitches (appearing as MEPs in the EMG).

The first experiment investigated the role of μ power for M1 excitability. 16 participants underwent one session of single-pulse TMS of the left M1, triggered by overall 10 individual power deciles in pseudorandomized order, partitioned into 4 'blocks' of stimulation over time. The data revealed, after stratification for confounding inter-trial-intervals (ITIs) and normalization to block average, a weak positive linear relationship contrary to the proposed inhibitory role of μ, which has however since been replicated several times in other studies. This discrepancy can be explained e.g. by an in fact facilitatory nature of μ, by a postcentral and thus sensory cortical (S1) source of the targeted oscillations, reversing the inhibitory effect in sign to a facilitatory one through S1-to-M1 feedforward inhibition, or by a shift of most excitable power values dependent on stimulus strength.

For the main experiment, we applied a paired associative stimulation (PAS) pro-

tocol intended to induce positive plasticity (strengthening of synaptic connection outlasting the intervention), combining electrical stimulation of the right median nerve at the wrist with a TMS of the left M1 in a temporally sensitive manner. After an extensive screening to pre-select suitable subjects with a sufficiently strong μ rhythm (to ensure accurate performance of the real-time EEG targeting), 16 participants completed 4 sessions (one condition each). We expected to induce more positive plasticity during more excitable brain states, i.e., μ troughs rather than μ peaks. In light of our findings on μ power from the first experiment (weak influence as compared to ITIs and intrinsic variability over time) and overall contradictory evidence as to its (facilitatory versus inhibitory) role, high vs. low power were not explicitly compared. TMS during PAS was applied at (1) μ peaks, (2) μ troughs, (3) at medium μ powers and (4) open-loop. (3) and (4) both served as controls. The intervention failed to evoke a significant change in MEP amplitudes from baseline irrespective of condition. Possible explanations can be found in the intra- and interindividual variability of decisive parameters across sessions (e.g. baseline amplitudes and absolute μ powers during PAS), which however did not significantly depend on the targeted condition and were thus not true confounders. The number of sessions might still have introduced a further measure of variability. Varying PAS ITIs (due to EEG-triggering) could have also impeded plasticity induction, and the involvement of two cortical regions (S1 and M1) might have complicated the identification of one relevant brain state.

Currently, plasticity-inducing TMS protocols in research and clinical trials evoke variable and transient effects. Improvements to enable routine application might come from EEG-triggering and/or combining with traditional motor training (physiotherapy). Regardless of our nil results in plasticity induction, EEG-triggered TMS remains a promising instrument in research and therapy.

7 Deutsche Zusammenfassung

In dieser Arbeit werden zwei Experimente vorgestellt, bei denen EEG-getriggerte transkranielle Magnetstimulation (TMS) an gesunden Probanden eingesetzt wurde, um die Rolle des sensomotorischen 8-14Hz μ-Rhythmus auf die kortikospinale Erregbarkeit (*CSE*) und die Induktion positiver Plastizität zu untersuchen. Unser Ziel war es, für Plastizitätsinduktion günstige Zeitpunkte im EEG zu identifizieren, um in Zukunft die Effektivität solcher zurzeit oft noch unzuverlässigen Anwendungen zu steigern. Unser EEG-TMS System interpretierte Oszillationen im EEG in Echtzeit und löste einen Stimulus aus, wenn bestimmte, vorher festgelegte Eigenschaften zutrafen. Die 'Gehirnwellen' im EEG entstehen durch synchronisierte Fluktuationen des Membranpotentials kortikaler Neurone, welche aufgrund ihrer intrakortikalen Kommunikationsfunktion wertvolle Informationen über neuronale Erregbarkeit vermitteln. Im Gegensatz zu "*open-loop*" TMS ermöglicht EEG-TMS nicht nur eine präzisere Erforschung der Funktion von Gehirnwellen, sondern auch die Umsetzung der gewonnenen Erkenntnisse in effizientere therapeutische Anwendungen. Speziell Oszillationen im Alpha-Frequenzbereich (8-14Hz) spielen eine bedeutsame Rolle, indem sie den Informationsfluss im Gehirn durch Hemmung aktuell irrelevanter Areale steuern, und zwar laut einer führenden Theorie als "asymmetrisch gepulste Inhibition" mit einem Maximum der Hemmung während der Hochpunkte ("*Peaks*") und während hoher "*Power*" ($\sim$ Amplitude). Der "μ*-Rhythmus*", Wellen in alpha-Frequenz über dem sensomotorischen Kortex, scheint für diese Areale eine analoge Rolle wie das okzipitale Alpha für den visuellen Kortex zu spielen. Die *CSE* lässt sich durch die Amplitude der ausgelösten kontralateralen Muskelzuckungen (MEPs im EMG) quantifizieren.

Im Vorexperiment erforschten wir den Einfluss der *Power* der μ-Wellen auf die *CSE*. 16 Teilnehmer wurden in einer Sitzung mit Einzelpuls-TMS des linken M1 stimuliert. Die Pulse wurden durch die momentane *Power* ausgelöst, 10 Dezile des individuellen μ-Powerspektrums wurden in pseudorandomisierter Reihenfolge angesteuert, verteilt auf 4 Stimulationsblöcke. Nach Berücksichtigung der "*Inter-Trial-Intervalle*" (*ITIs*, bekannter "*Confounder*") und Normalisierung pro Block zeigten unsere Daten eine schwache positiv-lineare Korrelation zwischen μ *Power* und MEP-Amplitude, welche somit im Widerspruch zur angenommenen hemmenden Wirkung von μ steht, aber mittlerweile in mehreren anderen Studien repliziert wurde. Diese Diskrepanz kann z.B. durch eine tatsächlich fazilitatorische Wirkung erklärt werden, oder auch durch eine anatomisch dem sensorischen Kortex (S1) zuzuordnende Quelle der angesteuerten μ-Wellen, was über hem-

mende Interneurone von S1 auf M1 zu einer 'Vorzeichenumkehrung' der Effektrichtung führen könnte. Weiterhin wird eine Abhängigkeit der 'erregbarsten' *Power*-Werte von der Stimulusstärke diskutiert.

Im Hauptexperiment sollte mit '*paarig-assoziativer Stimulation*' (*PAS*) (intervallsensitive Kombination von Elektrostimulation des rechten Nervus medianus mit TMS des linken M1) positive Plastizität (die Intervention überdauernde Stärkung von Synapsen) induziert werden. Dem ging ein umfangreiches "*Screening*" zur Identifikation geeigneter Probanden mit ausgeprägtem μ-Rhythmus (für präzise EEG-Triggerung) voraus. Letztlich absolvierten 16 Teilnehmer je 4 Sitzungen (eine pro Trigger-Bedingung). Unsere Hypothese war hierbei, mehr Plastizität nach Stimulation während der Tiefpunkte ("*Troughs*") als während der *Peaks* zu erzielen, also mehr synaptische 'Formbarkeit' während höherer Erregbarkeit. In Anbetracht der schwachen Ergebnisse des Vorexperiments sowie einer widersprüchlichen Beweislage bezüglich einer fazilitatorischen oder inhibitorischen Funktion wurden hohe und niedrige *Power* nicht explizit miteinander verglichen. TMS während PAS wurde durch (1) μ-*Peaks*, (2) μ-*Troughs*, (3) mittlere μ-*Power* und (4) *open-loop* getriggert. (3) und (4) dienten jeweils als Kontrollbedingung. PAS konnte, unabhängig von der EEG-Bedingung, keine signifikante Veränderung der MEP-Amplituden vom Ausgangswert hervorrufen. Die fehlende Wirkung könnte durch intra- und interindividuelle Schwankungen gewisser Parameter zwischen den Sitzungen erklärt werden (z.B. MEP-Ausgangswerte, absolute μ-*Power* während *PAS*), die sich jedoch nicht als systematische *Confounder* zwischen EEG-Bedingungen herausstellten.
Die, im Gegensatz zu open-loop-Studien, schwankenden ITIs während der *PAS* könnten die Wirkung ebenfalls beeinträchtigt haben. Weiterhin waren zwei verschiedene Kortexareale (S1 und M1) am Protokoll beteiligt, was die Identifikation einer relevanten EEG-Eigenschaft erschwerte.

Gegenwärtig rufen Plastizitäts-induzierende TMS-Protokolle in der Forschung und in Studien mit Schlaganfallpatienten schwankende und zeitlich begrenzte Wirkungen hervor. Durch EEG-Triggerung und / oder die Kombination mit klassischer Physiotherapie könnte eine verbesserte Effektivität und somit eine routinemäßige Anwendung erreicht werden. Trotz unserer negativen Ergebnisse bleibt EEG-getriggerte TMS ein vielversprechendes Instrument in Forschung und Klinik.

8 Bibliography

References

[Ai and Ro, 2014] Ai, L. and Ro, T. (2014). The phase of prestimulus alpha oscillations affects tactile perception. *J NEUROPHYSIOL*, 111(6):1300–1307. PMID: 24381028.

[Ameli et al., 2009] Ameli, M., Grefkes, C., Kemper, F., Riegg, F. P., Rehme, A. K., Karbe, H., Fink, G. R., and Nowak, D. A. (2009). Differential effects of high-frequency repetitive transcranial magnetic stimulation over ipsilesional primary motor cortex in cortical and subcortical middle cerebral artery stroke. *ANN NEUROL*, 66(3):298–309.

[Anderson and Ding, 2011] Anderson, K. and Ding, M. (2011). Attentional modulation of the somatosensory mu rhythm. *NEUROSCIENCE*, 180:165–180.

[Avenanti et al., 2012] Avenanti, A., Coccia, M., Ladavas, E., Provinciali, L., and Ceravolo, M. (2012). Low-frequency rTMS promotes use-dependent motor plasticity in chronic stroke. *NEUROLOGY*, 78(4):256–264.

[Awiszus, 2003] Awiszus, F. (2003). Chapter 2: TMS and Threshold hunting. In Paulus, W., Tergau, F., Nitsche, M., Rothwell, J., Ziemann, U., and Hallett, M., editors, *Transcranial Magnetic Stimulation and Transcranial Direct Current Stimulation*, volume 56 of *Supplements to Clinical Neurophysiology*, pages 13–23. Elsevier.

[Bagnato et al., 2005] Bagnato, S., Curra, A., Modugno, N., Gilio, F., Quartarone, A., Rizzo, V., Girlanda, P., Inghilleri, M., and Berardelli, A. (2005). One-hertz subthreshold rTMS increases the threshold for evoking inhibition in the human motor cortex. *EXP BRAIN RES*, 160(3):368–374.

[Baur et al., 2020] Baur, D., Galevska, D., Hussain, S., Cohen, L. G., Ziemann, U., and Zrenner, C. (2020). Induction of LTD-like corticospinal plasticity by low-frequency rTMS depends on pre-stimulus phase of sensorimotor μ-rhythm. *BRAIN STIMUL*, 13(6):1580–1587.

[Berger et al., 2014] Berger, B., Minarik, T., Liuzzi, G., Hummel, F. C., and Sauseng, P. (2014). EEG oscillatory phase-dependent markers of corticospinal excitability in the resting brain. *BIOMED RES INT*, 2014:936096.

[Berger, 1929] Berger, H. (1929). Über das Elektroenkephalogramm des Menschen. *Archiv für Psychiatrie und Nervenkrankheiten*, 87(1):527–570.

[Bergmann, 2018] Bergmann, T. O. (2018). Brain state-dependent brain stimulation. *Frontiers in Psychology*, 9:2108.

[Bergmann et al., 2016] Bergmann, T. O., Karabanov, A., Hartwigsen, G., Thielscher, A., and Siebner, H. R. (2016). Combining non-invasive transcranial brain stimulation with neuroimaging and electrophysiology: Current approaches and future perspectives. *NEUROIMAGE*, 140:4–19. Transcranial electric stimulation (tES) and Neuroimaging.

[Bergmann et al., 2019] Bergmann, T. O., Lieb, A., Zrenner, C., and Ziemann, U. (2019). Pulsed Facilitation of Corticospinal Excitability by the Sensorimotor mu-Alpha Rhythm. *J NEUROSCI*, 39(50):10034–10043.

[Bergmann et al., 2008] Bergmann, T. O., Mölle, M., Marshall, L., Kaya-Yildiz, L., Born, J., and Roman Siebner, H. (2008). A local signature of LTP-and LTD-like plasticity in human NREM sleep. *EUR J NEUROSCI*, 27(9):2241–2249.

[Bi and Poo, 1998] Bi, G.-q. and Poo, M.-m. (1998). Synaptic Modifications in Cultured Hippocampal Neurons: Dependence on Spike Timing, Synaptic Strength, and Postsynaptic Cell Type. *J NEUROSCI*, 18(24):10464–10472.

[Biernaskie and Corbett, 2001] Biernaskie, J. and Corbett, D. (2001). Enriched rehabilitative training promotes improved forelimb motor function and enhanced dendritic growth after focal ischemic injury. *J NEUROSCI*, 21(14):5272–5280.

[Blausen.com staff, 2014] Blausen.com staff (2014). Medical gallery of Blausen Medical 2014. *WikiJournal of Medicine*, 1(2). Accessed: 2021-06-12.

[Bliss and Collingridge, 1993] Bliss, T. V. and Collingridge, G. L. (1993). A synaptic model of memory: long-term potentiation in the hippocampus. *NATURE*, 361(6407):31–39.

[Brach and VanSwearingen, 2002] Brach, J. S. and VanSwearingen, J. M. (2002). Physical Impairment and Disability: Relationship to Performance of Activities of Daily Living in Community-Dwelling Older Men. *PHYS THER*, 82(8):752–761.

[Burn et al., 1997] Burn, J., Dennis, M., Bamford, J., Sandercock, P., Wade, D., and Warlow, C. (1997). Epileptic seizures after a first stroke: the Oxfordshire Community Stroke Project. *BMJ*, 315(7122):1582–1587.

[Caria et al., 1997] Caria, M. A., Kaneko, T., Kimura, A., and Asanuma, H. (1997). Functional Organization of the Projection From Area 2 to Area 4 gamma in the Cat. *J NEUROPHYSIOL*, 77(6):3107–3114. PMID: 9212260.

[Carmichael, 2006] Carmichael, S. T. (2006). Cellular and molecular mechanisms of neural repair after stroke: making waves. *ANN NEUROL*, 59(5):735–742.

[Chang et al., 2010] Chang, W. H., Kim, Y.-H., Bang, O. Y., Kim, S. T., Park, Y. H., and Lee, P. K. (2010). Long-term effects of rTMS on motor recovery in patients after subacute stroke. *J REHABIL MED*, 42(8):758–764.

[Charlton et al., 2003] Charlton, C. S., Ridding, M. C., Thompson, P. D., and Miles, T. S. (2003). Prolonged peripheral nerve stimulation induces persistent changes in excitability of human motor cortex. *J NEUROL SCI*, 208(1-2):79–85.

[Chen et al., 1997] Chen, R., Classen, J., Gerloff, C., Celnik, P., Wassermann, E. M., Hallett, M., and Cohen, L. G. (1997). Depression of motor cortex excitability by low-frequency transcranial magnetic stimulation. *NEUROLOGY*, 48(5):1398–1403.

[Cirillo et al., 2009] Cirillo, J., Lavender, A. P., Ridding, M. C., and Semmler, J. G. (2009). Motor cortex plasticity induced by paired associative stimulation is enhanced in physically active individuals. *J PHYSIOL*, 587(24):5831–5842.

[Conde et al., 2019] Conde, V., Tomasevic, L., Akopian, I., Stanek, K., Saturnino, G. B., Thielscher, A., Bergmann, T. O., and Siebner, H. R. (2019). The non-transcranial TMS-evoked potential is an inherent source of ambiguity in TMS-EEG studies. *NEUROIMAGE*, 185:300–312.

[Darling et al., 2006] Darling, W. G., Wolf, S. L., and Butler, A. J. (2006). Variability of motor potentials evoked by transcranial magnetic stimulation depends on muscle activation. *EXP BRAIN RES*, 174(2):376–385.

[Das et al., 2019] Das, B. B., Kumar, P., Kar, D., Ram, S. K., Babu, K. S., and Mohapatra, R. K. (2019). A spatio-temporal model for EEG-based person identification. *MULTIMED TOOLS APPL*, 78(19):28157–28177.

[Deng et al., 2014] Deng, Z.-D., Lisanby, S. H., and Peterchev, A. V. (2014). Coil design considerations for deep transcranial magnetic stimulation. *CLIN NEUROPHYSIOL*, 125(6):1202–1212.

[Di Lazzaro et al., 2004] Di Lazzaro, V., Oliviero, A., Pilato, F., Saturno, E., Dileone, M., Mazzone, P., Insola, A., Tonali, P., and Rothwell, J. (2004). The physiological basis of transcranial motor cortex stimulation in conscious humans. *CLIN NEUROPHYSIOL*, 115(2):255–266.

[Di Lazzaro and Ziemann, 2013] Di Lazzaro, V. and Ziemann, U. (2013). The contribution of transcranial magnetic stimulation in the functional evaluation of microcircuits in human motor cortex. *FRONT NEURAL CIRCUIT*, 7:18.

[Di Pino et al., 2014] Di Pino, G., Pellegrino, G., Assenza, G., Capone, F., Ferreri, F., Formica, D., Ranieri, F., Tombini, M., Ziemann, U., Rothwell, J. C., et al. (2014). Modulation of brain plasticity in stroke: a novel model for neurorehabilitation. *NAT REV NEUROL*, 10(10):597.

[Dugué et al., 2011] Dugué, L., Marque, P., and VanRullen, R. (2011). The Phase of Ongoing Oscillations Mediates the Causal Relation between Brain Excitation and Visual Perception. *J NEUROSCI*, 31(33):11889–11893.

[Eldaief et al., 2013] Eldaief, M. C., Press, D. Z., and Pascual-Leone, A. (2013). Transcranial magnetic stimulation in neurology: a review of established and prospective applications. *NEUROL CLIN PRACT*, 3(6):519–526.

[Fitzgerald et al., 2006] Fitzgerald, P. B., Fountain, S., and Daskalakis, Z. J. (2006). A comprehensive review of the effects of rTMS on motor cortical excitability and inhibition. *CLIN NEUROPHYSIOL*, 117(12):2584–2596.

[Frantseva et al., 2008] Frantseva, M. V., Fitzgerald, P. B., Chen, R., Möller, B., Daigle, M., and Daskalakis, Z. J. (2008). Evidence for impaired long-term potentiation in schizophrenia and its relationship to motor skill learning. *CEREB CORTEX*, 18(5):990–996.

[Fratello et al., 2006] Fratello, F., Veniero, D., Curcio, G., Ferrara, M., Marzano, C., Moroni, F., Pellicciari, M. C., Bertini, M., Rossini, P. M., and De Gennaro, L. (2006). Modulation of corticospinal excitability by paired associative stimulation: reproducibility of effects and intraindividual reliability. *CLIN NEUROPHYSIOL*, 117(12):2667–2674.

[Galvani, 1792] Galvani, L. (1792). *De viribus electricitatis in motu musculari comentarius cum joannis aldini dissertatione et notis; accesserunt epistolae ad animalis electricitatis theoriam pertinentes*. Apud Societatem Typographicam.

[Gho and Valera, 1988] Gho, M. and Valera, F. J. (1988). A quantitative assessment of the dependency of the visual temporal frame upon the cortical rhythm. *J PHYSIOL-PARIS*, 83(2):95–101.

[Grau et al., 2001] Grau, A. J., Weimar, C., Buggle, F., Heinrich, A., Goertler, M., Neumaier, S., Glahn, J., Brandt, T., Hacke, W., and Diener, H.-C. (2001). Risk Factors, Outcome, and Treatment in Subtypes of Ischemic Stroke. *STROKE*, 32(11):2559–2566.

[Grundey et al., 2012] Grundey, J., Thirugnanasambandam, N., Kaminsky, K., Drees, A., Skwirba, A. C., Lang, N., Paulus, W., and Nitsche, M. A. (2012). Neuroplasticity in Cigarette Smokers Is Altered under Withdrawal and Partially Restituted by Nicotine Exposition. *J NEUROSCI*, 32(12):4156–4162.

[Gualtierotti and Paterson, 1954] Gualtierotti, T. and Paterson, A. S. (1954). Electrical stimulation of the unexposed cerebral cortex. *J PHYSIOL*, 125(2):278.

[Haegens et al., 2011] Haegens, S., Nácher, V., Luna, R., Romo, R., and Jensen, O. (2011). alpha-Oscillations in the monkey sensorimotor network influence discrimination performance by rhythmical inhibition of neuronal spiking. *P NATL ACAD SCI USA*, 108(48):19377–19382.

[Hannula et al., 2005] Hannula, H., Ylioja, S., Pertovaara, A., Korvenoja, A., Ruohonen, J., Ilmoniemi, R. J., and Carlson, S. (2005). Somatotopic blocking of sensation with navigated transcranial magnetic stimulation of the primary somatosensory cortex. *HUM BRAIN MAPP*, 26(2):100–109.

[Hassanzahraee et al., 2019] Hassanzahraee, M., Zoghi, M., and Jaberzadeh, S. (2019). Longer Transcranial Magnetic Stimulation Intertrial Interval Increases Size, Reduces Variability, and Improves the Reliability of Motor Evoked Potentials. *BRAIN CONNECT*, 9(10):770–776.

[Hebb, 1949] Hebb, D. O. (1949). *The organization of behavior: A neuropsychological theory*. New York JOHN WILEY & SONS, Inc. London CHAPMAN & HALL, Limited.

[Herring et al., 2015] Herring, J. D., Thut, G., Jensen, O., and Bergmann, T. O. (2015). Attention Modulates TMS-Locked Alpha Oscillations in the Visual Cortex. *J NEUROSCI*, 35(43):14435–14447.

[Hjorth, 1975] Hjorth, B. (1975). An on-line transformation of EEG scalp potentials into orthogonal source derivations. *ELECTROEN CLIN NEURO*, 39(5):526–530.

[Horvath et al., 2011] Horvath, J. C., Perez, J. M., Forrow, L., Fregni, F., and Pascual-Leone, A. (2011). Transcranial magnetic stimulation: a historical evaluation and future prognosis of therapeutically relevant ethical concerns. *J MED ETHICS*, 37(3):137–143.

[Hoy and Fitzgerald, 2010] Hoy, K. E. and Fitzgerald, P. B. (2010). Brain stimulation in psychiatry and its effects on cognition. *NAT REV NEUROL*, 6(5):267–275.

[Huang et al., 2005] Huang, Y.-Z., Edwards, M. J., Rounis, E., Bhatia, K. P., and Rothwell, J. C. (2005). Theta Burst Stimulation of the Human Motor Cortex. *NEURON*, 45(2):201–206.

[Hussain et al., 2018] Hussain, S. J., Claudino, L., Bönstrup, M., Norato, G., Cruciani, G., Thompson, R., Zrenner, C., Ziemann, U., Buch, E., and Cohen, L. G. (2018). Sensorimotor Oscillatory Phase–Power Interaction Gates Resting Human Corticospinal Output. *CEREB CORTEX*, 29(9):3766–3777.

[Ilmoniemi et al., 1999] Ilmoniemi, F. J., Ruohonen, J., and Karhu, J. (1999). Transcranial magnetic stimulation–A new tool for functional imaging. *Crit. Rev. Biomed. Eng*, 27:241–284.

[Ingham et al., 2011] Ingham, D., Tucker, K. J., Tsao, H., and Hodges, P. W. (2011). The effect of pain on training-induced plasticity of the corticomotor system. *EUR J PAIN*, 15(10):1028–1034.

[Inghilleri et al., 2004] Inghilleri, M., Conte, A., Currà, A., Frasca, V., Lorenzano, C., and Berardelli, A. (2004). Ovarian hormones and cortical excitability. An rTMS study in humans. *CLIN NEUROPHYSIOL*, 115(5):1063–1068.

[Iscan et al., 2016] Iscan, Z., Nazarova, M., Fedele, T., Blagovechtchenski, E., and Nikulin, V. V. (2016). Pre-stimulus Alpha Oscillations and Inter-subject Variability of Motor Evoked Potentials in Single- and Paired-Pulse TMS Paradigms. *FRONT HUM NEUROSCI*, 10:504.

[Jensen and Mazaheri, 2010] Jensen, O. and Mazaheri, A. (2010). Shaping functional architecture by oscillatory alpha activity: gating by inhibition. *FRONT HUM NEUROSCI*, 4:186.

[Johnson et al., 2013] Johnson, M. D., Lim, H. H., Netoff, T. I., Connolly, A. T., Johnson, N., Roy, A., Holt, A., Lim, K. O., Carey, J. R., Vitek, J. L., and He, B. (2013). Neuromodulation for Brain Disorders: Challenges and Opportunities. *IEEE T BIO-MED ENG*, 60(3):610–624.

[Jones et al., 2009] Jones, S., Pritchett, D., Sikora, M., and Stufflebeam, S. (2009). Hä mä lä inen MS, Moore CI. Quantitative analysis and biophysically realistic neural modeling of the MEG mu rhythm: rhythmogenesis and modulation of sensory-evoked responses. *J NEUROSCI*, 102:3554–3572.

[Jones et al., 2010] Jones, S. R., Kerr, C. E., Wan, Q., Pritchett, D. L., Hämäläinen, M., and Moore, C. I. (2010). Cued Spatial Attention Drives Functionally Relevant Modulation of the Mu Rhythm in Primary Somatosensory Cortex. *J NEUROSCI*, 30(41):13760–13765.

[Jones et al., 1999] Jones, T. A., Chu, C. J., Grande, L. A., and Gregory, A. D. (1999). Motor skills training enhances lesion-induced structural plasticity in the motor cortex of adult rats. *J NEUROSCI*, 19(22):10153–10163.

[Kamke et al., 2012] Kamke, M. R., Hall, M. G., Lye, H. F., Sale, M. V., Fenlon, L. R., Carroll, T. J., Riek, S., and Mattingley, J. B. (2012). Visual Attentional Load Influences Plasticity in the Human Motor Cortex. *J NEUROSCI*, 32(20):7001–7008.

[Kang et al., 2010] Kang, J.-S., Terranova, C., Hilker, R., Quartarone, A., and Ziemann, U. (2010). Deficient Homeostatic Regulation of Practice-Dependent Plasticity in Writer's Cramp. *CEREB CORTEX*, 21(5):1203–1212.

[Karabanov et al., 2021] Karabanov, A. N., Madsen, K. H., Krohne, L. G., and Siebner, H. R. (2021). Does pericentral mu-rhythm "power" corticomotor excitability? – A matter of EEG perspective. *BRAIN STIMUL*, 14(3):713–722.

[Keil et al., 2014] Keil, J., Timm, J., SanMiguel, I., Schulz, H., Obleser, J., and Schönwiesner, M. (2014). Cortical brain states and corticospinal synchronization influence TMS-evoked motor potentials. *J NEUROPHYSIOL*, 111(3):513–519. PMID: 24198325.

[Kelly-Hayes et al., 2003] Kelly-Hayes, M., Beiser, A., Kase, C. S., Scaramucci, A., D'Agostino, R. B., and Wolf, P. A. (2003). The influence of gender and age on disability following ischemic stroke: the Framingham study. *J STROKE CEREBROVASC DIS*, 12(3):119–126.

[Khedr et al., 2004] Khedr, E. M., Gilio, F., and Rothwell, J. (2004). Effects of low frequency and low intensity repetitive paired pulse stimulation of the primary motor cortex. *CLIN NEUROPHYSIOL*, 115(6):1259–1263.

[Kim et al., 2006] Kim, Y.-H., You, S. H., Ko, M.-H., Park, J.-W., Lee, K. H., Jang, S. H., Yoo, W.-K., and Hallett, M. (2006). Repetitive transcranial magnetic stimulation–induced corticomotor excitability and associated motor skill acquisition in chronic stroke. *STROKE*, 37(6):1471–1476.

[Klimesch et al., 2007] Klimesch, W., Sauseng, P., and Hanslmayr, S. (2007). EEG alpha oscillations: the inhibition–timing hypothesis. *BRAIN RES REV*, 53(1):63–88.

[Koessler et al., 2017] Koessler, L., Colnat-Coulbois, S., Cecchin, T., Hofmanis, J., Dmochowski, J. P., Norcia, A. M., and Maillard, L. G. (2017). In-vivo measurements of human brain tissue conductivity using focal electrical current injection through intracerebral multicontact electrodes. *HUM BRAIN MAPP*, 38(2):974–986.

[Koski et al., 2004] Koski, L., Mernar, T. J., and Dobkin, B. H. (2004). Immediate and long-term changes in corticomotor output in response to rehabilitation: correlation with functional improvements in chronic stroke. *NEUROREHAB NEURAL RE*, 18(4):230–249.

[Kujirai et al., 2006] Kujirai, K., Kujirai, T., Sinkjaer, T., and Rothwell, J. C. (2006). Associative Plasticity in Human Motor Cortex During Voluntary Muscle Contraction. *J NEUROPHYSIOL*, 96(3):1337–1346. PMID: 16723411.

[Kumpulainen et al., 2012] Kumpulainen, S., Mrachacz-Kersting, N., Peltonen, J., Voigt, M., and Avela, J. (2012). The optimal interstimulus interval and repeatability of paired associative stimulation when the soleus muscle is targeted. *EXP BRAIN RES*, 221(3):241–249.

[Kwon et al., 2014] Kwon, T. G., Kim, Y.-H., Chang, W. H., Bang, O. Y., and Shin, Y.-I. (2014). Effective method of combining rTMS and motor training in stroke patients. *RESTOR NEUROL NEUROS*, 32(2):223–232.

[Lan et al., 2017] Lan, L., Zhang, X., Li, X., Rong, X., and Peng, Y. (2017). The efficacy of transcranial magnetic stimulation on migraine: a meta-analysis of randomized controlled trails. *J HEADACHE PAIN*, 18(1):1–7.

[Lan and Gee, 1994] Lan, N. C. and Gee, K. W. (1994). Neuroactive steroid actions at the GABAA receptor. *HORM BEHAV*, 28(4):537–544.

[Lang et al., 2006] Lang, N., Harms, J., Weyh, T., Lemon, R. N., Paulus, W., Rothwell, J. C., and Siebner, H. R. (2006). Stimulus intensity and coil characteristics influence the efficacy of rTMS to suppress cortical excitability. *CLIN NEUROPHYSIOL*, 117(10):2292–2301.

[Larsen et al., 2018] Larsen, D. B., Graven-Nielsen, T., Hirata, R. P., and Boudreau, S. A. (2018). Differential corticomotor excitability responses to hypertonic saline-induced muscle pain in forearm and hand muscles. *NEURAL PLAST*, 2018.

[Laufs et al., 2003] Laufs, H., Kleinschmidt, A., Beyerle, A., Eger, E., Salek-Haddadi, A., Preibisch, C., and Krakow, K. (2003). EEG-correlated fMRI of human alpha activity. *NEUROIMAGE*, 19(4):1463–1476.

[Lecturio Staff, 2020] Lecturio Staff (2020). The Lecturio Medical Concept Library. Hand. `https://www.lecturio.com/concepts/hand/`. Accessed: 2021-06-12.

[Linkenkaer-Hansen et al., 2004] Linkenkaer-Hansen, K., Nikulin, V. V., Palva, S., Ilmoniemi, R. J., and Palva, J. M. (2004). Prestimulus oscillations enhance psychophysical performance in humans. *J NEUROSCI*, 24(45):10186–10190.

[Lövsund et al., 1980] Lövsund, P., Öberg, P., Nilsson, S., and Reuter, T. (1980). Magnetophosphenes: a quantitative analysis of thresholds. *MED BIOL ENG COMPUT*, 18(3):326–334.

[Madsen et al., 2019] Madsen, K. H., Karabanov, A. N., Krohne, L. G., Safeldt, M. G., Tomasevic, L., and Siebner, H. R. (2019). No trace of phase: Corticomotor excitability is not tuned by phase of pericentral mu-rhythm. *BRAIN STIMUL*, 12(5):1261–1270.

[Maeki and Ilmoniemi, 2010] Maeki, H. and Ilmoniemi, R. J. (2010). EEG oscillations and magnetically evoked motor potentials reflect motor system excitability in overlapping neuronal populations. *CLIN NEUROPHYSIOL*, 121(4):492–501.

[Mathewson et al., 2009] Mathewson, K. E., Gratton, G., Fabiani, M., Beck, D. M., and Ro, T. (2009). To See or Not to See: Prestimulus alpha-Phase Predicts Visual Awareness. *J NEUROSCI*, 29(9):2725–2732.

[Mathewson et al., 2011] Mathewson, K. E., Lleras, A., Beck, D. M., Fabiani, M., Ro, T., and Gratton, G. (2011). Pulsed out of awareness: EEG alpha oscillations represent a pulsed-inhibition of ongoing cortical processing. *FRONT PSYCHOL*, 2:99.

[Matthews, 1999] Matthews, P. (1999). The effect of firing on the excitability of a model motoneurone and its implications for cortical stimulation. *J PHYSIOL*, 518(Pt 3):867–882.

[Mazaheri and Jensen, 2008] Mazaheri, A. and Jensen, O. (2008). Asymmetric Amplitude Modulations of Brain Oscillations Generate Slow Evoked Responses. *J NEUROSCI*, 28(31):7781–7787.

[Mazaheri and Jensen, 2010] Mazaheri, A. and Jensen, O. (2010). Rhythmic pulsing: linking ongoing brain activity with evoked responses. *FRONT HUM NEUROSCI*, 4:177.

[Meder et al., 2021] Meder, A., Liepelt-Scarfone, I., Sulzer, P., Berg, D., Laske, C., Preische, O., Desideri, D., Zipser, C. M., Salvadore, G., Tatikola, K., et al. (2021). Motor cortical excitability and paired-associative stimulation-induced plasticity in amnestic mild cognitive impairment and Alzheimer's disease. *CLIN NEUROPHYSIOL*.

[Mills et al., 1992] Mills, K., Boniface, S., and Schubert, M. (1992). Magnetic brain stimulation with a double coil: the importance of coil orientation. *ELECTROEN CLIN NEURO*, 85(1):17–21.

[Mochizuki et al., 2006] Mochizuki, H., Ugawa, Y., Terao, Y., and Sakai, K. L. (2006). Cortical hemoglobin-concentration changes under the coil induced by single-pulse TMS in humans: a simultaneous recording with near-infrared spectroscopy. *EXP BRAIN RES*, 169(3):302–310.

[Müller et al., 2007] Müller, J. F. M., Orekhov, Y., Liu, Y., and Ziemann, U. (2007). Homeostatic plasticity in human motor cortex demonstrated by two consecutive sessions of paired associative stimulation. *EUR J NEUROSCI*, 25(11):3461–3468.

[Müller-Dahlhaus et al., 2008] Müller-Dahlhaus, J. F. M., Orekhov, Y., Liu, Y., and Ziemann, U. (2008). Interindividual variability and age-dependency of motor cortical plasticity induced by paired associative stimulation. *EXP BRAIN RES*, 187(3):467–475.

[Murase et al., 2004] Murase, N., Duque, J., Mazzocchio, R., and Cohen, L. G. (2004). Influence of interhemispheric interactions on motor function in chronic stroke. *ANN NEUROL*, 55(3):400–409.

[Murray and Keller, 2011] Murray, P. D. and Keller, A. (2011). Somatosensory response properties of excitatory and inhibitory neurons in rat motor cortex. *Journal of Neurophysiology*, 106(3):1355–1362. PMID: 21653707.

[Müller-Dahlhaus et al., 2010] Müller-Dahlhaus, F., Ziemann, U., and Classen, J. (2010). Plasticity Resembling Spike-Timing Dependent Synaptic Plasticity: The Evidence in Human Cortex. *FRONT SYNAPTIC NEUROSCI*, 2:34.

[Nitsche et al., 2007] Nitsche, M. A., Roth, A., Kuo, M.-F., Fischer, A. K., Liebetanz, D., Lang, N., Tergau, F., and Paulus, W. (2007). Timing-dependent modulation of associative plasticity by general network excitability in the human motor cortex. *J NEUROSCI*, 27(14):3807–3812.

[O'Driscoll and Leach, 1998] O'Driscoll, K. and Leach, J. P. (1998). "No longer Gage": an iron bar through the head: Early observations of personality change after injury to the prefrontal cortex. *BMJ*.

[Ogata et al., 2019] Ogata, K., Nakazono, H., Uehara, T., and Tobimatsu, S. (2019). Prestimulus cortical EEG oscillations can predict the excitability of the primary motor cortex. *BRAIN STIMUL*, 12(6):1508–1516.

[Oldfield, 1971] Oldfield, R. (1971). The assessment and analysis of handedness: The Edinburgh inventory. *NEUROPSYCHOLOGIA*, 9(1):97–113.

[Oostenveld et al., 2011] Oostenveld, R., Fries, P., Maris, E., and Schoffelen, J.-M. (2011). FieldTrip: open source software for advanced analysis of MEG, EEG, and invasive electrophysiological data. *COMPUT INTEL NEUROSC*, 2011.

[Opie et al., 2020] Opie, G. M., Pourmajidian, M., Ziemann, U., and Semmler, J. G. (2020). Investigating the influence of paired-associative stimulation on multi-session skill acquisition and retention in older adults. *CLIN NEUROPHYSIOL*, 131(7):1497–1507.

[Osipova et al., 2008] Osipova, D., Hermes, D., and Jensen, O. (2008). Gamma power is phase-locked to posterior alpha activity. *PLOS ONE*, 3(12):e3990.

[Palmer et al., 2018] Palmer, J. A., Wolf, S. L., and Borich, M. R. (2018). Paired associative stimulation modulates corticomotor excitability in chronic stroke: a preliminary investigation. *RESTOR NEUROL NEUROSCI*, 36(2):183–194.

[Parent, 2004] Parent, A. (2004). Giovanni Aldini: from animal electricity to human brain stimulation. *CAN J NEUROL SCI*, 31(4):576–584.

[Peinemann et al., 2004] Peinemann, A., Reimer, B., Löer, C., Quartarone, A., Münchau, A., Conrad, B., and Siebner, H. R. (2004). Long-lasting increase in corticospinal excitability after 1800 pulses of subthreshold 5 Hz repetitive TMS to the primary motor cortex. *CLIN NEUROPHYSIOL*, 115(7):1519–1526.

[Penfield, 1950] Penfield, W. (1950). The Cerebral Cortex of Man: A Clinical Study of Localization of Function. *JAMA-J AM MED ASSOC*, 144(16):1412–1412.

[Picht et al., 2011] Picht, T., Schmidt, S., Brandt, S., Frey, D., Hannula, H., Neuvonen, T., Karhu, J., Vajkoczy, P., and Suess, O. (2011). Preoperative Functional Mapping for Rolandic Brain Tumor Surgery: Comparison of Navigated Transcranial Magnetic Stimulation to Direct Cortical Stimulation. *NEUROSURGERY*, 69(3):581–589.

[Player et al., 2012] Player, M. J., Taylor, J. L., Alonzo, A., and Loo, C. K. (2012). Paired associative stimulation increases motor cortex excitability more effectively than theta-burst stimulation. *CLIN NEUROPHYSIOL*, 123(11):2220–2226.

[Quartarone et al., 2006] Quartarone, A., Rizzo, V., Bagnato, S., Morgante, F., Sant'Angelo, A., Girlanda, P., and Roman Siebner, H. (2006). Rapid-rate paired associative stimulation of the median nerve and motor cortex can produce long-lasting changes in motor cortical excitability in humans. *J PHYSIOL*, 575(2):657–670.

[Rajagovindan and Ding, 2011] Rajagovindan, R. and Ding, M. (2011). From Prestimulus Alpha Oscillation to Visual-evoked Response: An Inverted-U Function and Its Attentional Modulation. *J COGNITIVE NEUROSCI*, 23(6):1379–1394.

[Ridding et al., 2000] Ridding, M. C., Brouwer, B., Miles, T. S., Pitcher, J. B., and Thompson, P. D. (2000). Changes in muscle responses to stimulation of the motor cortex induced by peripheral nerve stimulation in human subjects. *EXP BRAIN RES*, 131(1):135–143.

[Ridding and Ziemann, 2010] Ridding, M. C. and Ziemann, U. (2010). Determinants of the induction of cortical plasticity by non-invasive brain stimulation in healthy subjects. *J PHYSIOL*, 588(13):2291–2304.

[Ritter et al., 2009] Ritter, P., Moosmann, M., and Villringer, A. (2009). Rolandic alpha and beta EEG rhythms' strengths are inversely related to fMRI-BOLD signal in primary somatosensory and motor cortex. *HUM BRAIN MAPP*, 30(4):1168–87.

[Rosen and Asanuma, 1972] Rosen, I. and Asanuma, H. (1972). Peripheral afferent inputs to the forelimb area of the monkey motor cortex: input-output relations. *EXP BRAIN RES*, 14(3):257–273.

[Rosenkranz et al., 2007] Rosenkranz, K., Kacar, A., and Rothwell, J. C. (2007). Differential modulation of motor cortical plasticity and excitability in early and late phases of human motor learning. *J NEUROSCI*, 27(44):12058–12066.

[Roy-O'Reilly and McCullough, 2018] Roy-O'Reilly, M. and McCullough, L. D. (2018). Age and Sex Are Critical Factors in Ischemic Stroke Pathology. *ENDOCRINOLOGY*, 159(8):3120–3131.

[Sale et al., 2007] Sale, M. V., Ridding, M. C., and Nordstrom, M. A. (2007). Factors influencing the magnitude and reproducibility of corticomotor excitability changes induced by paired associative stimulation. *EXP BRAIN RES*, 181(4):615–626.

[Sale et al., 2008] Sale, M. V., Ridding, M. C., and Nordstrom, M. A. (2008). Cortisol Inhibits Neuroplasticity Induction in Human Motor Cortex. *J NEUROSCI*, 28(33):8285–8293.

[Salmelin and Hari, 1994] Salmelin, R. and Hari, R. (1994). Spatiotemporal characteristics of sensorimotor neuromagnetic rhythms related to thumb movement. *NEUROSCIENCE*, 60(2):537–550.

[Sauseng et al., 2009] Sauseng, P., Klimesch, W., Gerloff, C., and Hummel, F. C. (2009). Spontaneous locally restricted EEG alpha activity determines cortical excitability in the motor cortex. *NEUROPSYCHOLOGIA*, 47(1):284–8.

[Schalk, 2015] Schalk, G. (2015). A general framework for dynamic cortical function: the function-through-biased-oscillations (FBO) hypothesis. *FRONT HUM NEUROSCI*, 9:352.

[Schaworonkow et al., 2018a] Schaworonkow, N., Caldana Gordon, P., Belardinelli, P., Ziemann, U., Bergmann, T. O., and Zrenner, C. (2018a). mu-Rhythm Extracted With Personalized EEG Filters Correlates With Corticospinal Excitability in Real-Time Phase-Triggered EEG-TMS. *FRONT NEUROSCI*, 12:954.

[Schaworonkow et al., 2018b] Schaworonkow, N., Triesch, J., Ziemann, U., and Zrenner, C. (2018b). EEG-triggered TMS reveals stronger brain state-dependent modulation of motor evoked potentials at weaker stimulation intensities. *BRAIN STIMUL*, 12:100–118.

[Schubert et al., 2009] Schubert, R., Haufe, S., Blankenburg, F., Villringer, A., and Curio, G. (2009). Now You'll Feel It, Now You Won't: EEG Rhythms Predict the Effectiveness of Perceptual Masking. *J COGNITIVE NEUROSCI*, 21:2407–19.

[Schulz et al., 2014] Schulz, H., Übelacker, T., Keil, J., Müller, N., and Weisz, N. (2014). Now I am ready—now I am not: the influence of pre-TMS oscillations and corticomuscular coherence on motor-evoked potentials. *CEREB CORTEX*, 24(7):1708–1719.

[Siebner et al., 2009] Siebner, H. R., Hartwigsen, G., Kassuba, T., and Rothwell, J. C. (2009). How does transcranial magnetic stimulation modify neuronal activity in the brain? Implications for studies of cognition. *CORTEX*, 45(9):1035–1042.

[Siebner et al., 2004] Siebner, H. R., Lang, N., Rizzo, V., Nitsche, M. A., Paulus, W., Lemon, R. N., and Rothwell, J. C. (2004). Preconditioning of low-frequency repetitive transcranial magnetic stimulation with transcranial direct current stimulation: evidence for homeostatic plasticity in the human motor cortex. *J NEUROSCI*, 24(13):3379–3385.

[Siebner and Ziemann, 2007] Siebner, H. R. and Ziemann, U. (2007). *Das TMS-Buch: Handbuch der transkraniellen Magnetstimulation*. Springer-Verlag.

[Singh et al., 2014] Singh, A. M., Neva, J. L., and Staines, W. R. (2014). Acute exercise enhances the response to paired associative stimulation-induced plasticity in the primary motor cortex. *EXP BRAIN RES*, 232(11):3675–3685.

[Smith et al., 1999] Smith, M., Keel, J., Greenberg, B., Adams, L., Schmidt, P., Rubinow, D., and Wassermann, E. (1999). Menstrual cycle effects on cortical excitability. *NEUROLOGY*, 53(9):2069–2069.

[Smith et al., 2002] Smith, M. J., Adams, L. F., Schmidt, P. J., Rubinow, D. R., and Wassermann, E. M. (2002). Effects of ovarian hormones on human cortical excitability. *ANN NEUROL*, 51(5):599–603.

[Sommer et al., 2018] Sommer, M., Ciocca, M., Chieffo, R., Hammond, P., Neef, A., Paulus, W., Rothwell, J. C., and Hannah, R. (2018). TMS of primary motor cortex with a biphasic pulse activates two independent sets of excitable neurons. *BRAIN STIMUL*, 11(3):558–565.

[Stefan et al., 2002] Stefan, K., Kunesch, E., Benecke, R., Cohen, L. G., and Classen, J. (2002). Mechanisms of enhancement of human motor cortex excitability induced by interventional paired associative stimulation. *J PHYSIOL*, 543(2):699–708.

[Stefan et al., 2000] Stefan, K., Kunesch, E., Cohen, L. G., Benecke, R., and Classen, J. (2000). Induction of plasticity in the human motor cortex by paired associative stimulation. *BRAIN*, 123(3):572–584.

[Stefan et al., 2004] Stefan, K., Wycislo, M., and Classen, J. (2004). Modulation of Associative Human Motor Cortical Plasticity by Attention. *J NEUROPHYSIOL*, 92(1):66–72. PMID: 14724259.

[Stefan et al., 2006] Stefan, K., Wycislo, M., Gentner, R., Schramm, A., Naumann, M., Reiners, K., and Classen, J. (2006). Temporary occlusion of associative motor cortical plasticity by prior dynamic motor training. *CEREB CORTEX*, 16(3):376–385.

[Stolk et al., 2019] Stolk, A., Brinkman, L., Vansteensel, M. J., Aarnoutse, E., Leijten, F. S., Dijkerman, C. H., Knight, R. T., de Lange, F. P., and Toni, I. (2019). Electrocorticographic dissociation of alpha and beta rhythmic activity in the human sensorimotor system. *Elife*, 8:e48065.

[Suppa et al., 2013] Suppa, A., Biasiotta, A., Belvisi, D., Marsili, L., La Cesa, S., Truini, A., Cruccu, G., and Berardelli, A. (2013). Heat-evoked experimental pain induces long-term potentiation-like plasticity in human primary motor cortex. *CEREB CORTEX*, 23(8):1942–1951.

[Suppa et al., 2017] Suppa, A., Quartarone, A., Siebner, H., Chen, R., Di Lazzaro, V., Del Giudice, P., Paulus, W., Rothwell, J., Ziemann, U., and Classen, J. (2017). The associative brain at work: Evidence from paired associative stimulation studies in humans. *CLIN NEUROPHYSIOL*, 128(11):2140–2164.

[Swayne et al., 2008] Swayne, O. B., Rothwell, J. C., Ward, N. S., and Greenwood, R. J. (2008). Stages of Motor Output Reorganization after Hemispheric Stroke Suggested by Longitudinal Studies of Cortical Physiology. *CEREB CORTEX*, 18(8):1909–1922.

[Takeuchi et al., 2008] Takeuchi, N., Tada, T., Toshima, M., Chuma, T., Matsuo, Y., and Ikoma, K. (2008). Inhibition of the unaffected motor cortex by 1 hz repetitive transcranial magnetic stimulation enhances motor performance and training effect of the paretic hand in patients with chronic stroke. *J REHABIL MED*, 40(4):298–303.

[Tarri et al., 2018] Tarri, M., Brihmat, N., Gasq, D., Lepage, B., Loubinoux, I., De Boissezon, X., Marque, P., and Castel-Lacanal, E. (2018). Five-day course of paired associative stimulation fails to improve motor function in stroke patients. *ANN PHYS REHABIL MED*, 61(2):78–84.

[Tecchio et al., 2008] Tecchio, F., Zappasodi, F., Pasqualetti, P., Gennaro, L. D., Pellicciari, M., Ercolani, M., Squitti, R., and Rossini, P. (2008). Age dependence of primary motor cortex plasticity induced by paired associative stimulation. *CLIN NEUROPHYSIOL*, 119(3):675–682.

[Thickbroom et al., 2006] Thickbroom, G. W., Byrnes, M. L., Edwards, D. J., and Mastaglia, F. L. (2006). Repetitive paired-pulse TMS at I-wave periodicity markedly increases corticospinal excitability: A new technique for modulating synaptic plasticity. *CLIN NEUROPHYSIOL*, 117(1):61–66.

[Thies et al., 2018] Thies, M., Zrenner, C., Ziemann, U., and Bergmann, T. O. (2018). Sensorimotor mu-alpha power is positively related to corticospinal excitability. *BRAIN STIMUL*, 11(5):1119–1122.

[Thomson et al., 2011] Thomson, R. H., Daskalakis, Z. J., and Fitzgerald, P. B. (2011). A near infra-red spectroscopy study of the effects of pre-frontal single and paired pulse transcranial magnetic stimulation. *CLIN NEUROPHYSIOL*, 122(2):378–382.

[Thomson et al., 2012] Thomson, R. H., Maller, J. J., Daskalakis, Z. J., and Fitzgerald, P. B. (2012). Blood oxygenation changes resulting from trains of low frequency transcranial magnetic stimulation. *CORTEX*, 48(4):487–491.

[Thut et al., 2006] Thut, G., Nietzel, A., Brandt, S. A., and Pascual-Leone, A. (2006). alpha-Band Electroencephalographic Activity over Occipital Cortex Indexes Visuospatial Attention Bias and Predicts Visual Target Detection. *J NEUROSCI*, 26(37):9494–9502.

[Todd et al., 2010] Todd, G., Kimber, T. E., Ridding, M. C., and Semmler, J. G. (2010). Reduced motor cortex plasticity following inhibitory rTMS in older adults. *CLIN NEUROPHYSIOL*, 121(3):441–447.

[Triesch et al., 2015] Triesch, J., Zrenner, C., and Ziemann, U. (2015). Chapter 5 - modeling tms-induced i-waves in human motor cortex. In Bestmann, S., editor, *Computational Neurostimulation*, volume 222 of *Progress in Brain Research*, pages 105–124. Elsevier.

[Tsang et al., 2015] Tsang, P., Bailey, A. Z., and Nelson, A. J. (2015). Rapid-rate paired associative stimulation over the primary somatosensory cortex. *PLOS ONE*, 10(3):e0120731.

[Turco et al., 2018] Turco, C. V., El-Sayes, J., Savoie, M. J., Fassett, H. J., Locke, M. B., and Nelson, A. J. (2018). Short- and long-latency afferent inhibition; uses, mechanisms and influencing factors. *BRAIN STIMUL*, 11(1):59 – 74.

[Valera et al., 1981] Valera, F. J., Toro, A., Roy John, E., and Schwartz, E. L. (1981). Perceptual framing and cortical alpha rhythm. *NEUROPSYCHOLOGIA*, 19(5):675–686.

[van Dijk et al., 2008] van Dijk, H., Schoffelen, J.-M., Oostenveld, R., and Jensen, O. (2008). Prestimulus Oscillatory Activity in the Alpha Band Predicts Visual Discrimination Ability. *J NEUROSCI*, 28(8):1816–1823.

[VanRullen et al., 2011] VanRullen, R., Busch, N., Drewes, J., and Dubois, J. (2011). Ongoing EEG phase as a trial-by-trial predictor of perceptual and attentional variability. *FRONT PSYCHOL*, 2:60.

[Vaseghi et al., 2015] Vaseghi, B., Zoghi, M., and Jaberzadeh, S. (2015). Inter-pulse Interval Affects the Size of Single-pulse TMS-induced Motor Evoked Potentials: A Reliability Study. *BASIC CLIN NEUROSCI*, 6(1):44–51.

[Wagner et al., 2009] Wagner, T., Rushmore, J., Eden, U., and Valero-Cabre, A. (2009). Biophysical foundations underlying TMS: setting the stage for an effective use of neurostimulation in the cognitive neurosciences. *CORTEX*, 45(9):1025–1034.

[Wagner et al., 2007] Wagner, T., Valero-Cabre, A., and Pascual-Leone, A. (2007). Noninvasive Human Brain Stimulation. *ANNU REV BIOMED ENG*, 9(1):527–565. PMID: 17444810.

[Watt and Desai, 2010] Watt, A. and Desai, N. (2010). Homeostatic plasticity and STDP: keeping a neuron's cool in a fluctuating world. *FRONT SYNAPTIC NEUROSCI*, 2:5.

[Weise et al., 2006] Weise, D., Schramm, A., Stefan, K., Wolters, A., Reiners, K., Naumann, M., and Classen, J. (2006). The two sides of associative plasticity in writer's cramp. *BRAIN*, 129(10):2709–2721.

[Wischnewski and Schutter, 2016] Wischnewski, M. and Schutter, D. J. (2016). Efficacy and time course of paired associative stimulation in cortical plasticity: Implications for neuropsychiatry. *CLIN NEUROPHYSIOL*, 127(1):732–739.

[Wolters et al., 2003] Wolters, A., Sandbrink, F., Schlottmann, A., Kunesch, E., Stefan, K., Cohen, L. G., Benecke, R., and Classen, J. (2003). A Temporally Asymmetric Hebbian Rule Governing Plasticity in the Human Motor Cortex. *J NEUROPHYSIOL*, 89(5):2339–2345. PMID: 12612033.

[Woolley et al., 1997] Woolley, C. S., Weiland, N. G., McEwen, B. S., and Schwartzkroin, P. A. (1997). Estradiol increases the sensitivity of hippocampal CA1 pyramidal cells to NMDA receptor-mediated synaptic input: correlation with dendritic spine density. *J NEUROSCI*, 17(5):1848–1859.

[Yanagisawa et al., 2012] Yanagisawa, T., Yamashita, O., Hirata, M., Kishima, H., Saitoh, Y., Goto, T., Yoshimine, T., and Kamitani, Y. (2012). Regulation of Motor Representation by Phase–Amplitude Coupling in the Sensorimotor Cortex. *J NEUROSCI*, 32(44):15467–15475.

[Yavari et al., 2018] Yavari, F., Jamil, A., Samani, M. M., Vidor, L. P., and Nitsche, M. A. (2018). Basic and functional effects of transcranial electrical stimulation (tES)—an introduction. *NEUROSCI BIOBEHAV REV*, 85:81–92.

[Yerkes et al., 1968] Yerkes, R. M., Dodson, J. D., et al. (1968). The relation of strength of stimulus to rapidity of habit-formation. In Boe, E. E. and Church, R. M., editors, *Punishment: Issues and experiments.*, Century psychology series,The Century psychology series. - New York : Appleton., pages 27–41. Ardent Media.

[Zarkowski et al., 2006] Zarkowski, P., Shin, C. J., Dang, T., Russo, J., and Avery, D. (2006). EEG and the variance of motor evoked potential amplitude. *CLIN EEG NEUROSCI*, 37(3):247–51.

[Zhang and Ding, 2010] Zhang, Y. and Ding, M. (2010). Detection of a weak somatosensory stimulus: role of the prestimulus mu rhythm and its top-down modulation. *J COGNITIVE NEUROSCI*, 22(2):307–22.

[Ziemann et al., 2004] Ziemann, U., Ilić, T., Pauli, C., Meintzschel, F., and Ruge, D. (2004). Learning modifies subsequent induction of long-term potentiation-like and long-term depression-like plasticity in human motor cortex. *J NEUROSCI*, 24(7):1666–72.

[Zilberter et al., 2009] Zilberter, M., Holmgren, C., Shemer, I., Silberberg, G., Grillner, S., Harkany, T., and Zilberter, Y. (2009). Input Specificity and Dependence of Spike Timing–Dependent Plasticity on Preceding Postsynaptic Activity at Unitary Connections between Neocortical Layer 2/3 Pyramidal Cells. *CEREB CORTEX*, 19(10):2308–2320.

[Zilles et al., 1997] Zilles, K., Schleicher, A., Langemann, C., Amunts, K., Morosan, P., Palomero-Gallagher, N., Schormann, T., Mohlberg, H., Bürgel, U., Steinmetz, H., Schlaug, G., and Roland, P. E. (1997). Quantitative analysis of sulci in the human cerebral cortex: Development, regional heterogeneity, gender difference, asymmetry, intersubject variability and cortical architecture. *HUM BRAIN MAPP*, 5(4):218–221.

[Zrenner et al., 2018] Zrenner, C., Desideri, D., Belardinelli, P., and Ziemann, U. (2018). Real-time EEG-defined excitability states determine efficacy of TMS-induced plasticity in human motor cortex. *BRAIN STIMUL*, 11(2):374–389.

9 Erklärung zum Eigenanteil

Die Arbeit wurde in der Universitätsklinik Tübingen in der Abteilung für Neurologie mit Schwerpunkt Neurovaskuläre Erkrankungen sowie am Hertie-Institut für klinische Hirnforschung in der “Brain Networks and Plasticity” (BNP) Forschungsgruppe unter Betreuung von Prof. Dr. Til Ole Bergmann und Prof. Dr. med. Ulf Ziemann durchgeführt.

Prof. Bergmann hat die Studien entworfen, die Steuerung der EEG-getriggerten Stimulation programmiert, Drittmittelfinanzierung eingeholt (DFG Projektnummer 362546008) und die Daten statistisch ausgewertet. Dr. med. Christoph Zrenner hat das ‘Real-Time System’ entwickelt. Die beschriebenen Experimente habe ich nach Einarbeitung durch Prof. Bergmann eigenständig durchgeführt.

Die Ergebnisse des ersten in dieser Dissertation beschriebenen Experiments (‘MUPEX’) wurden bereits veröffentlicht:
Sensorimotor μ-power is positively related to corticospinal excitability
Autoren: Thies, Miriam, Zrenner, Christoph, Ulf Ziemann, Til Ole Bergmann
Magazin: Brain Stimulation September–October 2018, 11 (5) 1119-1122
DOI: 10.1016/j.brs.2018.06.006
Übernommene Graphiken und Textstellen in der vorliegenden Dissertationsschrift sind im Text gekennzeichnet.

Ich versichere, das Manuskript selbständig verfasst zu haben und keine weiteren als die von mir angegebenen Quellen verwendet zu haben.

Hannover, den 28.08.2021

Miriam El Hilany-Thies (geb. Thies)

10 Acknowledgments

I would like to thank my husband, without whom the typesetting, graphics and author of this thesis would be a mess.
My grandfather for a lifetime of endlessly helpful, unfailingly motivated and competent academic support regardless of the field.
My parents for finally teaching me the importance of backing up data.
And my best friend for teaching me that discipline and joy are not mutually exclusive.

I am also grateful to Professor Ziemann for ‘taking me in’ as a doctoral student upon my unsolicited e-mail from Munich, and to Professor Bergmann for all the help provided and his reliable and unbureaucratic availability for questions and troubles during and after measurements.

11 Attachments

11.1 Detailed description of an exemplary measuring session

- Setup: Subjects were seated in a comfortable upright position in a chair with arm- and footrests. The Localite infrared camera was placed ca. 1.5 m to the front and left side, a crosshair was displayed on the wall opposite the chair at subjects' eye level. Subjects were instructed to fix their gaze on this crosshair throughout EEG recording to avoid artifact-generating eye movements and shifts of visual attention which could have introduced confounding changes in µ power. The screen for NeurOne (EEG and EMG recording software) and Matlab (scripts for stimulation and graphs of resulting MEPs and SSEPs) and the Localite screen were visible for the experimenter, but not for the subject-
- Participant's head circumference was measured to choose the appropriate size of EEG cap (54, 56 or 58cm)
- The EEG cap was adjusted, positioning the central Cz electrode in the middle between nasion and inion and both tragi, respectively.
- EEG electrodes were prepared: Within each ring electrode, the hair was pushed aside using the blunt end of a wooden applicator, then the skin beneath was cleaned by rubbing EEG-specific peeling paste on it with the cotton tip of the applicator. Finally, electrode gel was applied through a syringe with a blunt tip. This process was repeated as necessary until impedance of all electrodes was below 5kOhm as indicated by the NeurOne Impedance testing.
- A layer of cling film was snugly placed over the EEG cap, followed by a net cap. These layers have the triple purpose of providing a surface to fix the tracker on, preventing the gel from drying out and thus losing its conductive quality, and preventing certain kind of EEG artifacts.
- The neuronavigation tracker was placed on the right frontal area of the subject's head to not obstruct coil positioning over the left motor cortex while remaining detectable to the infrared camera. To ensure stability of the tracker throughout the session (any displacement would cause an inaccuracy of the initial co-registration of the scalp and thus of the marked coil position), it was thoroughly fixed with tape.
- Approximately 100 points distributed across the scalp were co-registered in Localite, in addition to some fixed anatomical markers like nasion and tragi (based on MNI for MUPEX and MUPAS screening, on individual T1 MRI for

MUPAS main sessions). For MUPAS main sessions, the positions of all 64 electrodes were additionally co-registered.

- The EMG electrodes were fixed in a belly-tendon montage with the active electrode over the muscle belly (tactile location during contraction against resistance) and the reference over the distal tendon (in this case: over the radial side of the proximal interphalangeal joint of the respective digit).
- A vacuum pillow was snugly placed around the subject's neck and head for comfort and head fixation.
- A 3 min eyes-open resting state EEG was recorded to confirm a sufficient μ rhythm peak. For MUPAS, an additional 6 min resting state EEG as 'phase targeting test' followed.
- Hotspot search: different coil positions were tested to find the one that consistently elicited the biggest MEPs. Coil positioning relative to the registered scalp surface (based on MNI or ind. MRI) was recorded.
- Thresholding for TMS (and MNS): automatic SA-PEST Matlab script was run, the resulting SI was checked for plausibility and manually adjusted if necessary.
- Stimulation commenced, the experimenter maintaining constant visual control of EMG (to assure the absence of pre-innervation, which would in itself increase MEP size and thus act as a confounder) and EEG (no muscle or other artifacts) quality as well as coil position on hotspot (Localite screen). The coil was hand-held by the experimenter throughout.
- Between blocks of stimulation, the TMS coil was cooled with customary frozen gel cool packs as necessary. One such session lasted from about 2 hours (full MUPAS screening session) to about 4h 30min (MUPAS main session).

11.2 MUPAS single subject plots

For reasons of legibility, the figures depicting phase targeting, power spectra, and time courses of absolute and baseline-corrected MEPs for single subjects will be placed on the following full pages.

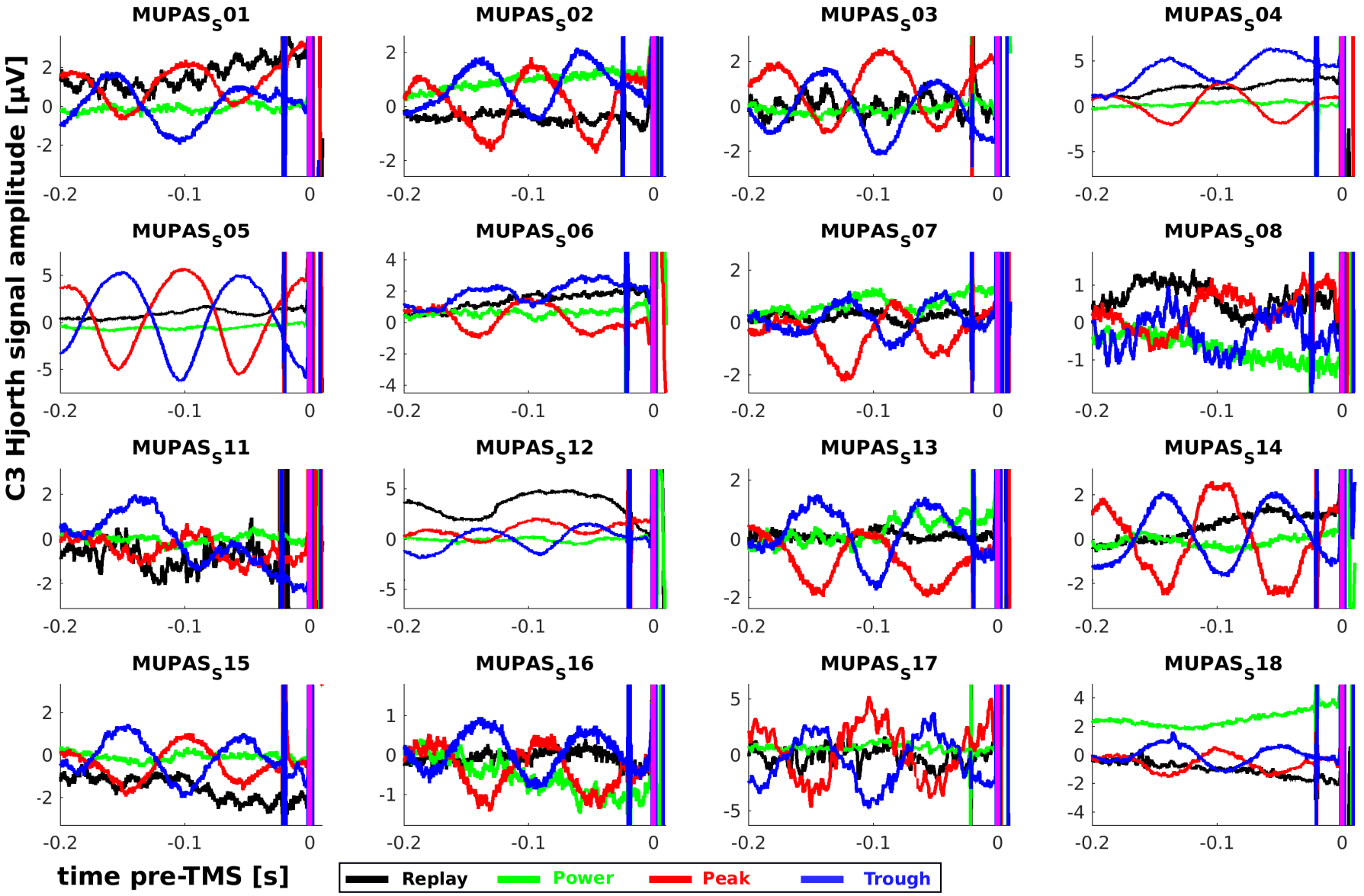

Figure 27: C3 Hjorth signal time-locked relative to delivery of TMS (time '0' on the x-axis) per condition for each participant. Subject numbers 9 and 10 are missing due to exclusion prior to completion of sessions (see 4.6.2)

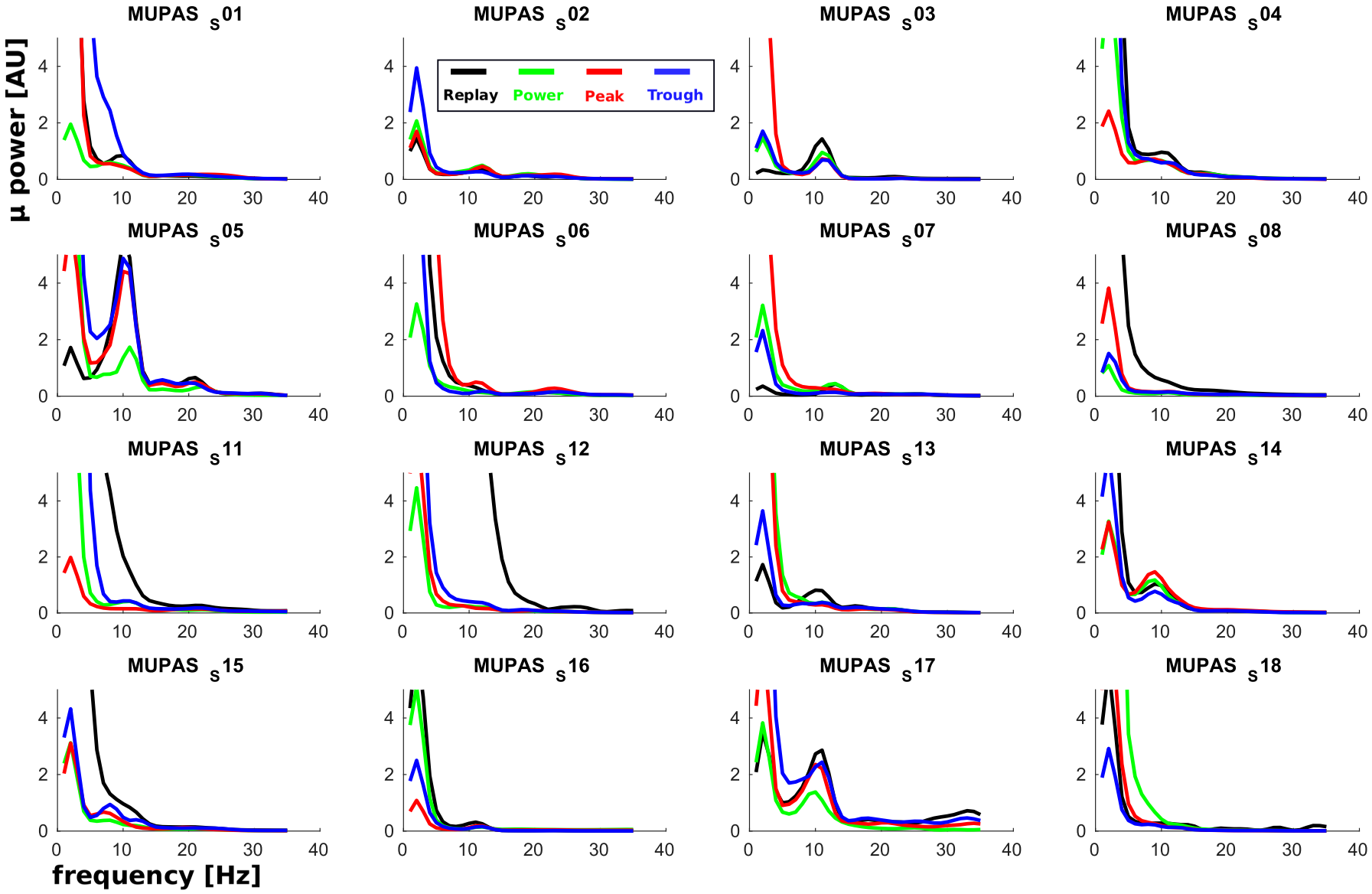

Figure 28: FFT-calculated pre-TMS C3 Hjorth signal power spectra per single subject. Subject numbers 9 and 10 are missing due to exclusion prior to completion of sessions (see 4.6.2)

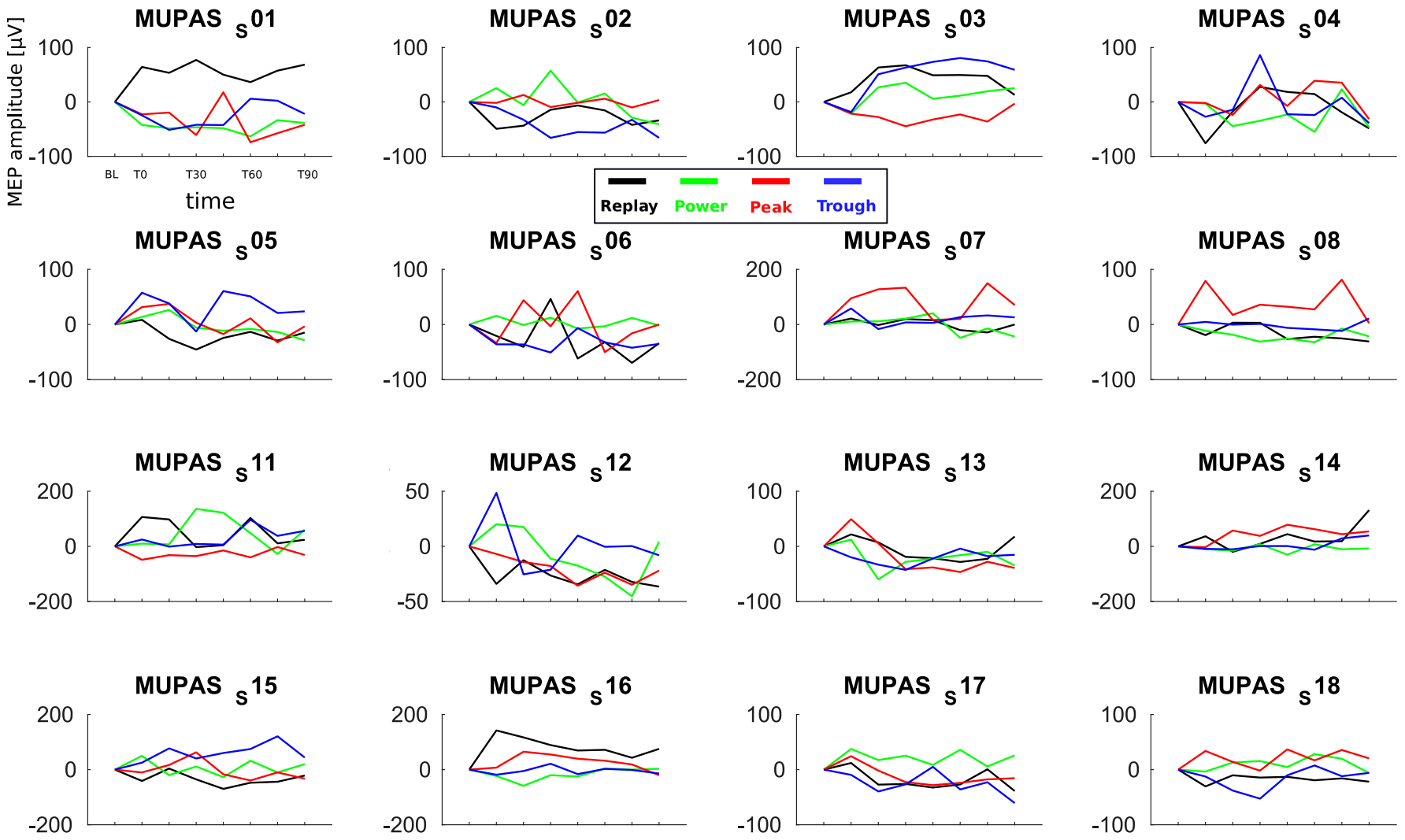

Figure 29: Change from baseline amplitude across time-points in the different conditions, plotted for each participant. Note the varying scaling of the y axis due to considerable differences in deviations from baseline between subjects. Subject numbers 9 and 10 are missing due to exclusion prior to completion of sessions (see 4.6.2)

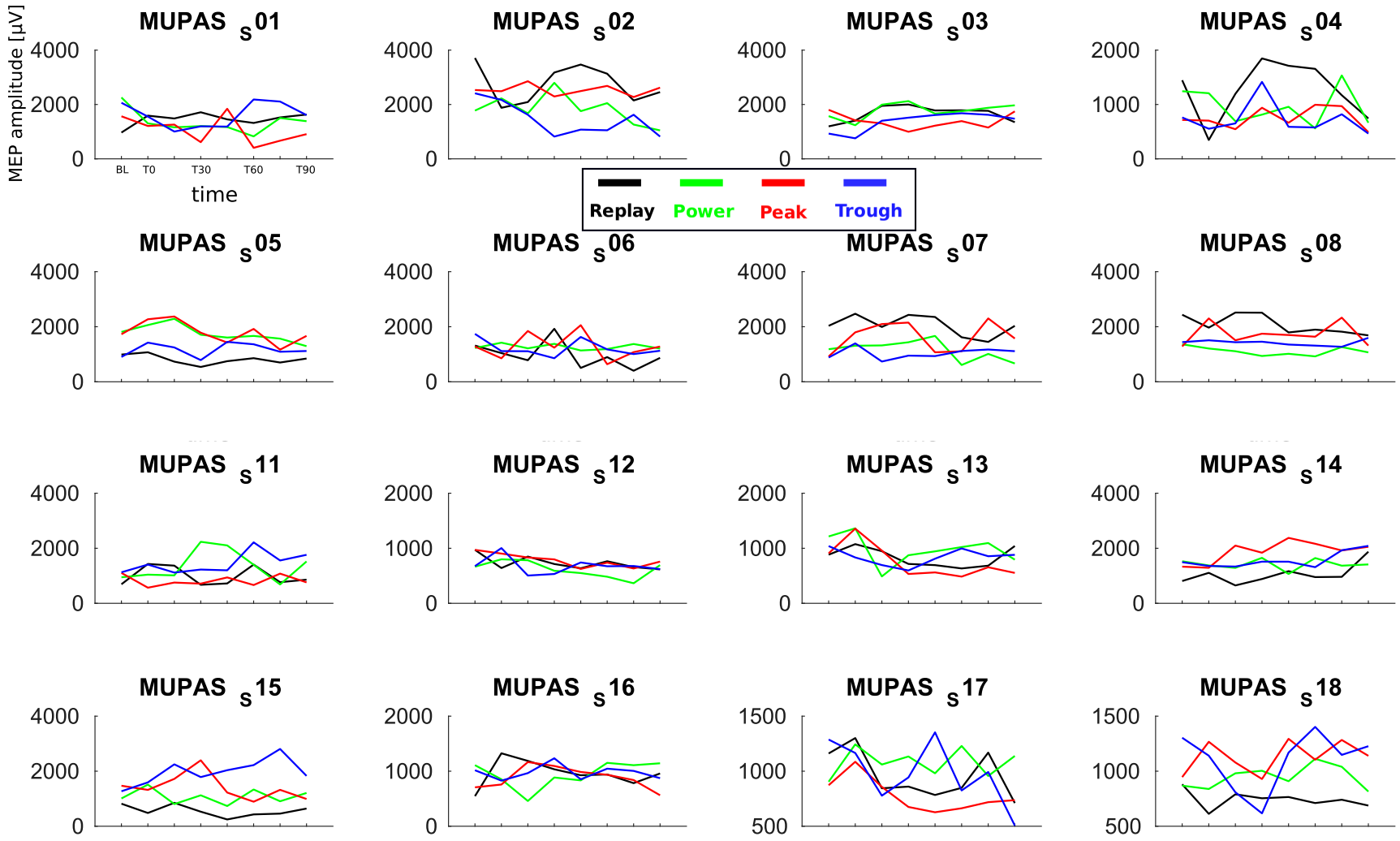

Figure 30: Absolute MEP amplitudes across time-points in the different conditions, plotted for each participant. Note the varying scaling of the y axis due to considerable differences in MEP sizes between subjects. Subject numbers 9 and 10 are missing due to exclusion prior to completion of sessions (see 4.6.2)